MASSEY UNIVERSITY

DOCTOR OF PHILOSOPHY IN PHYSICS

Structure-Rheology Relationships of Protein-Polysaccharide Complexes at Oil/Water Interfaces

---

Author:
Sashikumar RAMAMIRTHAM

Supervisor:
Prof. Martin Williams

Co-supervisor:
A/Prof. Catherine Whitby

Other supervisors:
Dr. Davoud Zare
Dr. Mike Weeks

A thesis presented in partial fulfillment of the requirements for the degree of Doctor of Philosophy in Physics

at

Biophysics and Soft Matter Group
School of Fundamental Science

PhD Duration : 2017 - 2021

Declaration of Authorship

I, Sashikumar RAMAMIRTHAM, declare that this thesis titled, "Structure-Rheology Relationships of Protein-Polysaccharide Complexes at Oil/Water Interfaces" and the work presented in it are my own. I confirm that:

- This work was done wholly or mainly while in candidature for a research degree at this University.
- Where any part of this thesis has previously been submitted for a degree or any other qualification at this University or any other institution, this has been clearly stated.
- Where I have consulted the published work of others, this is always clearly attributed.
- Where I have quoted from the work of others, the source is always given. With the exception of such quotations, this thesis is entirely my own work.
- I have acknowledged all main sources of help.
- Where the thesis is based on work done by myself jointly with others, I have made clear exactly what was done by others and what I have contributed myself.

Signed: 

Date: 30/09/2021

PREAMBLE

Life, the condition that distinguishes organisms from inorganic substances, manifests from intricately evolved functioning molecules carrying out specific physiological roles. Proteins are one of the oldest types of molecule, if not the oldest, which originated on earth more than 3 billion years ago. Encoded in the cell's genetic material, proteins are the supreme functioning biomolecules. Each protein molecule is entrusted with a unique set of functions which is carried out by its dynamic structure that can be rearranged by changing the surrounding solution environment. Although all the proteins can be derived from 20 constitutive amino acids, modelling and measuring protein structures to understand their possible functions has not been straightforward. The major breakthroughs so far have risen mainly from technological advancements such as X-ray crystallography and nuclear magnetic resonance (NMR) with artificial intelligence being the recent addition. Most proteins, especially globular proteins, irreversibly adsorb at interfaces between two substances, such as air/water and oil/water interfaces. Such interfaces also play a vital role in many of the physiological functions of organisms. Recent advances in interfacial techniques and their sensitivities makes it feasible to perceive protein monolayers. In this way, it is possible to use interfaces as a platform to investigate the protein structure in solution prior to adsorption.

Abstract

The complexation of proteins with polysaccharides to form bio-complexes is being utilized in a variety of applications including food formulations, microencapsulation, protein separation and bioactive deliveries. Understanding the impact of these biomolecules on each other with discernment will not only improve our existing usages but also aid in devising newer applications. The duo of β-lactoglobulin (β-lg), a surface active globular whey protein, and pectin, a plant-derived polysaccharide, is the model protein-polysaccharide system of this study. β-lg and pectin have been reported to undergo complexation driven by electrostatic attraction leading to contrasting interfacial rheological properties depending on the fine structures of the polysaccharide. The aim of this thesis is to understand the role of fine structures of the polysaccharide in protein adsorption and the interfacial film formation.

Given that β-lg is the interfacially active molecule in this study, assemblies of β-lg at dodecane/water interfaces at pHs 3 and 4, and at different conditions of ionic strength, salt type and temperature were studied. These parameters were tuned to vary the relative amounts of two native species, namely, monomer and its smallest aggregate, the dimer, while the interface was monitored using rheology and tensiometry. Unfolding of β-lg dimers at the interface triggers the formation of disulfide linkages between the free thiol groups located at cys121 of the monomers. In this way, it is demonstrated here for the first time that β-lg dimers are the smallest elastic network building unit of the protein. A higher concentration of dimers increases the final interfacial elastic strength of the network. The lack of the elastic film forming ability of β-lg monomer is attributed to the absence of multiple free thiol groups. Moreover, β-lg monomer exhibited minimal reduction in interfacial tension akin to a pure buffer solution. This fundamental relation between the quaternary structure of β-lg and its subsequent interfacial network suggests a possible interfacial role in its biological function. Besides, these results will also be used as control for assessing the

behaviors of β-lg/polysaccharide complexes.

In the next phase of this study, transient interfacial rheology of pre-mixed solutions of β-lg and polysaccharides with different lengths and charge densities at pHs 3 and 4 are presented. It was found that, while the interfacial activity of β-lg/pectin complexes is dictated by the amount of charge on the polysaccharide, the kinetics of the complexed β-lg's adsorption and its subsequent interfacial film formation is largely controlled by the contiguity of the charges on the polysaccharide molecule. Using subphase injection techniques, it is further shown that the structure of the β-lg in the protein/polysaccharide complex prior to adsorption is the major contributor to the lag time duration before the onset of an elastic film formation. This is exemplified by the contrasting behaviors of β-lg/pectin complexes with high polysaccharide charge density as compared to β-lg/pectin complexes with low polysaccharide charge density, where the latter can be used as a one shot delivery system to obtain reinforced oil/water interfaces. It is further proposed that the mechanism by which a polysaccharide molecule reinforces β-lg interfacial film is by concatenating multiple protein units and establishing cross-links in the aqueous subphase.

The final phase of this study presents microrheology measurements of oil/water interfaces laden with β-lg and β-lg/polysaccharide complexes. Microrheology further ascertains the viscous nature of β-lg monomer laden interfaces and the elastic nature of the interfaces with β-lg dimers. In addition, the presence of heterogeneity in the entangled films made of β-lg dimers in the form of confinements was also observed. A sharp transition was exhibited from an inelastic to elastic interface occurring around a surface dimer concentration of 56 $ng.m^{-2}$ at pH 3, 15 mM NaCl. Further, a slightly denser interface was observed for almost all the β-lg/polysaccharide complexes at pH 4. The heterogeneity that was observed at dimeric interfaces was not seen for interfaces with β-lg/polysaccharide complexes indicating the presence of the polysaccharide molecules beneath the interfacial film. On the whole, this thesis demonstrates the advantages of using of interfacial rheological techniques to tease out the structure-rheology relationships of biomolecules such as proteins and protein/polysaccharide complexes and thereby provide valuable insights about molecular manipulations.

Acknowledgements

Although the fruit of this thesis will bear my name as the author, the roots are many. The anchor of this project has been, Bill Williams, to whom I'm greatly indebted to for making my journey a thoroughly enjoyable one. The other major support for this project has been Catherine Whitby, whose untiring guidance has played a huge role. I thank both of them for providing me the freedom and guidance to carry out this study as well as rekindling my passion to learn. I extend my gratitude to Davoud Zare for introducing me to interfacial rheometry, for giving valuable inputs and for conceiving this project. The project would not have been possible without the financial funding of AgResearch Ltd, New Zealand and the able support of Dr. Mike Weeks and Dr. Brandon Haigh in the initial stages. I would also like to extend my thanks to the MacDiarmid institute for supporting me financially during the tough times of COVID19. Braydon Nikolaison was an excellent summer student who helped me carry out the emulsion studies reported in this thesis. The chamber used for microrheology was masterfully engineered by Olaf Griewaldt along with Steve Denby, some of the best mechanical engineers I have worked with. A big shout out to Dr. Rob Ward for all his help in providing me with the syringe pumps and helping me design the subphase injection experiments. The mass spectrometry of the protein samples were done by David Lun. I thank Dr. Allan Raudsepp for providing me the glycerol/water tracking data used for two-point microrheology analysis. I appreciate Riddet Institute and Maggie Zoe for letting me use their zeta sizer and tensiometry instruments. The 3D prints used in this study would not have been possible without the assistance of Sam Brooke and Ben Westberry. Natisha Megan was quintessential in sorting out the import of protein powder from Germany. I have to mention Dr. Trevor Loo and Harikrishnan Kurup for sorting out some of the chemistry. Although the protein denaturation experiments were not successful, I'm very thankful to Robert Wieliczko and Carolina Thum from AgResearch for their time. The illuminating discussions with

Geoff Jameson has been extremely useful in the critical stages of this project.

This acknowledgement will not be complete without mentioning the large group of people from Massey University for providing me their unwavering support throughout the project. Some of these people are Peter Lewis (Windows wizard), Paul Hocquard & Penny Abercrombie (procurement experts), Ann Truter; Cynthia Cresswell; Debbie Mcknight; Catherine Norman and Fiona Richmond (five women who constitute the soul of the School of Fundamental Sciences). I was blessed with some of the best lab mates who made this journey even more memorable with all the hikes, cookies and pints. I'm privileged to acquire the life-long friendships of the "werewolf" gang (Susav, Nimisha, Ben, Josiah, Shikeale and Kate) and my lunch buddies (Maulik, Hari, Joel and Chanjiev). I extend my gratitude to the acquaintances I have made through MacDiarmid Emerging Scientists Association (MESA). I have to mention my flat mates of the "haunted" house (Abhipray, Rayson, Sai and Ashray) for keeping me sane and grounded. Last but not the least, I can't find enough words to describe the support and love of my mother (Vijayalakshmi) who instilled the curiosity to learn, my father (Ramamirtham) who always had my back, my brother (Hari), sister-in-law (Revathy) and my niece (Parikshitha) for their constant affection and support.

This project was funded by New Zealand Ministry of Business, Innovation & Employment (MBIE Contract C10X1502) and AgResearch Ltd, NZ.

This thesis is dedicated to all the medical professionals who embodied the spirit of humanity in fighting the COVID19 pandemic.

Contents

List of Figures

List of Tables

List of Abbreviations

β-lg	**Beta-L**actoglobulin
LMP	**L**ow **M**ethylesterified **P**ectin
HMP	**H**igh **M**ethylesterified **P**ectin
HMP$_B$	**B**locky **H**igh **M**ethylesterified **P**ectin
HMP$_R$	**R**andom **H**igh **M**ethylesterified **P**ectin
HG	**H**omo **G**alacturanon
DM	**D**egree of **M**ethylesterification
GalA	**G**alacturonic **A**cid
DWR	**D**ouble **W**all **R**ing
PDMS	**P**oly **D**i **M**ethyl **S**iloxane
PS	**P**oly **S**tyrene
MSD	**M**ean **S**quared **D**isplacement
MPT	**M**ultiple **P**article **T**racking
OPM	**O**ne **P**oint **M**icrorheology
TPM	**T**wo **P**oint **M**icrorheology

List of Symbols

Bo	Boussinesq number	1
G'	storage/elastic modulus	$\mathrm{Nm^{-2}}$ ($\mathrm{kgm^{-1}s^{2}}$)
G''	loss/viscous modulus	$\mathrm{Nm^{-2}}$ ($\mathrm{kgm^{-1}s^{2}}$)
G_i'	interfacial storage/elastic modulus	$\mathrm{Nm^{-1}}$ ($\mathrm{kgs^{2}}$)
G_i''	interfacial loss/viscous modulus	$\mathrm{Nm^{-1}}$ ($\mathrm{kgs^{2}}$)
ω	angular frequency	$\mathrm{rad\,s^{-1}}$
$\gamma_{o/w}$	oil/water interfacial tension	$\mathrm{Nm^{-1}}$ ($\mathrm{kgs^{2}}$)
τ	lag time	s

Chapter 1

Introduction

1.1 Soft Matter

Our planet is bestowed with a plethora of elemental arrangements connected through a multitude of interactions. It ranges from simple gases and life-giving water to meticulously evolved complex architectures of polymers and biological molecules. Investigating materials and their macroscopic properties has proven to be greatly beneficial for practical applications. Further understanding about the emergence of such macroscopic properties from a microscopic scale has permitted tailor-made materials to be designed for specific applications. The characteristics of interactions between matter's components are sometimes exhibited through their reaction to external stimuli. "Soft matter", or sometimes referred to as complex fluids, is a category of materials including polymers, gels, liquids, and other biological materials that can be deformed by forces that are applied by thermal fluctuations.[1] Therefore, it is necessary to experiment on assemblies of such physical systems on a macroscopic and microscopic scale to derive a holistic understanding. In the forthcoming pages of this chapter, biomolecules, particularly, proteins and polysaccharides will be introduced. The key structural and rheological properties of the model protein and polysaccharide used in this study will be outlined. Subsequently, the interface, the intended final destination of these biomolecules and the platform for measurements in this study will be addressed. This will be followed by a discussion about the current state of understanding of their interactions followed by a brief description of the rheological techniques employed. Lastly, the chapter will be concluded by describing the motivation and scope of this study.

1.2 Proteins

In order to understand the mechanism of life at a fundamental level, the structural understanding of biomolecules has gathered attention. By the mid 20th century, a great deal had been unearthed regarding proteins, such as their unfolding and their denaturation behaviour. In the spring of 1951, Linus Pauling, Robert Corey and Herman Branson published articles that proposed the structure of helical and sheet-like elements of proteins through X-ray diffraction patters.[2,3] Proteins were found to be intricate polyelectrolytes with highly specific physiological responses. Every protein is unique and has evolved to carry out specific functions. The complexity of protein molecules arise from the 20 different constituent amino acids and their multitudinous unique sequence options available for assembly. These amino acids could be hydrophilic and charged, such as lysine and arginine, or polar and uncharged, such as asparagine and glutamic acid. To compound things further, each amino acid's behavior in the protein chain could also be affected by its position and the neighbouring residues.

1.2.1 Structure

The amino acid sequence constituting a protein chain can arrange itself spatially in different ways leading to its secondary structure. The most common ones are α-helix and β-strands. Right-handed α-helices form the shape of a cork screw with the side chains on the outside. Usually, it has 3.6 residues/turn and a pitch of 0.54 nm/turn. This structure is stabilized by hydrogen (H)-bonding between the O of the peptide bond i and the NH of the peptide bond i+4. Although each H-bond is of the order of a k_BT (k_B:Boltzmann constant, T:Temperature), the cumulative bond energy of the α-helix is enough to form a stable structure at typical ambient temperature. On the other hand, a β-strand is an extended structure, albeit slightly twisted. Several of these β-strands can be arranged either parallel or anti-parallel to form β-sheets. H-bonds once again play an important role in stabilizing the structure. In most proteins, regions that form α-helices and β-strands are typically seen together. The above mentioned secondary structures play a key role in determining the tertiary structure of the proteins.

The commonly occurring tertiary structures are globular (such as β-lactoglobulin), fibrous (such as collagen) and disordered (such as casein). The monomeric protein units can aggregate to form oligomeric quaternary structures of different oligomers such as dimers, trimers, tetramers and so on. Globular proteins are the most prevalent in nature. These imperfectly spherical proteins typically have α-helices and β-strands roughly spanning their diameter and connected to each other by reverse turns. Their net hydrophobicity is high, enabling them to be used as emulsifiers in various applications. Globular proteins also have specific conformations in their native states which, when denatured, will lead to their unfolding. Such structural changes lead to a loss of their biological activity in most cases.

1.2.2 Solubility

The solubility of a substance is measured by its saturation concentration (C_{sat}) under equilibrium conditions with the crystals or fluid phase of the substance. Such definitions are difficult to apply for solutes like proteins which contain both polar and apolar groups. Given the tertiary structures of globular proteins, their solubility greatly depends on the surface groups which come into contact with the solvent. Generally, the larger number of surface polar groups, the greater the solubility in water. Often, increasing the ionic strength also improves the solubility of proteins and is referred to as *salting in*. However, higher ionic strengths usually tend to precipitate proteins (salting out) which also depend on the nature of ions as illustrated by the well known Hoffmeister series.[4] Hence, the nature of the salt ions in the solution also plays an important role in regulating the protein's structure.

1.2.3 Denaturation

Upon adsorption to air/water and oil/water interfaces protein molecules undergo mild denaturation. Such an unfolding has a great bearing on the network structure that might be formed at the interface. Globular proteins have evolved to present a stable native structure under physiological conditions. By changing the conditions, the native structures can be unfolded or refolded. Nonetheless, refolding is not always

possible and is prevented by many factors. Aggregation of the exposed hydrophobic residues, changes in configuration of peptide bonds, reshuffling of sulfur bridges and cross-linking reactions between side groups at high temperatures are some of the factors that hinder refolding of a denatured protein back to its native state.

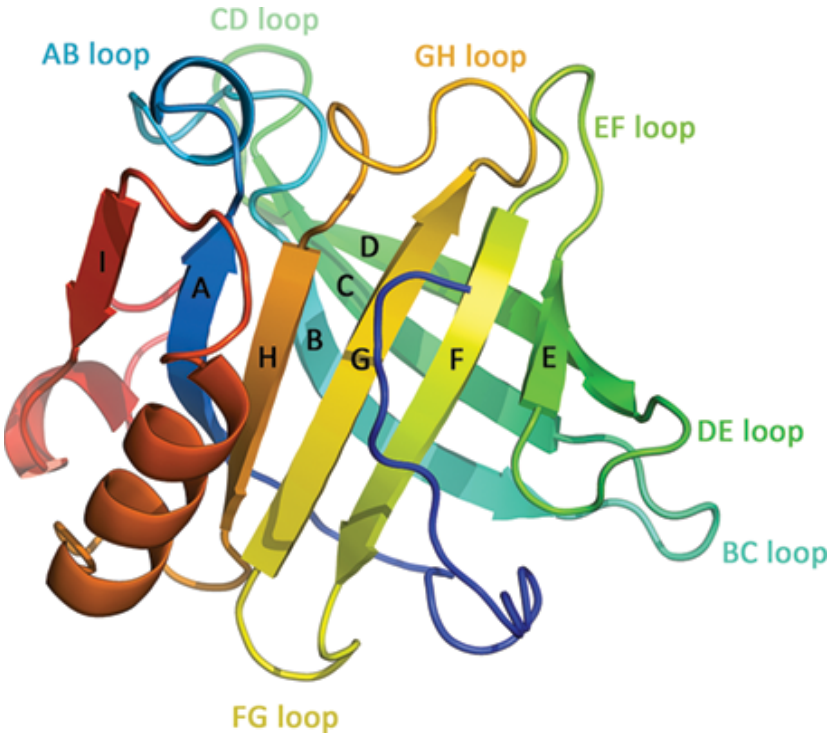

FIGURE 1.1: Crystal structure of β-lg monomer (PDB ID: 1BSO).[5]

1.3 β-Lactoglobulin

Milk is a foremost source of nutritive molecules including fats, carbohydrates, minerals and proteins for mammals. Most notably, it contains all the 9 essential amino acids that the human body cannot synthesize for itself. Hence, the admiration for milk proteins from both an industrial and an academic perspective is largely unsurprising. Milk proteins can be largely classified into two types, casein proteins and whey proteins. Whey proteins typically are obtained by precipitating soluble casein proteins through acid coagulation at pH 4.6, with further recovery through techniques such as chromatography.[6] The concentrated whey proteins consist of β-lactoglobulin,

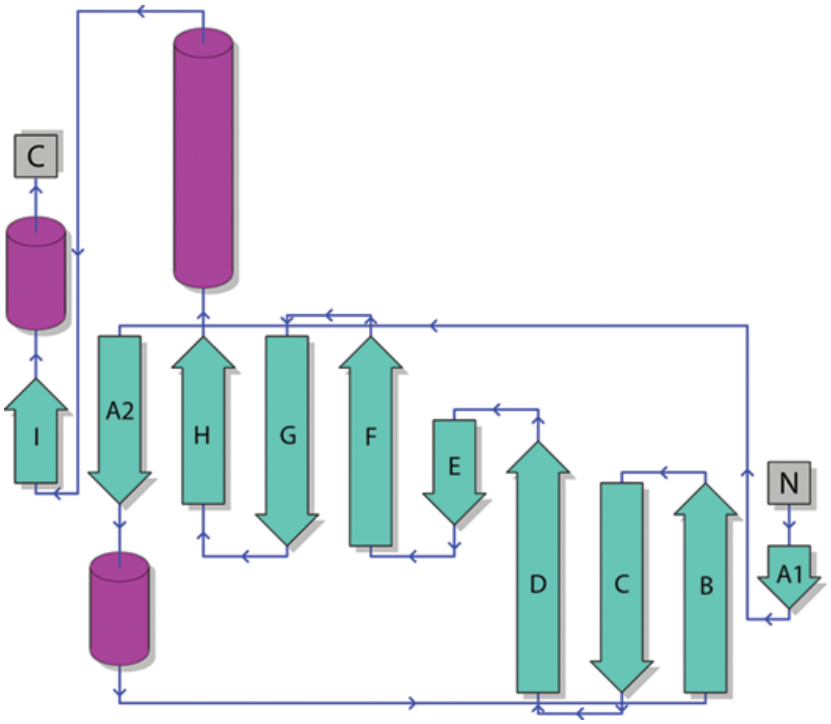

FIGURE 1.2: Corresponding topology structure of β-lg monomer (PDB ID: 1BSO).[5]

α-lactalbumin, bovine serum albumin, glycomacropeptide and other minor components. The primary component, β-lactoglobulin, generally accounts for about half of the total protein concentration in whey. It has been one of the important model proteins used in many studies related to biophysics and biochemistry.[7]

1.3.1 Structure

The structural conformation of a protein is the result of its energy landscape. Protein structures are folded and maintained by molecular interactions that are dictated by their environment. The balance between ordered, stable structure and disordered, unstable structure is key to enable a protein to perform its functions. This relationship between the structure of a protein and its function is called the structure-function relationship.[8] β-lg monomer is a small molecule (18.3 kDa) as shown in figure 1.1, that readily dissolves in aqueous solutions with an isoelectric point around pH 5.1. The two major genetic variants of β-lactoglobulin (βlg) are β-lg-A and β-lg-B. The latter can be obtained from β-lg-A by replacing Asp-64 and Val-118 with glycine and alanine respectively. Bovine βlg is present in the cow milk in the form of a noncovalent

homodimer.

β-lg was classified as a lipocalin protein after characterizing its atomic level resolution structure using X-ray crystallography.[9] Lipocalins are a family of proteins that share a similar structure to transport hydrophobic ligands. A typical lipocalin structure consists of an eight-stranded anti-parallel β-sheets as shown in figure 1.2, that is folded backwards to form an internal cavity enclosing hydrophobic residues, commonly referred as the calyx. This is accompanied by a three turn α-helix handle.[10]

Besides the delicate origami of arranging the amino acids, covalent bridging is important to maintain the integrity of the structure. Sulfurous proteins such as cysteine tie up different sections of a protein through disulfide bridging. The subtlety of disulfide bridges and thiol groups is particularly realized when encountering problems with unintended aggregation of recombinant proteins.[11] The impact of disulfide bonds on the folding and unfolding rates of proteins further signifies their importance in structural transitions of the protein.[11] Each monomer of β-lg contains five cysteine (cys) residues of which one has a free thiol group at cys121. The link cys106-cys119 connects neighbouring β-strands while the other link of cys66-cys160 connects the C-terminus to the CD-loop. The free thiol is situated just below the cys106-cys119 link hiding behind the α-helix.

1.4 Polysaccharides

Polysaccharides are long, sometimes branched biomolecules usually composed of one or more repeating monosaccharide units. They are typically a much bigger molecule ($\sim$ 50-100 kDa) when compared to proteins ($\sim$ 10-20 kDa). The monomers are bonded together through glycosidic bonds (-C-O-C-) between the monomers. Every monomer-monomer glycosidic bond is capable of undergoing rotation as well as assuming different configurations (α and β) and thus a polysaccharide molecule can assume numerous conformations. Linear polysaccharides are typically formed by 1,4-glycosidic bonds between the 1^{th} carbon of one monosaccharide and 4^{th} carbon of the other while 1,6-glycosidic bond leads to branching. In solutions, the long chains are constantly bombarded with solvent molecules causing fluctuations in their conformations.

Food related polysaccharides encompass many polyacids typically containing carboxyl groups (-COO^-) along the chain (for example pectin, gum arabic, alginate, xanthan gum). The number of charges carried is naturally a function of the molecular weight and pH. Polysaccharides are usually stiff, with a lot of side chains adding structural complexity. Moreover, charged polysaccharides contain ionizable groups whose counterions contribute to the ionic strength of the solution themselves and thus their interactions with other molecules. In addition, the pattern of glycosidic linkage plays a critical role in determining the flexibility and final structure of polysaccharide molecules. Further, for commercially available polysaccharides such as pectins, all the molecules in a polysaccharide sample do not have the same degree of polymerization (molecular weight). The molecular weight distribution depends on the pathway and conditions of synthesis and extraction. Thus, only an average molecular weight is typically specified for such polysaccharides.

1.4.1 Viscosity/Gelation

In many food systems, polysaccharides are primarily used as thickeners to increase the viscosity of the system. The polysaccharide chains begin to overlap beyond a critical concentration (C^*) which in turn is related to the intrinsic viscosity of the solution. At high concentrations, entanglements between polymer chains are considerable. The viscoelastic nature of the solution is dependent on the timescale of deformation and the dynamics of the entanglements. If the entanglements become permanent, then classical elastic gel behaviour results. At larger time scales, the tendency of the flexible polymer chains to come back to their original conformation compounded with the viscosity of the solvent, gives rise to a viscoelastic medium.

1.5 Pectin

Another fascinating biomolecule that has accumulated great interest over the years is pectin. Pectin is an important part of the plant cell wall which functions primarily as a hydrating agent and cementing material.[12] Pectin also imparts firmness and strength to the plant tissue through its links with the cellulose fibers.[13] This complex polysaccharide is commonly produced during the initial stages of primary cell wall

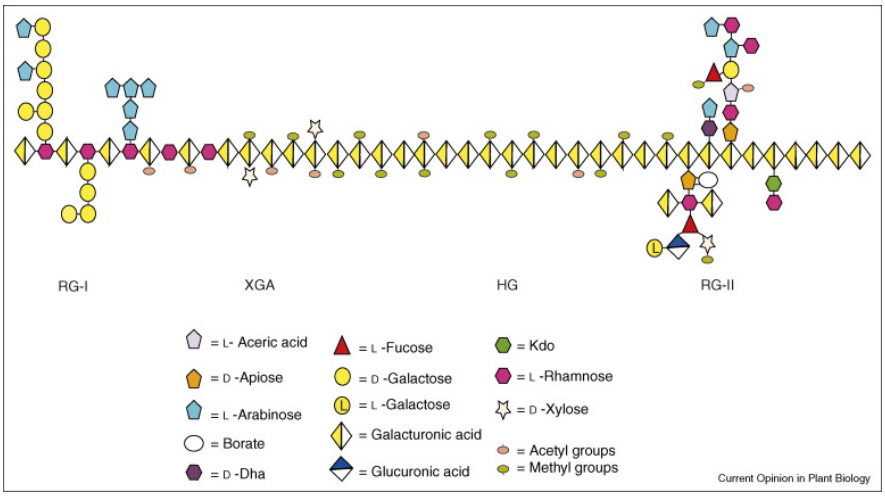

FIGURE 1.3: A schematic structure of pectin as given by Mohnen et al.[25]

growth and amounts to one third of dry substances in the cell wall of dicotyledons and some monocotyledons.[14] Despite multiple sources, commercial manufacture of pectin is limited by the potential gelling ability which depends on many factors including the fine structures. Currently, apple pomace and citrus peels are the primary sources of commercial pectin. Other sources include sugar beet and residues from seed heads of sunflowers.[15,16] Pectin production originated in the 20^{th} century when an apple juice manufacturer attempted to cook dried apple pomace which is the by-product after processing.[17] From there on, pectin has increased in popularity as an additive in beverages,[18,19] confectionery,[20] dairy[21] and meat products[22] in the food industry. Pectin was first discovered by Vauquelin (1790) and was later isolated by Braconnot,[23] who named it based on the greek word *pektikos* which means to congeal or curdle. Although the exact structure is yet to be realized pectin has been the focus of many investigations.[24]

Pectin is an anionic polysaccharide that is primarily made of covalently chained α-1,4-linked D-galacturonic acid (GalA) units, as shown in Figure 1.3. These GalA groups interconnect with varying degrees of methylesterfied and acetylatated carboxylate groups to form the backbone homogalacturonan (HG), which makes up 60-65% of total pectin.[26] This constitutes the "smooth region" of pectin. Further, C-2 and C-3 positions of some of these GalA units could be substituted with residues of xylose or apiose leading to xylogalacturonan or apiogalacturonan domains respectively.[27] In

some regions, the GalA units are interrupted with α-1,2-linked L-rhamnose- α-1,2-linked D-GalA units in turns of various lengths. Neutral sugar side chains of galactan, arabinan and arabinogalactans branch out of some of the L-rhamnose. This branched region of pectin is termed as Rhamnogalacturonan I (RG-I) and is also known as the "hairy region". The GalA residues of RG-I are not methyl-esterified, although the GalA residues of RG-I could be O-acetyl-esterified.[28] Rhamnogalacturonan II (RG-II) forms the other part of the hairy region albeit a minor one. It is a highly compact polymer made up of around 9 α-1,4-linked GalA units (of which some are methyl- esterified) with four structurally different polymeric side chains attached. These side chains contain eleven rare sugars including apiose, 2-O-methyl-l-fucose, 2-O-methyl-d-xylose, 3-C-carboxy- 5-deoxy-l-xylose (aceric acid), 3-deoxy-d-manno-octulosonic acid and 3-deoxy-d-lyxoheptulosaric acid.[29] An interesting aspect of RG-II is that it cross links two pectin molecules within the cell walls by borate ester links.

The primary focus on pectin especially from an industrial perspective stems from its exceptional ability to form gels in the presence of divalent ions or sugars and acid. Naturally, this property has been exploited in many food products where pectin is used as a thickening/gelling agent. The role of calcium-stabilized ionic bonds in retaining pectin in the cell wall has also been an area of discussion.[30,31] The behavior of the networks are dictated by molecular structure, intermolecular forces and the nature of the junction zones at which the polymers are cross-linked.[32] Hence, the total degree of methylesterification (DM) and the pattern of such groups along the backbone plays a crucial role in controlling the divalent ion binding affecting the texture of the pectin gel. Thus, based on the DM, pectins are classified into highly methylesterified pectin (HMP) with 50-80 % DM and low methylesterified pectin (LMP) with 20-50 % DM. Industrially produced pectins are mostly HMP. However, LMP is usually obtained from HMP by industrially controlled de-esterfication processes. Although many of the macromolecular properties of HMP and LMP are the same (the later being obtained from the former), the gelation occurs by different structural mechanisms.

Hydrogen bonding and hydrophobic interactions between the methyl esters play an important role in the gels of HMPs. The contribution of the latter to the free energy of junction zones is half that of the former.[33] Therefore, the pattern of methylesterification i.e. charges randomly distributed across the chain or occurring in chunks

FIGURE 1.4: A schematic state diagram depicting the interactions between anionic polysaccharide and globular protein from De Kruif et al.[44]

(block distribution) affects the gelation of HMPs along with temperature.[34,35,36] On the other hand, LMP gels are stabilized by ionic-cross linkages usually via calcium bridges between carboxylate groups of different chains which is described by the so-called "egg-box" model.[37,31,38] The gelation process starts with the initial dimerization of two macromolecules before subsequent aggregation of these dimers, making it a two-stage process.[39,40] The junctions are formed between unbranched, non-esterified GalA blocks bound together by Ca^{2+} ions. To achieve the stability of such "egg-boxes" at typical ambient temperatures requires of the order of six consecutive carboxyl groups on the interior of each participating chain.[41,38] Unsurprisingly, with decrease in DM, LMP-calcium mixtures ever more eagerly form gels with the strength related to the pattern and DM value.[42] Another variant of LMP is the amidated low methoxy pectin (AMLP) which will not be discussed here as it is outside the scope of this study but more information could be found elsewhere.[43]

1.6 Protein-Polysaccharide Interactions

The possible outcomes of protein-polysaccharide electrostatic interactions can be categorized into three types as shown in the figure 1.4. The figure depicts a schematic state diagram between a weakly anionic polysaccharide and a globular protein from the study made by De Kruif et al.[44] For a given protein/polysaccharide ratio both components are soluble above pH_c. From pH_c and below, the two components associate

to form soluble complexes. Upon decreasing pH further to below $pH_{\phi 1}$, these soluble complexes aggregate to eventually form complex coacervates.[44] At pH less than $pH_{\phi 2}$, a one phase system is again observed, due to protonation of the acid groups that reduce complexation. The value of $pH_{\phi 2}$ depends on the pK_a of the polysaccharide. The complexation in this study is predominantly studied at pH 4 where the protein and polysaccharide typically form soluble complexes. However, the total charge and its distribution on the polysaccharide backbone has been shown to affect the complexation and thereby alter β-lg's interfacial behavior.[45] In order to understand the impact of protein-polysaccharide complexation, interfaces, the typical destination of the protein, can be monitored.

1.7 Interfaces

Interfaces are the boundaries between two different substances or two different physical states of the same substance. Their properties are radically different and more complex in comparison to the bulk due to their asymmetric nature. Moreover, the actual thicknesses of most interfaces are of the order of few nanometers, usually containing a mixture of both the bulk phases. This has frustrated many researchers over the years including the revered Wolfgang Pauli who said *God made the bulk, the surface was invented by the devil*.[46] While scratching the surface sounds easy, understanding them has taken us centuries. Thanks to the technological advancements such as neutron scattering and X-ray diffraction we are beginning to understand the depths of the interface.

Interfaces form an intrinsic part of colloidal systems which are multi-component systems that are ubiquitous in nature. From the time Thomas Graham (*1805-1869*) identified them, colloidal science grew in popularity over the last 1.5 centuries and became a well established field of study through the efforts of Wolfgang Ostwald (*1883-1943*) and many other eminent scientists.[47] Colloids are fundamentally defined by the characteristic of having one phase dispersed in another. Emulsions are a class of colloids which comprises of at least one liquid dispersed in another immiscible liquid and a stabilizer to avoid the inherent coalescence and phase separation. The liquid that is dispersed in the form of droplets is the dispersed phase and the liquid around

these drops is the continuous phase. Such liquid-liquid dispersions have found wide spread industrial applications owing to the ease of their preparation.[48,49]

For a given liquid-liquid system, the chosen emulsifier plays a crucial role in dictating the properties of the emulsion among which stability is the main concern. The emulsifier stabilizes the system by residing at the interface between the two liquids and reducing the interfacial tension. While there are many mechanisms by which an emulsion can de-stabilize, viz. Ostwald Ripening, creaming and flocculation, the emulsifier prevents the primary mechanism of destabilization, namely, coalescence. In a simple emulsion, which consists of two immiscible liquids and one emulsifier, the interactions between the emulsifier molecules are of the primary concern. However, most of the systems encountered in the food industry contain multiple components such as thickening or gelling agents in both the liquid phases. Understanding the properties of such systems is far more complicated and challenging due to the diverse nature of interactions between the various components. Hence, the study of molecules at the interfaces has been the focus of many emulsion studies in the recent years.[50,51]

In spite of the recent upsurge in usage of solid particles as emulsifiers,[52,51] surface active molecules remain the most traditional and wide spread source of stabilizers. Naturally, biopolymers are widespread in food products such as creams, beverages, milk-based products and so on.[53] Amongst them, proteins and polysaccharides are major components due to their abundant availability from various sources. While polysaccharides are predominantly used as thickening or gelling agents, proteins are primarily used as emulsifiers as a consequence of their amphiphilic nature.[54] Therefore, the interactions between these two biopolymers intrigued scientists.[55] In this work, β-lactoglobulin and pectin will be used to study protein-polysaccharide interactions at the interface. Before stating the modus operandi and scope of this work, it is imperative to understand the nature of the components and their interactions along with the techniques available to study them.

1.7.1 Protein Interfacial Adsorption

A globular protein such as β-lg typically tries to hide its hydrophobic residues in aqueous solutions by wrapping around itself. Nonetheless, on the availability of a fluid/fluid interface, the alleviated hydrophobic residues can be stretched into the

non-aqueous phase. Hence, the fate of the protein usually culminates in an irreversible adsorption at the interface. The adsorption is driven by enthalpic gain from dehydration of hydrophobic surface patches and overall entropic gain from higher flexibility and the increased disordering of the unfolded amino acid chain. These irreversible adsorptions are more pronounced at interfaces with more hydrophobicity.[56] Simulation studies have also shown translating of β-lg beneath the interface, before finally adhering.[57]

As β-lg reshuffles at the interface, it undergoes various structural rearrangements. The protein molecule unravels its hydrophobic core, also known as calyx, into the oil phase.[57] As native β-lg molecules adsorb, their structural change triggers disulfide bridging[58,59] eventually leading to percolating networks. Viscoelastic properties of the gel-like networks crucially contribute to stabilizing emulsions by physically preventing droplet coalescence through sterically or electrostatically. Adsorption studies of β-lg at air/water and oil/water interfaces have consistently shown that stable emulsions are formed near the pI of the protein.[60,61] From a colloidal perspective, this observation has been primarily associated with screening of protein-protein electrostatic repulsion leading to the formation of denser networks. However, the role of ion-specific forces and their impact on aggregation properties have been largely ignored in such colloidal interpretations to date. These ion-specific effects on the protein structure, and subsequently on the interfacial assembly of β-lg, can be inferred by measuring the rheological properties of the interface. Therefore, it becomes imperative to understand the rheological techniques used to study interfaces, which will be introduced in the next section.

1.8 Rheology

All materials evolve with the effect of time and force. However, the time scales in which such effects can be perceived vary over many orders of magnitude. The common perception about the distinction of solids and fluids lies in their response to forces. Fluids dissipate any repercussions of an external stimuli while an elastic solid sustains and stores the input. Nevertheless, this only applies to the time scales we deal with in day to day life. In fact, solidity of a substance is only a time scale dependent

description as even some seemingly rigid solids under an applied force can flow given enough time.[62] Most materials exhibit solid-like properties, as well as liquid-like properties, at different time scales of probing. A wide number of soft matter systems such as emulsions, gels, pastes and foams have been shown to exhibit elastic (solid-like) behavior at short time scales and viscous (liquid-like) behavior at long time scales. They are therefore termed as viscoelastic fluids. Rheology is the study of such deformation and flow relationships of materials and their dependencies on applied force and time. The objective of rheology is to describe the interrelation between force, deformation and time for the given material. Measuring rheological properties provides a way to not only categorize materials but also helps to understand the microscopic origins of their macroscopic behaviors. The two major modes of deformation are in-plane deformations (ex. dilational and shear rheology) and out-of-plane deformations (ex. bending and torsion). Dilational rheology studies the response of the interface to changes in its area while the interfacial shape remains constant. In shear rheology, which is the method employed in this study, the response of the interface to changes in its shape are measured while maintaining the interfacial area constant.

1.8.1 Macrorheology

As the name suggests, macrorheology is the study of deformation and flow on a macroscopic or bulk or continuous scale of a material. In case of a rheometer, the deformations are applied by accurately designed instrument geometries. When energy is supplied to systems through external stimuli, the material can either dissipate the applied energy (viscous response) so it cannot be recovered or it can store the energy which can be latter recovered (elastic response). The typical response of a fluid is when the applied stress (σ) is proportional to the rate of deformation ($\dot{\gamma}$). Such fluids are classified as Newtonian fluids, although the concept of flow and viscosity precedes Newton.[63] For an ideal solid under deformation, stress is directly proportional to the strain (γ) rather than the rate of strain. While the above two systems form the two extremes of a spectrum, most materials encountered fall in between them and are classified as viscoelastic fluids. Further reading on rheology of viscoelastic fluids can be found elsewhere.[64]

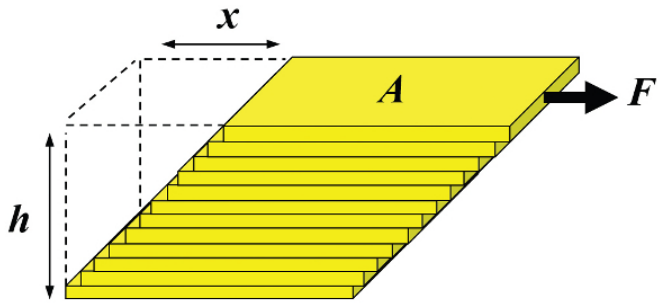

FIGURE 1.5: Mathematical definitions regarding a material under deformation. Image courtesy American Laboratory.

Shear rheology involves the application of a force parallel to the surface of a material as shown in figure 1.5. The resulting shear stress (σ) is given by $\frac{F}{A}$ and the corresponding strain is $\frac{x}{h}$. In this work, oscillatory shear typically in smaller amplitudes is employed to utilize its non-destructive and dynamic nature. Under such small deformations, the material is typically under 'linear' viscoelastic regime (LVR) where the relation between the input and output scales linearly causing no permanent damage to the material. In this method, a torque is applied through a probe geometry and the strain is varied sinusoidally with time as:

$$\gamma = \gamma_0 \sin(\omega t) \tag{1.1}$$

where γ_0 is the amplitude and ω is the frequency of the applied strain. For a viscoelastic fluid, the corresponding stress response of the material is given by

$$\sigma = \sigma_0 \sin(\omega t + \delta) \tag{1.2}$$

where σ_0 is the stress amplitude and δ is the phase angle. The measurement of the phase angle (δ), which can vary between 0 (purely elastic) and $\pi/2$ (purely viscous) provides a convenient method of viscoelastic quantification of a substance as shown in figure 1.6.

The corresponding storage modulus (G′) which signifies the recoverable input and loss modulus (G″) which signifies the unrecoverable input can be derived using,

$$G' = \frac{\sigma_0}{\gamma_0} \cos\delta \qquad G'' = \frac{\sigma_0}{\gamma_0} \sin\delta \tag{1.3}$$

FIGURE 1.6: Strain-stress responses of elastic, viscous and viscoelastic materials.[65]

Traditional rotational rheometers used for bulk (3-dimensional) measurements was modified to suit interfacial (2-dimensional) measurements. Other techniques for interfacial rheological characterization include deep-channel surface viscometers[66] and magnetic rod rheometers.[67] The sensitivity of rotational rheometers have greatly improved in recent times particularly in the last decade enabling measurement of molecular assemblies at delicate interfaces. In relation to shear rheology, bi-cone, Du-Noüy ring and double-wall ring (DWR) are the most commonly used geometries for interfacial measurements. Although bi-cone geometry is very reliable, the large contact area with the subphase limits its sensitivity and hence require higher sample concentrations. Du-Noüy ring which was designed to be more sensitive has been reported to have a few issues such as the dubious small gap assumption and the unaccounted contribution of the surface inside the ring. In this respect, DWR has many merits that overcomes the limitations of both these geometries.[68] Firstly, the square-edged cross-section enables efficient pinning at the interface as compared to the round-edged cross-section of Du-Noüy ring. The larger diameter of the ring also enables higher torque sensitivity. The patented design of DWR also enables similar shear rates in the inner and outer regions of the ring. Furthermore, the vertical struts holding the ring which gets immersed in the oil phase was shown to have negligible impact on the measurements. The rheometers used in this study are capable of measuring the

required phase angles and providing the moduli values. Further details pertaining to the interfacial rheology methodology will be provided in the experimental methodology section of Chapter 2.

1.8.2 Microrheology

Microrheology harnesses the innate thermal energy of a system to characterize its mechanical properties instead of applying an external stimuli. Thermal motion of molecules is imperceptible to human perception in both length scales and time scales. However, Albert Einstein[69] and Marian Smoluchowski[70] showed that the random motion of a colloidal particle in a fluid as observed by Robert Brown[71] is indeed due to their collisions with the surrounding atoms and molecules convincingly confirming their existence. One of the earliest particle tracking experiments was done by Jean Baptiste Perrin, who experimentally proved Einstein's theory in his work.[72] Multiple particle tracking (MPT) is a microrheology technique that is based on capturing the motion of small probe particles embedded in the system. The development of methods and algorithms to track the position of particles over time made this technique convenient to explore the short time scales that are not accessible using a conventional rheometer.[73] Furthermore, microrheology is useful in perceiving any heterogeneity of the system at much smaller length scales (nm) as compared to the length scales probed with macrorheology (μm).

The fundamental elements of passive microrheology involve recording the positions of the microscopic probe particles dispersed in the fluid over time. The series of images are then analysed to derive the properties such as the mean squared displacement which can be transformed through fluctuation dissipation theorems[74] to obtain the mechanical properties of the material.[75] The details of the theory and calculations are discussed further in the experimental methodology section of Chapter 4.

1.9 Research Questions and Scope of This Work

Protein molecules assemble at the interface and typically form viscoelastic interfaces which has found applications as food emulsifiers. However, the stability of these protein films are not always ideal in the conditions required for processing. A major

solution to this issue is the addition of polysaccharide to stabilize and reinforce the adsorbed protein molecules at the interface. Protein-polysaccharide complexes have found applications in food emulsification,[76] microencapsulation,[77, 78] fat substitution,[79], protein separation[80] and bioactive delivery.[81] Understanding the mechanisms of the underlying complexation can help us unravel strategies to tune them to various applications and can help in designing better recombinant β-lg for specific applications. Describing the behavior of β-lg/pectin complexes, the model system of this study, is also strongly urged by the demand from dairy industries for processing applications with implications in product stability. This study aims to first understand the rheological properties of β-lg/polysaccharide complexation and the possible parameters that can be used in order to tune their interfacial assemblies at dodecane/water interfaces.

Bovine β-lg's structure in solution is well studied compared to other proteins. Moreover, as it is touted as a transport protein, the structure-function relationship assumes critical importance. Gathering information about such molecular interactions of proteins will eventually lead to a quantitative understanding of cellular systems which involves self-assembly, chemical reactions and phase transitions. As β-lg is the surface active component in this study, it is crucial to first understand the protein's behavior in the absence of polysaccharide to later measure the impact of complexation.[7] The protein's behavior at different ionic conditions has been primarily attributed to the electrostatic interactions, leaving the role of its quaternary structure unclear. Therefore, in an attempt to gain a structure-rheology understanding of the protein molecule, chapter 2 will aim to study the relation between the self-association properties of β-lg and interfacial properties. This chapter will also demonstrate the sensitivity of interfacial rheometry to perceive such fundamental relationships. This will be carried out by modifying the monomer/dimer ratio in the solution through various parameters such as ionic strength, nature of salt and temperature at low protein concentrations. The inferences from rheology will be verified using interfacial tension measurements, which is the auxiliary technique used in this study.

Complexation of various polysaccharides with β-lg has been shown to exhibit contrasting interfacial properties.[82] The dissociation of complexes and the accompanying

transfer of the protein to the interface has been proposed as the critical step in determining how interfacial properties of such systems evolve. To scrutinize this hypothesis, β-lg was complexed with polysaccharides of different overall charges (LMP and HMP) and charge pattern (blocky and random). Further, to analyze the effect of binding site strength of the polysaccharide partner, the protein was complexed with shorter polysaccharides and oligosaccharides. The above mentioned studies at pH 4, dimeric solutions, and pH 3, monomeric solutions, will be utilized to unravel the mechanism of protein/polysaccharide complexation. This will be complemented with interfacial tension measurements and preliminary emulsion studies to capture the wholesome behavior of protein/polysaccharide complexes.

The final result chapter aims at further investigating the roles of β-lg self-association and polysaccharide complexation at oil/water interfaces using passive microrheology providing a qualitative comparison with macrorheology. β-lg assemblies at pHs 3 and 4 will be measured to scrutinize the inferences obtained using macrorheology in chapter 2. Any presence of heterogeneity in the β-lg films will also be explored using different probe particle sizes. The transition from monomeric to dimeric interfaces, if any, will be captured by performing interfacial measurements at different monomer/dimer ratios. The impact of polysaccharide on the topology of β-lg films will be investigated by carrying out particle tracking measurements at interfaces laden with β-lg/polysaccharide complexes employed in chapter 3. Overall, the combined results of interfacial rheometer and microrheology will provide comprehensive mechanical information and structural inferences about interfacial assemblies of protein/polysaccharide complexes.

Chapter 2

Beta-Lactoglobulin at the Interface

2.1 Background

β-lg is a model protein with multiple structo-functional regions that can be exploited to instigate process-induced conformational changes. Such mechanisms have been realized in many studies on emulsification/foaming.[83,84,85] For instance, β-lg can form supramolecular aggregates with different structures of various aspect ratios when subjected to heat treatment at different solution conditions.[86] Denaturation of β-lg by the addition of chemical denaturants such as guanidinium chloride is another commonly employed method. However, in this study, denaturation and structural changes induced by the interfacial adsorption of native β-lg is of the primary concern.

As alluded to in the previous chapter, β-lg monomer comprises of 9 β-strands (A-I) and one main α-helix of which the I-strand contributes towards the dimer interface. The remaining 8 anti-parallel β-strands (A-H) are folded backwards into a β-barrel forming a central cavity or calyx. The inside of this calyx is lined primarily with hydrophobic residues (residues 70-123) of the β-strands. Small hydrophobic ligands such as retinol have been shown to bind to this calyx region of β-lg.[87] One of the primary markers for structural changes is the aromatic tryptophan residue trp19 residing at the bottom of the calyx in the protein's hydrophobic interior as shown in figure 2.1 Fluorescent measurements show a redshift of its emission maximum when it is exposed to a more hydrophilic environment. Circular dichroism (CD) measurements are another way of monitoring the protein's overall tertiary and secondary structure in near-UV and far-UV regions respectively. Further, the reactivity of the lone thiol group at cys121 to reagents such as the Ellman's reagent can also be used to decipher

the structural changes of β-lg.[88] The cys121 group is usually hidden behind the α-helix in the solution (figure 2.1) but gets exposed when the protein unfolds its hydrophobic residues after denaturation.

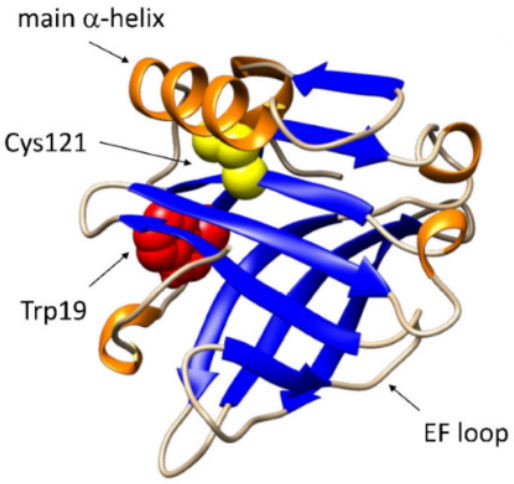

FIGURE 2.1: Native structure of β-lg monomer highlighting important structural regions such as cys121 (yellow) hidden behind the main α-helix and Trp19 (red) inside the β-barrel.[89]

2.2 β-lg Interfacial Adsorption

The thermodynamic stability of a protein determines the ease of its conformational changes at different environments such as a fluid/fluid interface.[90] The higher the thermodynamic stability of the protein the lower its rate of network formation but higher the final strength of the network. Disulfide bonds are one of the key factors to influence a protein's thermodynamic stability. β-lg has two disulfide bonds which makes the structure barely stable with an instability index of 40.12[91] as compared to a stable protein such as lysozyme[92] which contains four disulfide bonds with an index of 20.93. Hence, it is not entirely surprising that β-lg molecules have been shown to undergo considerable restructuring at fluid/fluid interfaces. Such conformational changes primarily revolve around the exposure and unfolding of hydrophobic residues particularly of the calyx into the non-aqueous, hydrophobic phase.

β-lg undergoes irreversible denaturation eventually losing its globular-like tertiary structure and undergoes significant changes in secondary structure upon adsorption

to fluid/fluid interfaces due to unfolding and structural rearrangements.[93] Indeed, the nature of the hydrophobic phase has been shown to play an important role in dictating such protein structural rearrangements.[94] At air/water interfaces, the structural rearrangements of β-lg are limited due to the absence of solvent molecules that can interact with the hydrophobic residues and facilitate spatial rearrangements through hydrophobic interactions. Multiple studies have reported weak β-lg films at air/water interfaces which has generally been attributed to the lack of considerable structural re-arrangements rendering the protein molecules devoid of any linkages through covalent bonding.[61,56,95]

Assemblies of β-lg at oil/water interfaces undergo considerable secondary structural rearrangement leading to viscoelastic film formation. β-lg contains around $\sim$ 36% β-sheets and 14% α-helix when present in the solution.[93] Initial studies on the conformational behavior at oil/water interfaces reported the loss of β-sheet structure after adsorption. However, the concomitant increase in unordered structure or ordered α-helix structure remained ambiguous.[96,97] Using synchrotron radiation circular dichroism spectroscopy, Zhai et al. (2010) reported an increase of α-helix content from 14% to 25% upon adsorption along with a considerable loss of tertiary structure akin to thermal denaturation due to binding of hexadecane (oil) molecules inside the hydrophobic β-barrel.[93]

The nature of the oil is another important parameter that has been shown to decide the protein interfacial film rheology. In particular, oil polarity has been shown to impact the assemblies of β-lg assemblies.[98] In case of polar oils, a higher affinity of the oil molecules to the exterior hydrophilic residues of the protein was suggested to retard the protein unfolding leading to slower build of interfacial films . Furthermore, β-lg adsorption effectiveness was found to be in the order of apolar oil/water > air/water > polar oil/water interfaces. The quicker buildup of interfacial strength at short chain apolar, n-alkane/water interfaces was attributed to the better penetration of the short chains into the hydrophobic core of β-lg.

β-lg monomer in solution is roughly spherical with a diameter of around 3.5 nm. β-lg dimer can be approximated to a prolate ellipsoid with a long axis of 6.9 nm and short axis of 3.5 nm.[95] Neutron reflectivity measurements have been employed to measure the thickness and coarseness of the interfacial protein films. At apolar/water and

air/water interfaces, β-lg film thickness was around 1.5 nm which is nearly half the thickness at polar/water interfaces showing considerable unfolding and restructuring in non-polar oils.[94] However, the surface roughness of protein films at apolar/water interface indicated a higher degree of dissolved hydrophobic residues as compared to that of air/water interface. The thin layers reported at air/water interfaces was attributed to flattening of β-lg monomers.[95]

2.3 Monomer-Dimer Equilibrium

While β-lg molecules spontaneously adsorb at the interface, the protein units are in a monomer-dimer equilibrium in the bulk. Native β-lg molecules in solution commonly exist in two quaternary states, namely, the monomer and the dimer. Although β-lg is overwhelmingly dimeric at conditions typically associated with milk, the monomer-dimer equilibrium can be altered by pH, ionic strength and temperature. β-lg at lower concentrations (10 mg/mL) exists in monomer-dimer equilibrium at pH < 4 and pH > 5.2. While dimers are favoured with increase ionic strength, the monomer are favoured with increase in temperature. It is useful to recall that the protein's isoelectric point is $\sim$ 5.1, below which its overall charge is positive. At pH 3 and 5 mM ionic strength, β-lg almost completely exists in the monomeric form at room temperature. An increase in the ionic strength pushes the equilibrium towards the dimeric form. At higher salt concentrations, the anions surround the positively charged subunits reducing the electrostatic repulsions between two monomer units enabling dimerization.[99] Sakurai et al. (2001) demonstrated that the higher chaotropic ClO_4^- anion was more effective in promoting dimerization than Cl^- ions.[100] These results point out the role of anionic binding in the burial of hydrophobic patches during dimer formation. The chaotropic anions promote the electrostatic interaction of Asp33 and Arg40 residues in the AB loop of each monomer along with anti-parallel association of the ninth β-strands (I). They also found that native dimer concentration can be increased by reducing the temperature. The hydrophobic effect at higher salt concentrations promotes dimerization which was quantified in a later study.[101]

Hydrophobic effects and electrostatic interactions dispute the association/dissociation equilibrium dynamics between β-lg monomers. Native dimer formation originates

mainly through hydrogen bonds between β-strand I of each monomer (mainly residues 146-150) arranged in anti-parallel direction.[99] At higher ionic strengths and lesser protein net charge, the dimer is stabilized by intrinsic hydrophobic interactions and specific intermolecular electrostatic shielding by counterions. Recent molecular dynamics (MD) simulations investigating the mechanism of dissociation have led to the suggestion that the dimer can dissociate using two plausible routes, a direct aligned unbinding where by the dimers dissociate without any prior rearrangements and an indirect dissociation where each monomers undergo either sliding or hoping before complete unbinding.[102] Mercandte et al. conducted a detailed investigation on the self-association of β-lg at various concentrations and pHs.[103] The results indicated that around the pH of 4.5 to 5.5, β-lg exists almost exclusively in a dimeric state. The study further emphasized the key role of electrostatics in the monomer/dimer equilibrium. The above mentioned trends are the same for both variants of β-lg, namely, β-lg-A and β-lg-B. Besides, both variants have exhibited the same near- and far-UV synchrotron radiation circular dichroism spectra.[93] Some studies have found evidence of even bigger oligomers such as octamers for β-lg-A near the isoelectric point.[104] Further, NMR spectroscopy has shown that the structure of the monomer at pH 2.6 is very similar to that of the subunits of the dimer at pH 6.2.[105]

While β-lg monomers continuously pair and split up in solution at certain rates, they also adsorb to surfaces spontaneously. As alluded to in chapter 1, β-lg's interfacial behavior has been primarily associated with the screening of protein-protein electrostatic repulsion leading to denser networks. However, the role of the quaternary structure and its impact on protein aggregation are largely disregarded in such colloidal interpretations. The concurrent change in self-association properties with the solution conditions naturally shifts the focus to the monomer-dimer interplay and raises the following questions:

- Is there any relation between the self-association state of β-lg and the rheology of its interfacial films?
- If so, how are the interfacial properties correlated to the two species, namely, the monomer and the dimer?

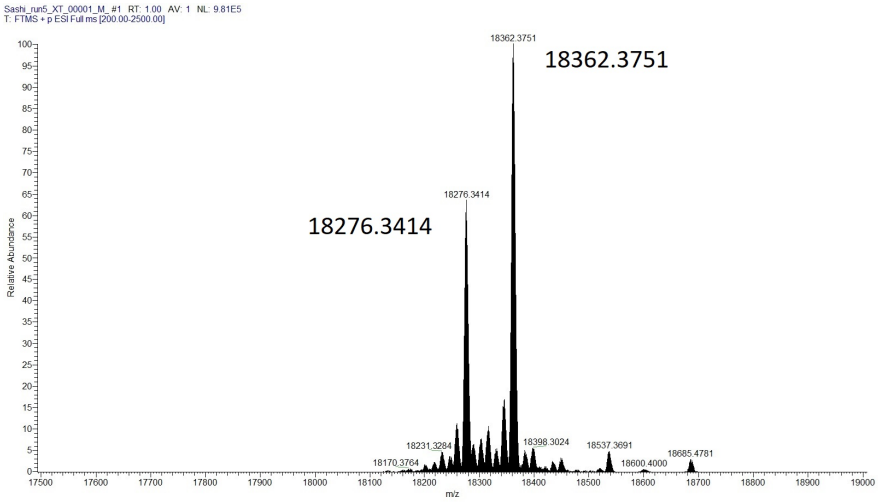

FIGURE 2.2: Mass spectrometry results (peak values enlarged) of β-lg solution in Milli-Q water. Instrument: Thermo Scientific Q-exactive focus hybrid quadrupole-orbitrap mass spectrometer.

- More importantly, is it feasible to use interfacial rheology to indirectly assess the effects of protein's quaternary structure?

In this chapter, the mechanical properties of β-lg assemblies at oil/water interfaces measured using oscillatory shear macrorheology and interfacial tension measurements are presented. Using the established methodology, the solution conditions such as the salt type, ionic strength and temperature were varied to study interfaces at different monomer/dimer ratios, while maintaining the total protein concentration. Since not many rheological studies have been performed with the above intentions, the protocol adopted and the preliminary experiments will be elaborated upon in some detail. These results will finally be discussed to draw out the major conclusions.

2.4 Materials and Methods

2.4.1 Materials

Purified β-lg was purchased from the food and bioprocess engineering group at the Technical University of Munich, Germany.[106] It is a mixture of β-lgA ($\sim$ 18.36KDa) and β-lgB ($\sim$ 18.27KDa) as shown by the mass spectroscopy data in figure 2.2. Other studies purchased from the same source have measured a total β-lg content > 99% and a ratio of β-lgA:β-lgB $\sim$ 1.22.[95] Once opened, the protein powder was packed in

multiple industrial foil bags, sealed with nitrogen gas and stored in the freezer at -4° C. Fresh protein powder was taken out roughly every 3 months. Milli-Q water with a resistivity 18.2 $M\Omega.cm$ was used for making all the solutions.

Protein solutions at different pHs were prepared using analytical grade hydrochloric acid (HCl), sodium hydroxide (NaOH) and sodium chloride (NaCl) (Fischer Scientific, $>$ 97 % purity, ACS grades). The more chaotropic sodium perchlorate ($NaClO_4$) was purchased from VWR chemicals (Belgium) at $>$ 97 % purity, ACS grade. Fresh protein stock solutions of 0.2 g.L^{-1} were prepared using filtered (pore size - 0.2 µm) electrolyte solutions and further diluted to 1 mg.L^{-1}. The pH 4 and pH 3 solutions were prepared by adjusting the pH using HCl. Since the proteins themselves contribute to the pH of the solution, all protein solutions were ensured to be in the intended pH using a SevenEasy pH meter (Mettler Toledo) before further measurements. Standard silicone oil (PDMS) samples were also purchased from Sigma Aldrich and were used for interfacial control measurements. The sample viscosities were 5, 100, 1000 cSt which corresponds to 4.5×10^{-3}, 0.096 and 0.97 Pa.s respectively.

Dodecane was chosen as the hydrophobic phase for the interfacial system for a number of reasons. Jotam et al. (2018) showed that for n-alkanes with chain length n $>$ 10, the interfacial film formation kinetics is dictated by the adsorption of β-lg rather than just diffusion.[56] In addition, the purity of the oil phase is also very important when measuring the protein film properties at the interface since most purchased oils have small traces of other chemicals. The known purification method along with previous literature results with interfacial rheology to compare made n-dodecane an ideal choice to study β-lg's interfacial properties.[56] Dodecane (anhydrous) was purchased from Sigma-aldrich (CAS 112-40-3) with $>$ 99 % purity. 100 mL of dodecane was continuously stirred overnight with 0.1 g of $FeCl_3.6H_2O$ (VWR Chemicals, $>$ 97 % purity, ACS reagent), 0.2 g of Na_2SO_4 (Sigma Aldrich, $>$ 99 % purity, ACS reagent), 0.04 g of KOH (VWR Chemicals, $>$ 85 % purity, ACS reagent) and 20 mL of silica gel (40-63 µm, Sigma Aldrich) to remove peroxides, residual water, alcohols and polar contaminants respectively.[56] Dodecane was freshly purified when necessary.

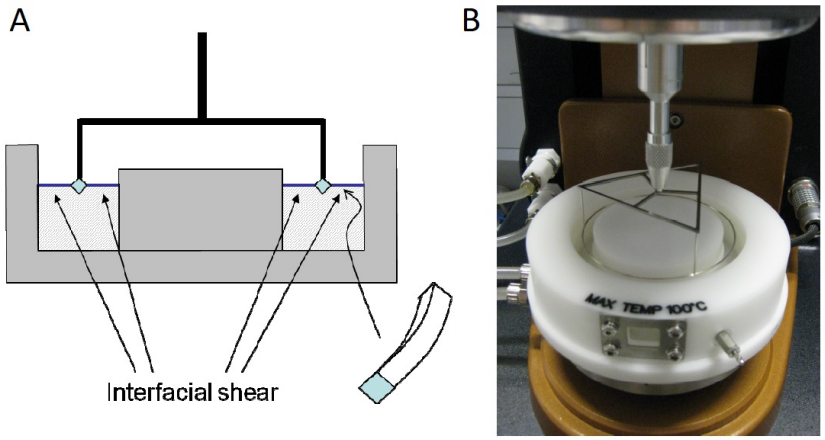

FIGURE 2.3: Cross sectional view of the DWR geometry (A) and the interfacial set up with DWR (B)[107]

2.4.2 Zeta potential Measurements

The zeta potential values reported were measured using a Zetasizer Nano ZS (Malvern Instruments, UK). β-lg solutions of 0.2 g/L with 5 mM of NaCl were used for the zeta potential measurements. The pH of the filtered (0.2 μm) solutions were adjusted by adding 0.1 M HCl and 0.1 M NaOH. At least six measurements were taken for each sample at 25 °C and the averaged values are reported.

2.4.3 Interfacial Shear Rheology

A discovery HR-2 rheometer from TA instruments (New Castle, DE, USA) was used with the interfacial setup using a DWR geometry of 1 mm thickness as shown in figure 2.3. The DWR has a square edged cross-section to enable it to pin to the interface as shown in the figure 2.3A. The ring is made out of Pt/Ir and the circular channel is made of Delrin, a material similar to that of Teflon.[107] The dimensions of the inner and outer radii of the DWR enables a uniform shear rate at the inner and outer ring sections. As the DWR inevitably drags the subphase along during the measurements, the interfacial shear rheology measurements are always overestimated due to the drag contribution from the subphase. The sub-phase drag correction is based on a finite difference calculation.[68] Briefly, the torque exerted on the ring is extracted from other contributions and iterated to match the intended applied torque. The relative contributions of surface to subphase drag is expressed in the form of Boussinesq number

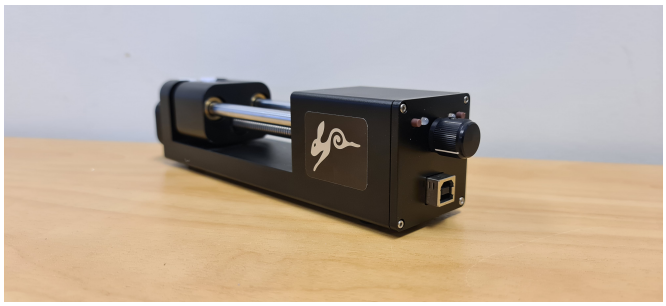

FIGURE 2.4: Syringe pumps obtained from White Rabbit Scientific Ltd, New Zealand

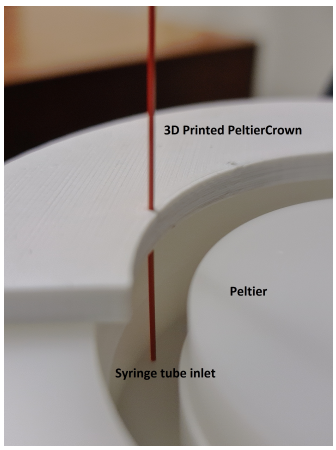

FIGURE 2.5: Microfluidic set up showing the inlet of the syringe pump tubing.

(B_o):

$$B_o = \eta_s/(\eta L) \tag{2.1}$$

where η_s is the surface viscosity and η is the bulk viscosity while L is the length scale associated with the technique. The interfacial stresses dominate while $B_o \gg 1$ and the subphase stresses dominate when $B_o \ll 1$.[68] For the DWR , L is 0.7 mm making $B_o \gg 1$ and as such the subphase correction is trivial unless the interface is extremely fragile $(< 10^{-5} Pa.s.m)$.

Experiments were carried with 20 mL of aqueous subphase after which the geometry was placed at the air/water interface. Subsequently, 10 mL of purified dodecane was added on top gently. The temperature was controlled using a Peltier trough was set at 25 °C unless specified otherwise. The DWR ring and the Peltier trough were thoroughly washed with water, acetone (Sigma Aldrich, $>$ 99.5 % purity, ACS

reagent) and isopropyl alcohol (Sigma Aldrich, $>$ 99.5 % purity, ACS reagent) before drying it in preparation for each measurement. Inertia and geometry calibrations were performed prior to each measurement in the suitable frequency and amplitude ranges. A draft shield is used to protect the sample from any convective disturbances from the environment. The dodecane/water interfaces were monitored by measuring interfacial properties at 0.1 % strain amplitude and 1 rad.s^{-1} angular frequency, with equilibration time per measurement of 60 seconds. All frequency sweeps were performed at 0.1 % strain amplitude and strain amplitude sweeps were performed at 1 rad.s^{-1}. Measurements were done in triplicate with reproducible values within a tolerance limit of 5%. For the convenient readability of time sweeps, every few data points are sometimes skipped to avoid crowding. In some of the results presented, only the G_i' values are shown for clarity and ease of reading. For these results, the corresponding G_i'' data can be found in appendix A.

Microfluidic syringe pumps were bought from White Rabbit Scientific Ltd, New Zealand as shown in figure 2.4. Glass syringes (Hamilton company) with a volume of 100 µl were used. The outer diameter of the syringe tubing made of teflon is 0.9 µm. The syringes and the tubings were thoroughly washed with water and buffer solutions before usage. The tubes were inserted through a 3D-printed rim on top of the Peltier trough as shown in figure 2.5. The tubes were around 5 mM from the DWR geometry while the tip of the tube was around 1 mm from the bottom of the Peltier trough. Flow rates of injection and withdrawal were very low (10s of nL.s^{-1}) in order to avoid causing considerable disturbance in the bulk phase. For rheology experiments involving microfluidic injections, the tubes remained inserted from the start till the completion of the experiments.

2.4.4 Interfacial Tension Measurements

The interfacial tension of dodecane drops in protein solutions were measured using a pendant drop tensiometer (KSV CAM200, Finland). A hooked needle (Biolin Scientific, Sweden) of gauge 22 was used to hang the inverted, pendant shaped oil drops in aqueous solutions at 25 °C. The volumes of the oil drops measured were in the range of 12 µL to 15 µL. The captured series of images were inverted along the vertical

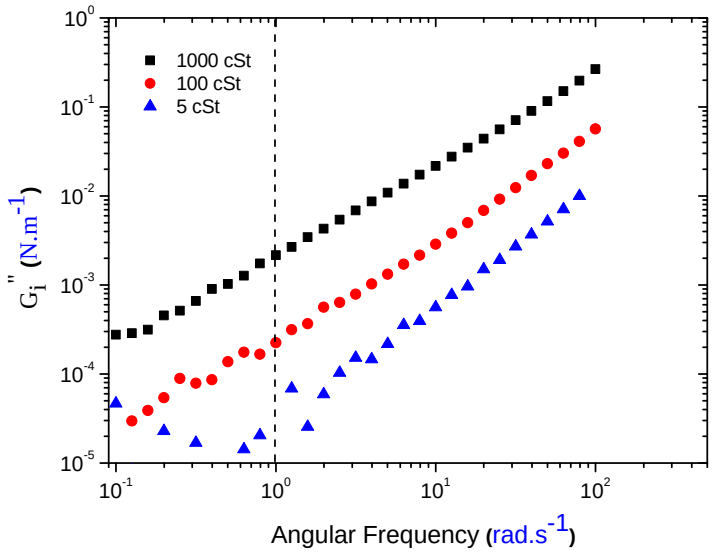

FIGURE 2.6: Frequency sweeps at 0.1 % strain amplitude performed on PDMS/water interfaces with the oil viscosities in the legends.

direction and the drop profiles were fitted to Young-Laplace equation to obtain the interfacial tension values.

2.5 Results and Discussion

2.5.1 Torque Reliability

Discovery HR-2 is a single head rheometer where the motor head applies a stress and measures the corresponding displacement (strain). The applied torque has to overcome the inertia of the instrument and the measurement geometry in order to obtain the contribution from the sample. At high frequencies and strain amplitudes, the torque required to overcome the inertia of the instrument dominates the torque, shearing the sample and thereby masking the material behavior. In such cases the loss modulus is proportional to the square of the angular frequency (ω^2).[107] In order to find a reliable range in which to measure the time evolution of mechanical properties of the interfaces, PDMS oils of three different viscosities were used to perform control experiments. Oscillatory frequency sweeps at 0.1 % strain amplitude at 25 °C are shown in figure 2.6. From figure 2.7, the torque response becomes inertia dominated beyond an angular frequency (ω) of 1 rad/sec for low viscosity oils and roughly below

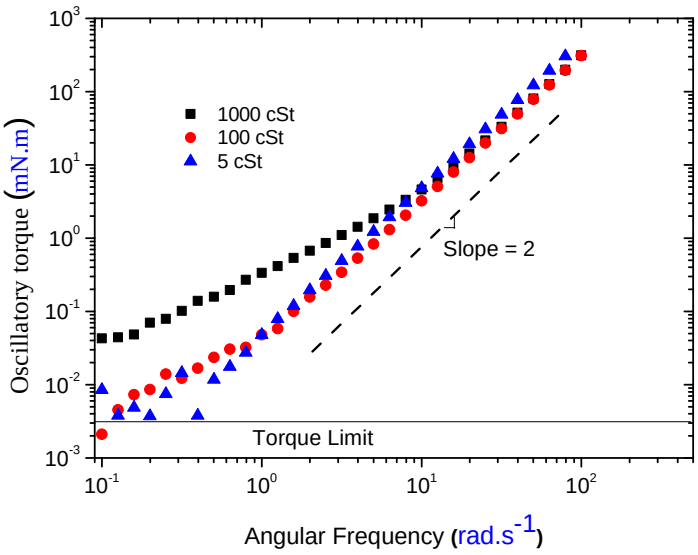

FIGURE 2.7: Torque data of the frequency sweeps at 0.1 % strain amplitude performed on PDMS/water interfaces with the oil viscosities in the legends.

an interfacial strength of $G_i'' \sim 10^{-4}$ Nm^{-1}. Hence, the reliability range was considered to be above the interface strengths of 10^{-4} Nm^{-1}, which corresponds to a Boussinesq number ~ 33.

2.5.2 Oil Purification

The nature of the hydrophobic phase has been shown to play a role in protein adsorption and the subsequent rheology of interfacial films.[56] Oils with higher polarity led to a slower build of weaker interfacial films for β-lg.[94] Hence, the oil was purified as mentioned in section 2.3.1 and the purity was verified with surface drop tensiometer measurements as shown in figure 2.8. In order to maintain the purity of oil for experimental comparisons, the oils were freshly purified whenever necessary and interfacial tension values were ensured to match with the reported values.

2.5.3 DWR Position

The position of the interface was identified by lowering the ring onto the aqueous phase at 10 $\mu m/sec$ until the measured axial force was < 0.01 N. At this point the ring is further lowered down to its measuring position by half its thickness (500 μm) and

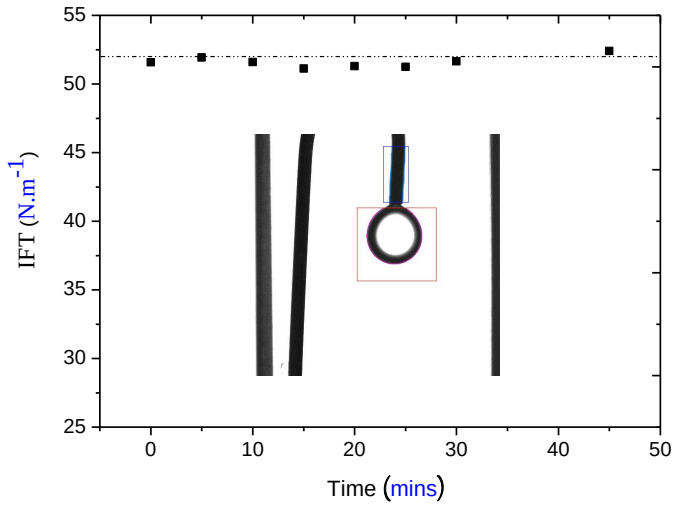

FIGURE 2.8: Interfacial tension (IFT) values obtained using a drop tensiometer at purified dodecane/water interface. The dashed line indicates the value reported in the literature. The inset shows a model inverted pendant drop image after length calibration (blue box) and curve fitting (red box).

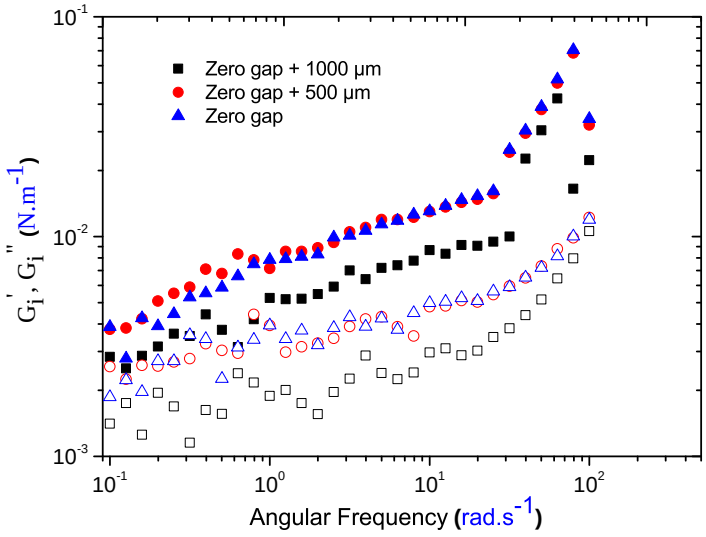

FIGURE 2.9: G'_i (solid) and G''_i (hollow) from frequency sweeps of 1 mg.L^{-1} β-lg solution at different geometry positions near dodecane/water interfaces.

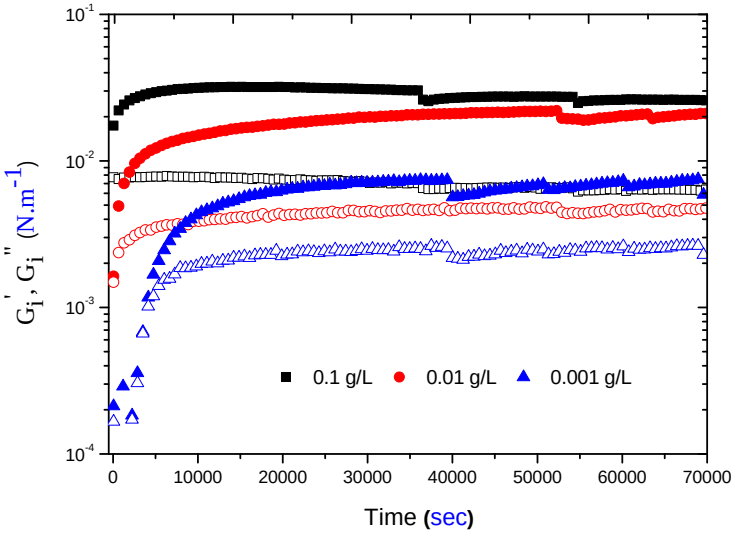

FIGURE 2.10: Time evolution of G_i' (solid) and G_i'' (hollow) at dodecane/water interfaces of various β-lg concentrations (pH 4, 5 mM NaCl).

the less dense liquid (oil) is added to the top. For experiments that involves delayed injection of salts into the subphase, the position of DWR might vary slightly during the experiments. To test the sensitivity to the geometry position at the interface, frequency sweeps were performed at dodecane/water interfaces with 1 mg.L^{-1} β-lg concentration as shown in figure 2.9. It can be observed that measurements taken when the center of the DWR is at the interface (zero gap) i.e. when half of the DWR is immersed into the subphase were similar to the measurements taken where only the bottom tip of DWR is touching the interface. Only when the geometry was lifted completely out of the interface (zero gap + 1000 μm) into the oil phase was a considerable change in G_i' and G_i'' observed. This shows that DWR is not too sensitive to the minor fluctuations happening around the 500 μm height region as long as the middle or bottom tip is in contact with the subphase. All the other experiments in this study are carried out with the DWR equally immersed in both the phases as much as possible

2.5.4 Protein Concentration

In order to carry out the experiments accurately, it is essential to have an interface that is sensitive to the proposed changes in the bulk. High concentrations of proteins can

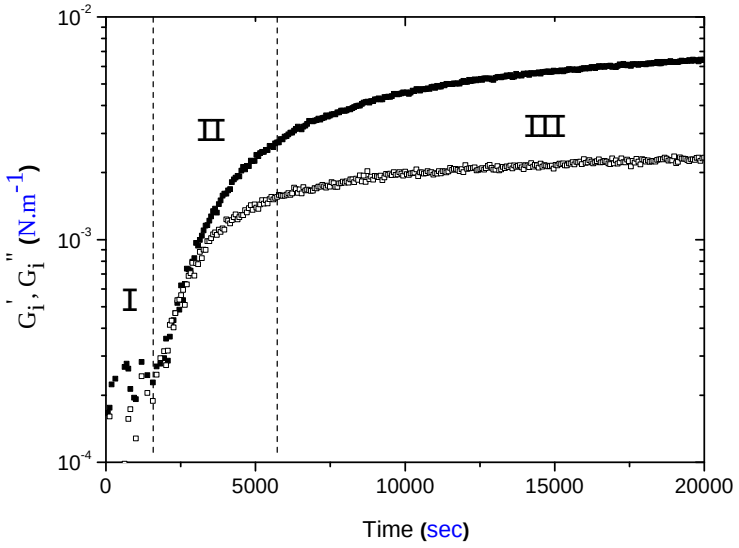

FIGURE 2.11: Time evolution of G_i' (solid) and G_i'' (hollow) at dodecane/water interfaces of 1 mg.L^{-1} β-lg solution (pH 4, 5 mM NaCl).

easily form multiple interfacial layers, crowding the interface to saturation. This renders the data devoid of any initial time dependent values owing to the fast build up of the interface. In order to gauge the protein concentrations needed for the interface sensitive to the properties of monolayer build-up, the mechanical properties of β-lg solutions at different concentrations were measured at pH 4 in 5 mM NaCl as shown in figure 2.10 A considerable period of induction was first observed at 1 mg.L^{-1} bulk concentration which was subsequently chosen for further experiments. The corresponding frequency sweeps of these interfaces can be found in figure A.1. The typical reproducibility of macrorheology measurements can be found at figure A.2.

Lag Time

β-lg adsorption follows three distinct steps as depicted in figure 2.11, akin to other protein molecules.[108] First, the molecules diffuse through the bulk and reach the interface. This step is mainly controlled by the temperature of the solution and the size of adsorbing molecules. When the surface concentration of protein reaches a certain threshold, the rheometer starts to sense a reliable interfacial elastic moduli (G_i'). The duration of the induction period (after which the protein network begins to establish itself at the interface) is generally referred to as the *lag time* (t_{lag}). The t_{lag} for this study

was defined as the time after which G_i' consistently rises above instrument's reliability limit of 10^{-4} Nm^{-1}.

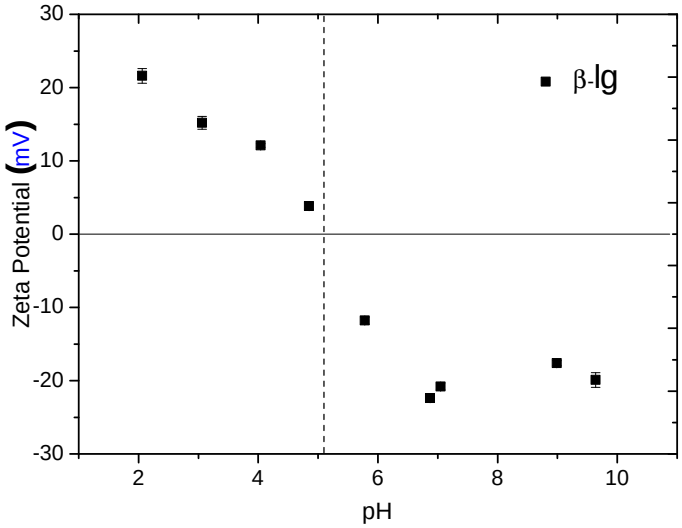

FIGURE 2.12: Zeta potentials of 0.2 $g.L^{-1}$ β-lg solutions at different pHs.

2.5.5 The Quaternary Structure Hypothesis

As alluded to earlier, changes in the solution pH can alter the structure as well as the net charge of β-lg. The zeta potential of β-lg at different pHs are shown in figure 2.12. Higher concentrations (0.2 $g.L^{-1}$) of β-lg were used due to the sensitivity of the zetasizer instrument. The isoelectric point (pI) of β-lg is consistent with the literature value observed elsewhere.[60] The transient shear interfacial properties of β-lg solutions (1 mg/L) at various pHs are shown in figure 2.13. At first glance, conditions at which β-lg carries a higher net charge i.e., a pH of 2 and 3 did not give rise to a viscoelastic interfacial layer. However, the protein managed to form a viscoelastic network despite its high net charge at pH 7. This suggests another factor in play that contributes in determining the rheology of β-lg laden interfaces. Another major structural change that occurs with the change in pH is the position of the monomer-dimer equilibrium. At a fixed protein concentration, the ratio of β-lg monomers to dimers is altered with changes in pH. While the monomer species is prevalent at pH 2 and 3, the dimer species dominate solutions at pH 4 and 7.[100,103] Therefore, the results shown in figure

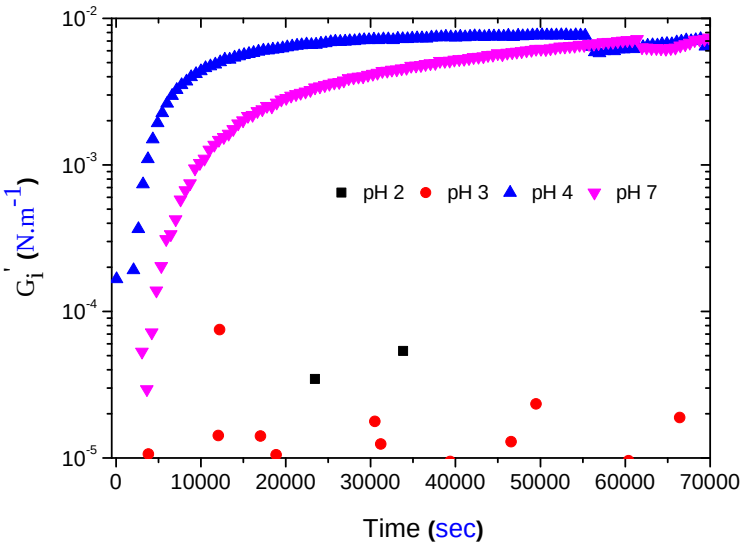

FIGURE 2.13: Time evolution of G_i' at dodecane/water interfaces with 1 mg.L^{-1} β-lg concentration and various pHs. Corresponding G_i'' data can be found in figure A.3.

2.13 can also be interpreted by the relative quantities of monomers and dimers. Hence, it is reasonable to hypothesize that the interfacial film properties are also related to the monomer-dimer equilibrium i.e. the quaternary structure of β-lg in the solution.

2.5.6 β-lg Dimers Build Elastic Interfaces

In order to test the aforementioned hypothesis, β-lg solutions were prepared with different relative amounts of monomers and dimers by modulating various parameters such as salt concentration, nature of salt, pH and temperature. The total β-lg solution concentration was kept constant at 1 mg.L^{-1}. The dimer populations listed in table 2.1 are derived from the dimerization equilibrium constants measured by Sakurai et al. (2001) at 20°C.[100] The Arrhenius equation was used to recalculate the values at the temperatures of the performed experiments. As dimerization equilibrium constants were not available at pH 4 due to sensitivity limits of measurements, an approximate value of 1 µM was assumed for calculations.[103]

In figure 2.14, two β-lg solutions with similar ionic strengths but different salts, namely, NaCl and $NaClO_4$, are compared. $NaClO_4$, the more chaotropic salt that is

TABLE 2.1: Dimer amounts of 1 mg.L^{-1} β-lg solutions at various solution conditions.

pH	C_{NaCl}(mM)	M_{Dimer} (g)
3	5	$1.74\pm0.95\times10^{-10}$
3	25	$1.69\pm0.35\times10^{-9}$
3	50	$1.24\pm0.37\times10^{-8}$
3	100	$2.47\pm0.26\times10^{-8}$
3	200	$8.75\pm0.15\times10^{-8}$
3	500	$2.68\pm0.23\times10^{-7}$
3	1000	$2.693\pm0.53\times10^{-7}$
3	50	$1.11\pm0.33\times10^{-7}$
3	50	$3.08\pm0.91\times10^{-7}$
3	50	$1.22\pm0.36\times10^{-6}$
3	20*	$4.62\pm1.5\times10^{-7}$
3	20**	$2.76\pm0.76\times10^{-6}$
4	5	$1.8\pm0.1\times10^{-6}$

* $NaClO_4$ was used at 25°C ** $NaClO_4$ was used at 15°C

known to promote dimer formation displays a higher G_i' and smaller t_{lag} values as compared to that of NaCl. For the same concentration of $NaClO_4$, when the experiment was conducted at a lower temperature of 15 °C as expected, G_i' increased. This is consistent with the above result, as reducing the temperature also promotes dimer formation.[100] β-lg solution at pH 4 and 5 mM NaCl (25 °C) contains a similar dimer population as the one at 15 °C. As expected, the pH 4 solution yielded a network of comparable G_i' but with a much smaller t_{lag} value. Based on this result, although the dimer populations are similar, the larger t_{lag} value at 15 °C can be explained by the slower diffusion of molecules. These results point to a correlation between the dimer concentration and the final interfacial strength as well as the t_{lag}.

It is worth reasserting that all of the above measured β-lg solutions had the same total protein concentration. While a higher concentration of β-lg dimers seem to promote the elastic strength, it is important to verify the corollary that β-lg monomers do not impart elasticity. Evolution of the strength of the interfaces of β-lg solutions with decreasing NaCl concentrations are shown in figure 2.15. Unsurprisingly, the final G_i' decreases with decreasing salt concentration. A similar trend with NaCl concentration can also be seen at pH 4 in figure A.6. This result is usually attributed to a decrease in Debye length. However, based on the previous results, it can be argued that a lower concentration of dimers also contribute towards the reduction of interfacial strength.

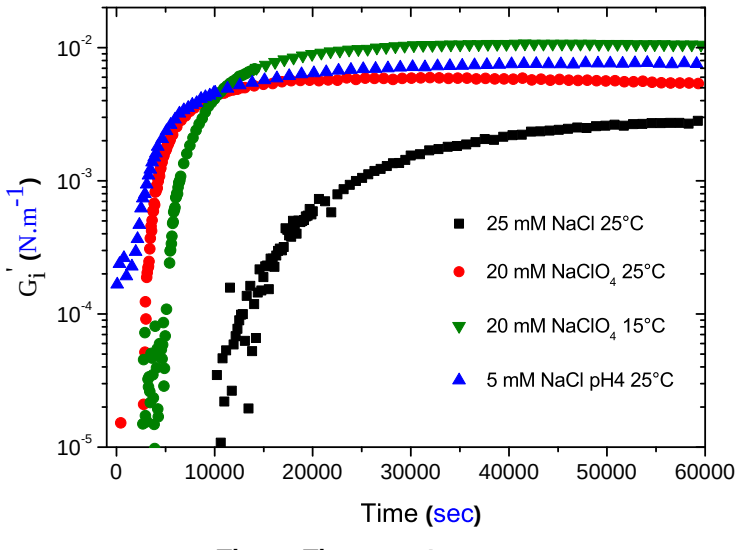

FIGURE 2.14: Time evolution of G_i' at dodecane/water interface with a subphase concentration of 1 mg.L^{-1} β-lg of various ionic conditions and temperature as mentioned. The corresponding dimer concentrations of the subphase can be found in Table 2.2. Corresponding G_i'' data can be found in figure A.4.

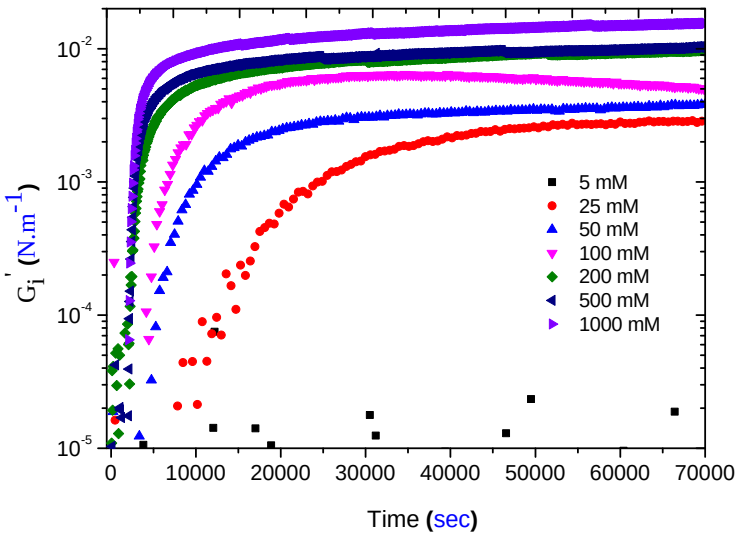

FIGURE 2.15: Time evolution of G_i' at dodecane/water interfaces with a subphase concentration of 1 mg.L^{-1} β-lg in various NaCl concentrations at pH 3. Corresponding G_i'' data can be found in figure A.5.

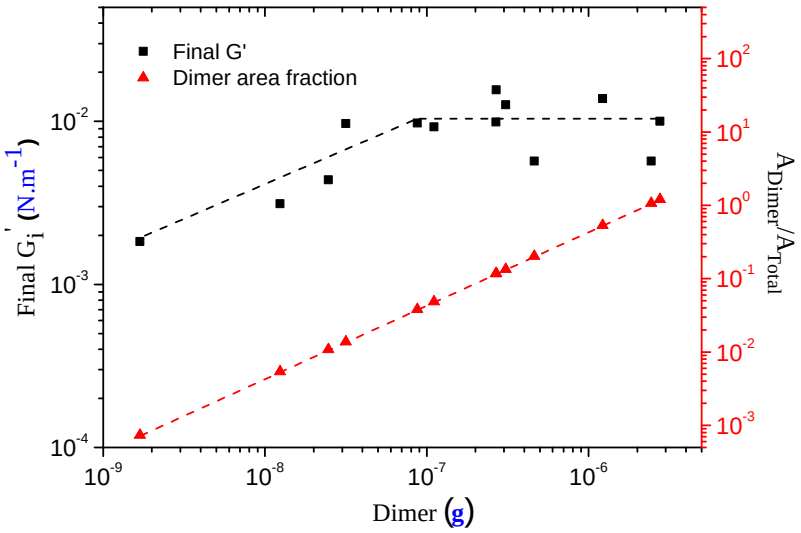

FIGURE 2.16: Final G_i' of dodecane/water interface at different β-lg dimer concentration. The right Y-axis denotes the corresponding calculated area fraction occupancy assuming complete dimer adsorption. The dotted line is to guide the eyes.

Fittingly, the solution at pH 3 and 5 mM NaCl, which is predominantly monomeric, failed to establish a viscoelastic network even after 20 hours.

These results establish that native β-lg dimers are the functional network forming units at the interface. In contrast, interfaces of predominantly monomeric solutions remained fluid-like. The G_i' followed a similar trend when various total protein concentrations were used at pH 3 and 50 mM NaCl as listed in table 2.2. When all these results are collapsed into a single graph as shown in figure 2.16, the correlation between dimer population (expressed as area fraction occupied by dimers) and the elastic strength is evident. In particular, a viscoelastic interface is observed even under unusually low area occupancy of 0.001 (pH 3, 25 mM NaCl). The implications of this will be elaborated in the discussion section.

Having established the distinct difference between rheological behaviors of β-lg monomers and dimers as seen in table 2.2, experiments monitoring their corresponding interfacial activities were undertaken. The evolution of the dynamic interfacial tension ($\gamma_{o/w}$) for protein solutions at various NaCl concentrations (C_{NaCl}) at a dodecane/water interface is shown in a semi-log plot in figure 2.17. After a brief lag

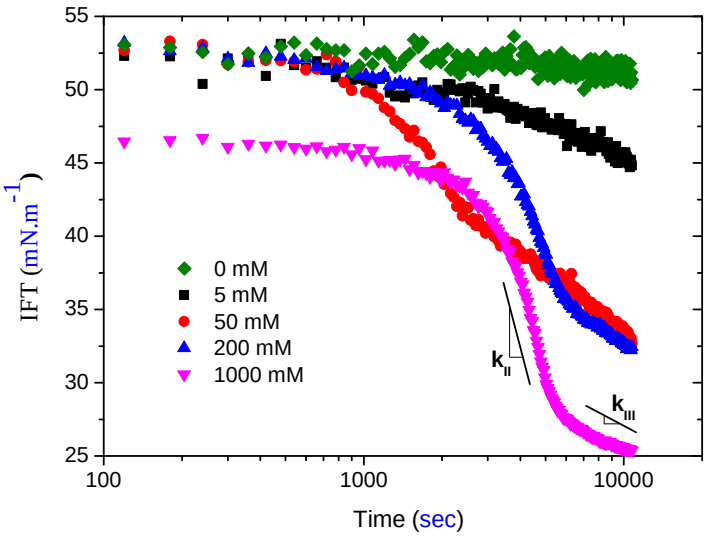

FIGURE 2.17: Time evolution of $\gamma_{o/w}$ (IFT) of dodecane pendant drop immersed in 1 mg.L^{-1} β-lg solution in various NaCl concentrations at pH 3. $k_{||}$ and $k_{|||}$ represent fitted slope values for second and third stage of the adsorption respectively.

period, diffusive β-lg molecules reduce $\gamma_{o/w}$ in two distinct stages indicating two different contributing processes. A steep drop in $\gamma_{o/w}$ with a slope of $k_{||}$ indicates the rate of protein adsorption leading to monolayer formation. Naturally, higher concentration of protein molecules leads to larger $k_{||}$ values. This stage is followed by $\gamma_{o/w}$ reduction at a much lower rate with a slope of $k_{|||}$, indicating a secondary process post-adsorption. Gelation due to post-adsorptional structural changes has previously been associated with $k_{|||}$ values for other protein solutions.[108] The substantial reduction in the initial $\gamma_{o/w}$ of 1 M NaCl solution due to the high salt concentration has also been observed elsewhere.[109]

TABLE 2.2: Interfacial properties of β-lg at dodecane/water interface at different solution conditions.

pH	C_{NaCl}(mM)	M_{Dimer} (g)	t_{lag} (s)	Final G_i' (mN/m)	$\gamma_{o/w}$ (mN/m)	k_{II} (mN/mlog(s))	k_{III} (mN/mlog(s))
3	5	$1.74\pm0.95\times10^{-10}$	-	-	44.1±0.64	-15.2±3.3	-
3	25	$1.69\pm0.35\times10^{-9}$	14216.8±2772	1.83±0.1	34.1±0.6	-18.1±3.6	-10.1±0.6
3	50	$1.24\pm0.37\times10^{-8}$	4526.±741	3.12±0.3	29.9±1.3	-28.6±4	-12.4±1.5
3	100	$2.47\pm0.26\times10^{-8}$	4120±44.5	4.37±0.12	28.4±2.1	-32.1±1	-14.2±2.5
3	200	$8.75\pm0.15\times10^{-8}$	2264.5±32	9.76±0.32	26.9±1.9	-41.9±1	-10.8±1
3	500	$2.68\pm0.23\times10^{-7}$	2264.7±57	9.91±0.29	26.3±1.2	-57.9±4.5	-7.9±0.8
3	1000	$2.693\pm0.53\times10^{-7}$	2138.7±13	15.6±0.4	25±1.4	-62.4±2.4	-8.7±1
3	50	$1.11\pm0.33\times10^{-7}$	1887.18±47	9.24±0.47	-	-	-
3	50	$3.08\pm0.91\times10^{-7}$	880.76±23	12.6±2.1	-	-	-
3	50	$1.22\pm0.36\times10^{-6}$	0	13.8±0.5	-	-	-
3	20*	$4.62\pm1.5\times10^{-7}$	3082.8±33	5.8±0.17	28.8±0.6	-39.6±0.4	-6.7±0.1
3	20**	$2.76\pm0.76\times10^{-6}$	5095.5±29	10.1±0.6	-	-	-
4	5	$1.8\pm0.1\times10^{-6}$	2704.8±19	8.6±0.54	36.9±0.5	-32.1±0.05	-6.4±2.1

* $NaClO_4$ was used at 25°C ** $NaClO_4$ was used at 15°C

The final $\gamma_{o/w}$ is lower at higher NaCl concentrations as seen in figure 2.17. Any effects arising out of the electrostatic nature of salt will be correlated to the Debye length in solution which in turn is proportional to the $\sqrt{C_{NaCl}}$. $k_{||}$ values are clearly correlated with $C_{NaCl}^{0.5}$ as shown in figure 2.18. Dampening of electrostatic repulsion at higher ionic strength enables denser packing of protein molecules. Such electrostatic effects are also observed at extreme pHs where β-lg carries a greater net charge. However, the $k_{||}$ value almost doubled when the experiment was carried out with $NaClO_4$ as seen in figure 2.19 suggesting the native dimer's involvement in $\gamma_{o/w}$ reduction in addition to electrostatics. $k_{|||}$ values on the contrary did not have any correlation with salt concentration as seen in figure 2.18. Since post-adsorptional changes in the oil phase are not affected by the aqueous phase ionic strength, salt concentration did not affect the $k_{|||}$ values greatly.

β-lg solution at pH 3 (5 mM NaCl) did not show any slope change of $\gamma_{o/w}$ with time as seen from figure 2.17 and hence no $k_{|||}$ value is reported. In conjunction with rheology measurements, the results show that β-lg dimers play the crucial role in this gelation phase of adsorption confirming their network forming tendency. Interestingly, the overall reduction in the $\gamma_{o/w}$ by monomers at pH3 and 0 mM NaCl was minimal, with the value itself indistinguishable from that of a pristine buffer/dodecane interface as shown in figure 2.20. Similar values were also observed under alkaline conditions of pH 10 that favour monomer formation (figure 2.20). Despite electrostatic repulsion between monomers, there should be a considerable number of protein molecules adsorbed at the interface. This questions the amphiphilic nature of β-lg monomers and suggests a barrier to adsorption at the interface since no influence on $\gamma_{o/w}$ is observed. The lack of $\gamma_{o/w}$ reduction might also be a direct consequence of lesser number of contact points at the oil/water interface.

2.5.7 Nature of β-lg Interfacial Films

To understand the nature of β-lg films formed at oil/water interfaces, frequency sweeps were performed subsequent to the time sweep measurements as shown in figure 2.21. Interfaces of β-lg solutions with high dimer surface concentration (pH 4, 5 mM NaCl) and low dimer surface concentration (pH 3, 25 mM NaCl) both exhibited a gel-like

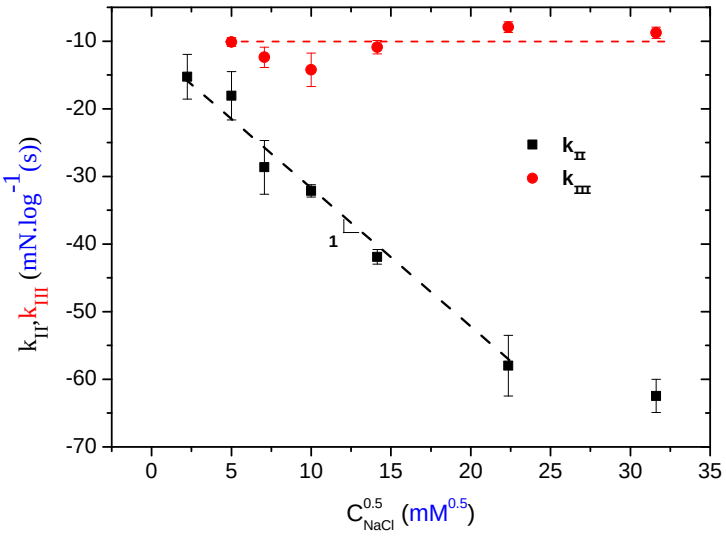

FIGURE 2.18: Slope values of $k_{||}$ and $k_{|||}$ derived from interfacial tension measurements plotted against the square root of salt concentration of the corresponding protein solutions. The dotted lines indicates a slope of 1 (black) and 0 (red).

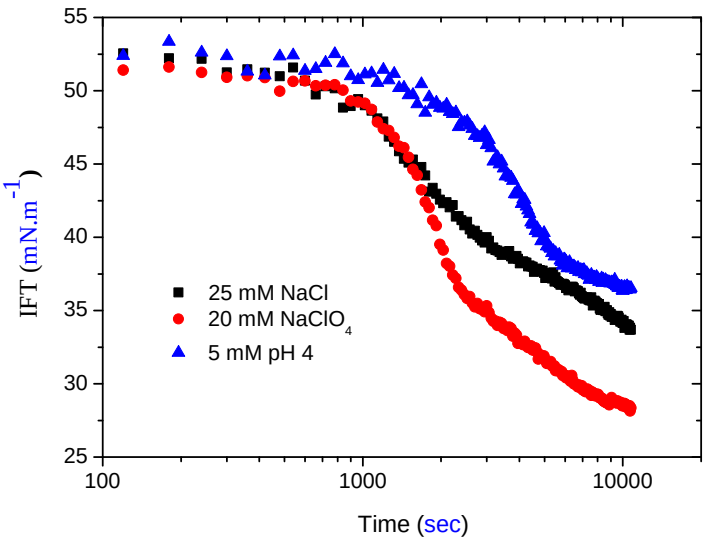

FIGURE 2.19: Time evolution of $\gamma_{o/w}$ (IFT) of dodecane pendant drop immersed in 1 mg.L^{-1} β-lg solution at various ionic conditions.

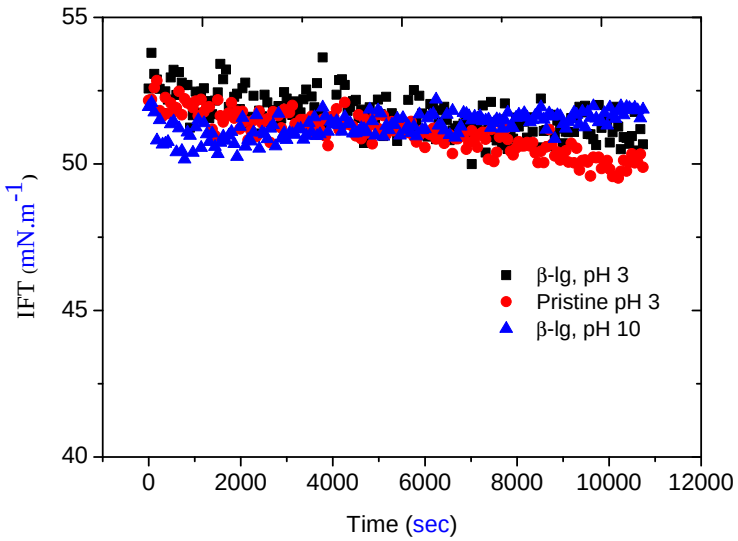

FIGURE 2.20: Time evolution of $\gamma_{o/w}$ (IFT) of dodecane pendant drops immersed in 1 mg.L^{-1} β-lg solution and pristine buffers with 0 mM NaCl.

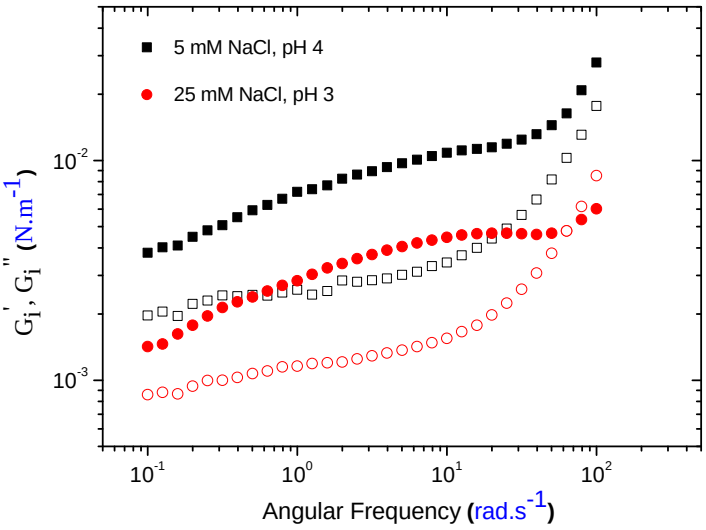

FIGURE 2.21: G_i' (solid) and G_i'' (hollow) from frequency sweeps with β-lg solutions (1 mg.L^{-1}) at dodecane/water interface with low (red) and high (black) dimer fractions.

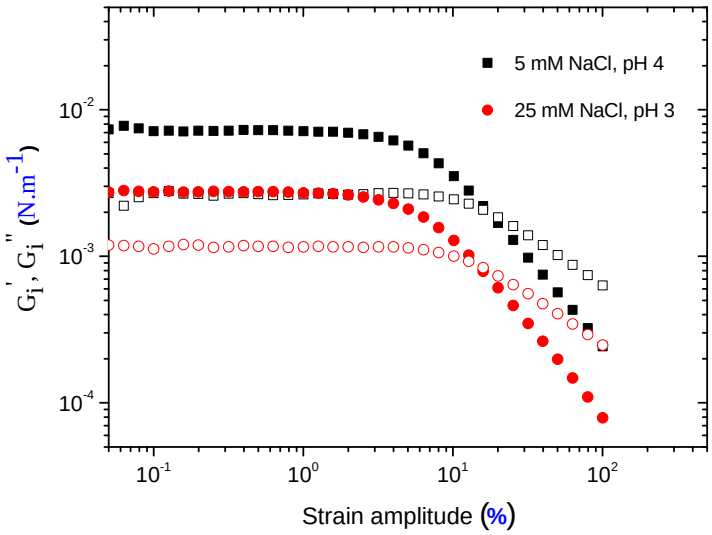

FIGURE 2.22: G_i' (solid) and G_i'' (hollow) from strain amplitude sweeps with β-lg solutions (1 mg.L^{-1}) at dodecane/water interface with low (red) and high (black) dimer fractions.

nature with $G_i' \gg G_i''$ with a weak frequency dependence, similar to the plateau region of a typical polymer melt. At very high frequencies (> 50 rad.s^{-1}), G_i' and G_i'' begins to strongly depend on the frequency, suggesting the interfacial network is at the onset of soft-glassy transition regime. To understand the interfacial network's behavior at large strain amplitudes, strain amplitude sweeps were performed as shown in figure 2.22. The cross over of G_i' and G_i'' which reflects the yielding of the network occurs at higher strain amplitudes for interfaces with higher dimer concentrations. The moduli decreases at higher oscillatory strain amplitudes depicting a typical shear thinning behavior for a polymer solution.[110] This can be explained by the alignment of the polymer chains along the shearing direction at higher strain rates thereby reducing the local viscous drag leading to lower moduli values.

2.5.8 Kinetics of β-lg Network Assembly

To understand the kinetic nature of β-lg assembly at the interface, measurements were performed by injecting 50 mM NaCl into the subphase of a pre-formed protein layer at pH 3. Initially, the NaCl concentration was zero and no appreciable G_i' was observed in the monomeric dominated interface for the first 20 hours as shown in figure 2.23A.

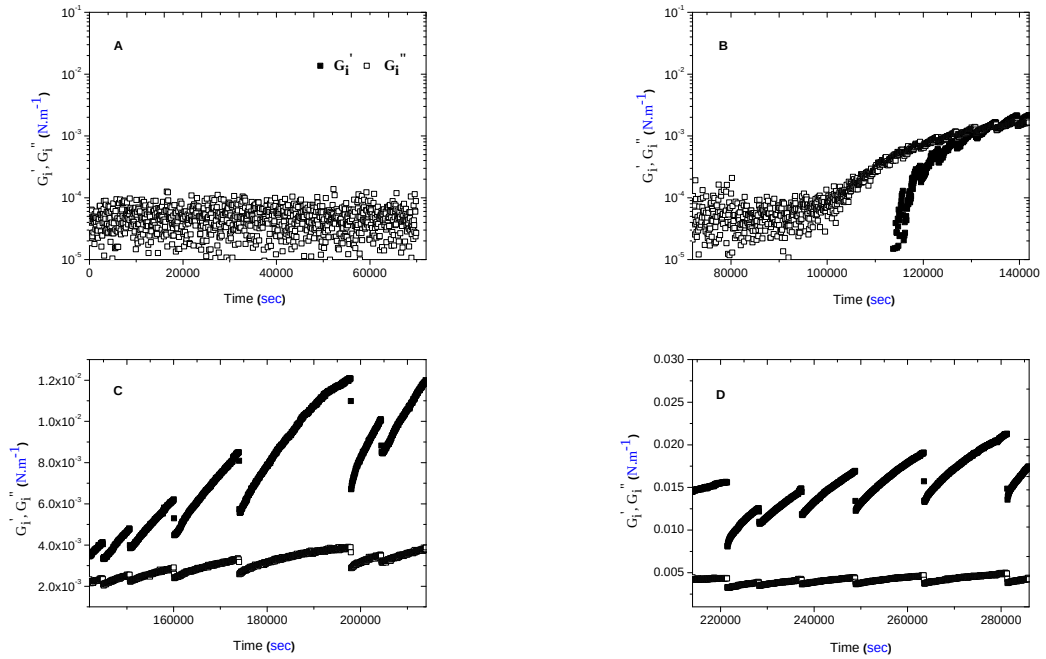

FIGURE 2.23: Time evolution of G_i' at dodecane/water interface with a subphase concentration of 1 mg.L^{-1} β-lg in pH 3 before (A) and after (B, C, D) the injection of 50 mM NaCl.

Subsequently, 50 mM NaCl was injected at a rate of 83 nL.s^{-1} using microfluidic syringe pumps while simultaneously withdrawing in order to maintain the volume of the subphase. Complete injection of NaCl was completed in 10 minutes and the evolution of the interfacial strength for the next 72 hours is shown in figure 2.23B, C and D. As expected, NaCl promotes strengthening of the interface through dimerization and reducing the Debye length. This strengthening of the interface further shows that dimerization of β-lg monomers is possible even at oil/water interfaces. Evidently, G_i' is not built up in a monotonous increase as one might have expected. Instead, the network undergoes abrupt breaking events leading to a drastic fall in G_i' and G_i''. This is followed by the gradual recovery to a higher G_i' and G_i''. It is also worth noting that the rise and fall in G_i' is much larger than that occurring in the G_i'' indicating that the pertaining events are more to do with the elastic nature of the interface.

To further check the consistency of this experiment and to verify if the observed kinetics is an artifact due to for example, microfluidic set up, the interface was observed at the same protein concentration and salt concentration as the previous experiment but a higher temperature of 40° C as shown in figure 2.24. A higher temperature

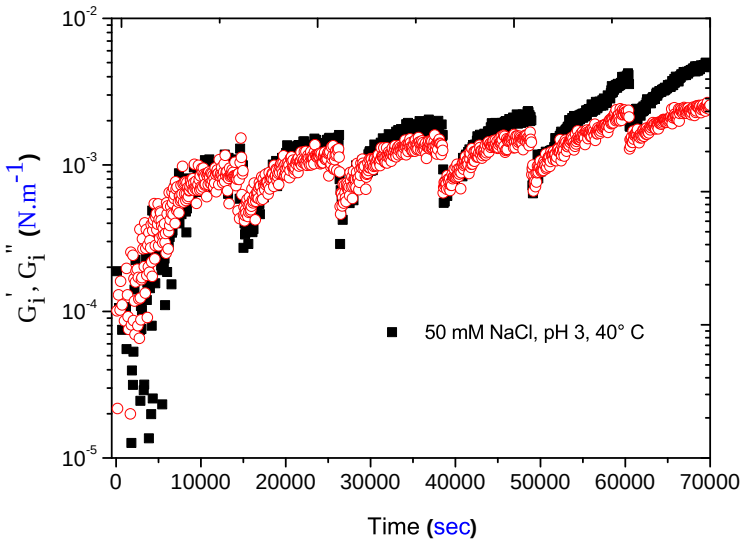

FIGURE 2.24: Time evolution of G_i' (solid) and G_i'' (hollow) at dodecane/water interface with a subphase concentration of 1 mg.L^{-1} β-lg in pH 3, 15 mM NaCl at a temperature of 40° C.

is expected to hasten the kinetics and thereby amplify the structure building mechanisms, if any. The measurements include drastic events where G_i' and G_i'' abruptly reduces and gradually builds up to a higher value akin to breaking and remaking. This suggests that the previous result with salt addition is not completely due to the microfluidic set up. However, possible sources of effects such as convection induced by air-conditioning or other mechanical sources were investigated and eliminated to the best of our knowledge. The experiments performed at higher temperature and the consistency of these events suggests that β-lg interfacial network formation is a non-equilibrium process in which internally built up stresses are continually redistributed.

Diffusive protein molecules from the solution should adsorb at random positions at the interface. This implies local concentration gradients might lead to molecules cross-linking in patches. It is possible that such a heterogeneous way of construction leads to local lateral stresses causing local fractures in the network during assembly. Such events might expose portions of the pristine interface where protein again adsorbs and rebuilds the film. The moduli values keep building up indefinitely over 72 hours as seen from figure 2.23. Such kinetics involving perpetual breaking and rebuilding as the network forms has not been measured before at the interface to the

knowledge of the author. Interestingly, other parameters such as oil polarity which could also contribute to interfacial stresses have been shown to play in role in β-lg interfacial network formation.[94]

2.5.9 Discussion

The results presented demonstrate that the interfacial properties achieved with β-lg can be adjusted by changing the bulk concentration of native dimer species. The dimer population plays a crucial role in $\gamma_{o/w}$ reduction and imparting elasticity to the network. On the contrary, β-lg monomers by themselves neither form viscoelastic networks nor reduce $\gamma_{o/w}$ appreciably. Unlike mobile surfactants which prevent coalescence between emulsion droplets mainly through Marangoni effects, protein molecules shield emulsion droplets against coalescence by forming a strong, elastic interfacial network. Hence, the ability to form a viscoelastic network at oil/water interfaces is quintessential in its application as an emulsifier. In industrial applications, most studies use high concentrations or high ionic strength. Consequently, surplus dimers easily achieve monolayer saturation. Nevertheless, weak interfaces of β-lg has been observed in monomer dominated conditions at low concentrations.[61]

The interfacial tension measurements showed two stages of adsorption, the first stage was correlated to the ionic strength while the second stage was not. This lack of correlation with the Debye length indicates that the second stage happens in the oil phase, presumably protein structural rearrangement. Neutron reflectivity and synchrotron measurements have shown significant rearrangements of adsorbed protein at air/water interfaces.[111,93] Disulfide bonds (S-S) between cysteine residues constitute a pivotal part of the architecture of globular proteins. These covalent bonds not only preserve the folded structure of a β-lg monomer but can also interlink two monomers to form a non-native dimer.[112] The free thiol group in native β-lg monomers is not exposed and therefore does not aggregate in the solution. When β-lg exposes its hydrophobic residues at the interface, interconnection propagates through disulfide bridging between free thiol groups at cys121. Similar exposure of β-lg's hydrophobic residues through denaturation in the bulk typically leads to 3-dimensional non-native aggregates.[113,114] However, protein aggregation at interfaces is confined to a 2-dimensional plane leading to the formation of long, linear non-native aggregates

through the formation of disulphide linked dimers. Dickinson and Matsumura observed such polymerization on emulsion droplets.[115] They further showed that inhibiting the free sulphur in cys121 hinders the formation of higher oligomers at an oil/water interface through such interlinking. Other studies also corroborate such cross-linking.[116] It has been observed however that the addition of a disulfide bond reducing agent such as dithiothreitol in the aqueous phase does not reduce the interfacial properties of β-lg indicating that the disulfide bridging is happening in the oil phase as one would expect.[94]

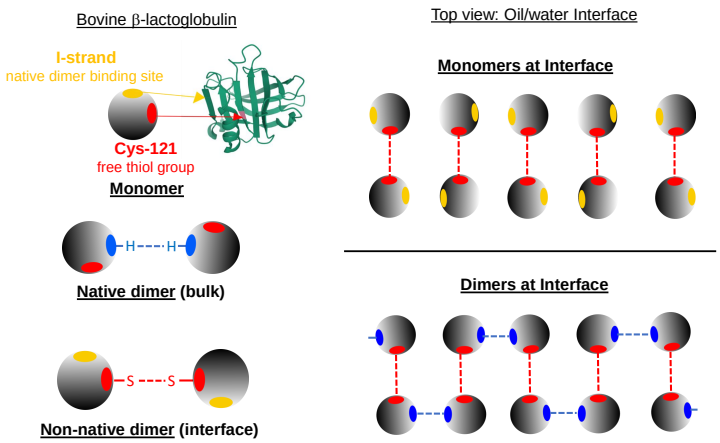

FIGURE 2.25: The image depicts native and non-native dimers of bovine β-lg monomer (left). The red dots indicate the free thiol group in cys121 and blue dots indicate the dimerization site. When monomers reach the oil/water interface (top right) discrete non-native dimers are formed through disulfide bonds (red). Dimerization connects monomers through hydrogen bonds (blue) cross-linking the molecules to form a continuous network.

Cross-linking has been shown to impart elasticity for various other polymers, most notably, rubber.[117] The decrease in protein chain mobility due to cross-linking causes external load to be applied on the chemical bonds connecting them. The rigid, cross-linked and non-flowing network is therefore capable of storing the applied stress which can later be recovered as signified by the G_i' values observed. In fact, it has been shown that cross-linking of β-lg films using glutaraldehyde imparts stiffness.[118] In this way, the capability of native β-lg dimers to form interconnected elastic networks can be understood based on the schematic shown in figure 2.25. When β-lg monomers

reach the interface they form discrete non-native dimers through disulfide bonds between cys121 (red dots). This arrangement lacks the required inter-connectivity to form a percolated network. Dimerization establishes supplemental links to the disulfide bonds creating extended networks and forming a strong elastic film. A threshold concentration of dimers is needed to form a large enough network to reach the sensitivity limits of rheometer. From table 2.2, $\sim$ 530 ng.m^{-2} of dimer (which covers roughly $1/1000^{th}$ of available interface) is seemingly sufficient for the rheometer to sense a network. These low values indicate a network made of high aspect ratio fibrils. In fact, long fibrils has been observed after thermal denaturation of β-lg rich whey protein below a pH of 3.5.[119] However, further experiments are needed to visualize such high aspect ratio fibrils at the interface.

The results from this study have shown that the elastic strength of interface is dictated by the quaternary structure of β-lg. Remarkably, another protein that exhibits analogous functionality owing to its quaternary structure and cysteine motifs is the biofilm surface layer protein-A (BslA) from *Bacillus subtilis*.[120] Monomers of this bacterial protein contain a hydrophobic cap which opens up at the interface similar to that of β-lg. BslA also has two free thiol groups that associate in solution to form dimers and tetramers. These higher oligomers have been shown to impart hydrophobicity while the monomeric BslA dictates biofilm architecture thus establishing bi-functionality through dimerization.[120,121] Besides, oligomerization and quaternary structure play a major role in the functionality of many secondary transport proteins.[122] These noteworthy similarities in the structural toggles and their subsequent functionalities suggests a potential interfacial role in the biological functions of β-lg.

2.6 Conclusion

Globular proteins such as β-lg are multi-functional with many levers available to modify their function through changes in the external environment through their responses to changing pH, temperature and some of the ion-specific behaviors.[123,100] The importance of the protein structure prior to adsorption on its subsequent interfacial properties has been demonstrated by thermal denaturation.[124] However, the relation

between β-lg self-association and its interfacial properties has not been characterized previously. In this study, we demonstrated that interfacial shear rheology can be employed to decode such quaternary structural dependencies of proteins provided the protein structural characterizations are available for the aqueous bulk conditions.

The interfacial shear rheology and complementary surface tension results presented in this chapter conclusively demonstrated a relationship between β-lg quaternary structure and the protein film properties at oil/water interfaces. The final interfacial strength of the network was found to have a direct correlation with the concentration of β-lg dimers. On the contrary, β-lg monomers neither reduced the interfacial tension nor built an elastic interface. Dimerization of adsorbed β-lg monomers at oil/water interfaces further exemplified this contrasting behavior. The origin behind this behavior is proposed to be the availability of thiol groups that can form disulfide linkages and thereby interconnect to form a continuous percolating network. β-lg monomers with a lone thiol group can only connect to another single monomer while β-lg dimers with two available thiol groups are capable of cross-linking. Moreover, the interfacial tension reduction in monomeric solution was indistinguishable from that of the buffer solution and therefore explains the low foamability under monomeric conditions observed elsewhere.[125] This suggests a higher structural stability for β-lg monomers in the solution and there by lesser number of contact points at the oil/water interface

The kinetics of β-lg interfacial film formation was also quicker for solutions at higher dimer concentrations. The complementary interfacial tension measurements depicted a two-stage adsorption process after an initial lag period. While the rate of reduction in the first stage had a dependency with the dimer concentration, the slope of the second stage remained relatively independent. This led to the proposal that the latter stage is caused by protein conformational changes post-adsorption. Furthermore, the rheology results obtained through subphase injection suggested that β-lg interfacial film formation might be a non-equilibrium process with constant stress redistribution involving breaking and rebuilding of the film. Overall, the behavior of β-lg assemblies at oil/water interfaces strongly depend on its monomer-dimer equilibrium. This inference will be carried forward to understand the protein's behavior when an anionic polysaccharide is added to the solutions.

Chapter 3

Beta-Lactoglobulin/Polysaccharide Complexes at the Interface

3.1 Background

Fruit based health beverages are finding a niche in the market.[126,127,128] They are a concoction of carbohydrates, proteins, pigments, organic acids and other minerals. These products are formulated and processed with shelf stability as a key requirement. Understanding the interactions between the components will therefore be helpful in formulating food products and designing processing conditions. Interactions between the components, especially pectin (either from the fruit, or as the typical carbohydrate stabiliser used in dairy beverages) and proteins, control the stability of such products by preventing milk protein precipitation by the formation of protein-polysaccharide complexes.[129,130] A typical example in the food industry is the usage of pectin to stabilize against the aggregation of casein micelles in acidified milk drinks.[131] Such protein-polysaccharide complexes have found applications in food emulsification,[76] microencapsulation,[77,78] fat substitution,,[79] protein separation[80] and bioactive delivery.[81] Complex formation between oppositely charged β-lg and pectin in acidic conditions is typically driven by electrostatic interactions between the anionic polysaccharide and the positive domains on the protein.[132,133] Other factors that affect the interactions are the ratio of protein to polysaccharide and the aqueous conditions (pH, ionic strength and temperature).[134,129,135]

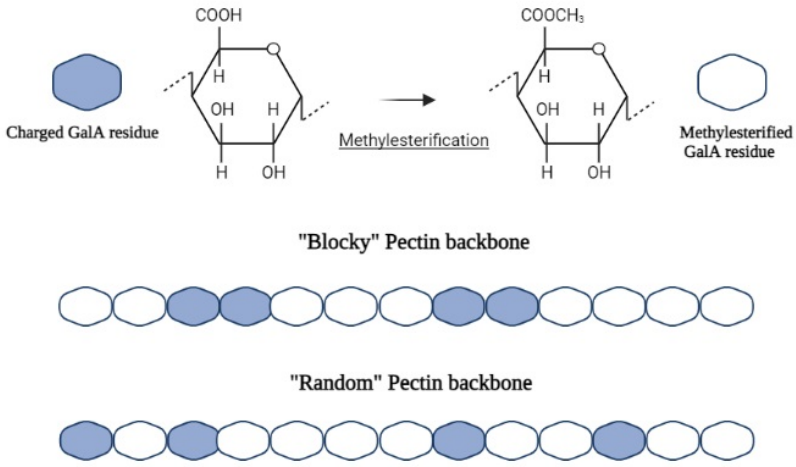

FIGURE 3.1: A schematic representing different pattern of charge distribution of pectin backbone.

3.2 β-lactoglobulin-Polysaccharide Interactions

When two polyelectrolytes carrying opposite charges encounter each other in conducive conditions, physical bonds form spontaneously.[136] It is relatively straightforward to assess the binding properties of homogeneous polyelectrolytes where the charged groups are uniformly distributed along the chain length using techniques like calorimetry. It has been shown that a critical chain length needs to be exceeded for such polyelectrolytes to complex.[137] With respect to pectin, it was found that an oligomer comprising of at least 7-8 GalA units is needed to complex with β-lg at pH 4.[138] When the charged residues are heterogeneously distributed along the chain, additional parameters such as the length and density of charged patches play a crucial role. The effects of such subtleties are feasible to study with β-lg/pectin complexes since adequate knowledge has been gained on tuning pectin's fine structures.[139] However, this heterogeneity leads to binding sites with different binding affinities and hence measurements such as binding isotherms assume an averaged character.[140]

Formation of β-lg/pectin complexes requires a minimum degree of charge density on the polysaccharide molecule corresponding to a DM of around 90 % at pH 4.[141] The complexation in acidic conditions is an exothermic process primarily driven by

the favorable electrostatic attraction.[136] While the enthalpic contribution dominates the drive for electrostatic association for a highly charged polysaccharides such as low-methyl esterified pectins (LMPs) of DM $<$ 40 %, considerable entropic contributions are also observed for highly methyl esterified pectins (HMPs) of DM $>$ 50 %.[140] The balance between the enthalpic and entropic contributions has been shown to depend on the local charge density of HMPs. Blocky HMPs (HMP_B) contain concentrated patches of negative charges (figure 3.1) driving the complexation primarily by the enthalpic contribution. This leads to the presence of some high-affinity binding sites on HMP_B similar to ones found in LMP. On the other hand, when the same amount of charges are more evenly spread on the polymer backbone such as in the case of random HMPs (HMP_R), less enthalpic contribution but a greater entropic contribution was observed. This higher entropic contribution has been suggested to arise as a consequence of the association of hydrophobic methyl esters of pectin molecules and the hydrophobic regions of β-lg resulting in the release of small counterions and water molecules from the surrounding solvation shells of the components.[140] At pH 4 and high ionic strengths (> 10 mM) shielding of electrostatic attraction decreases the enthalpic contribution. β-lg/HMP_R complexes was further reported to be more sensitive to ionic strengths.[140]

When β-lg is titrated into a pectin solution, a two-step binding process has been repeatedly observed through calorimetry.[136,139] The first step, occurring at low β-lg/pectin molar ratios, is driven by the change in enthalpy despite an unfavourable entropic change possibly due to surrendering of conformational freedom.[136] At higher β-lg/pectin molar ratios ($>$ 15), a second stage is observed with a diminished role of enthalpy and a favourable entropic contribution from the release of counterions and water molecules. Girard et al. (2003) interpreted the two steps as an initial formation of β-lg/pectin complexes as pectin molecules get decorated by protein, followed by their subsequent aggregation forming inter-complexes.[136] Later, Xu et al. (2018) measured a considerable loss in α-helix content of the protein upon binding to pectin.[139] Citing the similarity between these changes in secondary structure seen in the β-lg/pectin system to those observed in instances of β-lg/β-lg association, it was proposed that the complexed β-lg molecules could act as seeds for other β-lg molecules to bind on to them and form protein clusters. It was proposed that the

formation of β-lg rich clusters eventually leads to the generation of inter-complexes. SAXS and SANS experiments showed that the size of these β-lg rich clusters in complexes vary depending on the local charge distribution of the pectin.[139]

3.2.1 Interfacial Implications of β-lactoglobulin/Polysaccharide Complexation

As discussed in chapter 2, the structural rearrangement of β-lg plays a crucial role in its interfacial adsorption. Although the interfacial rheological properties can be modulated by controlling the solutions conditions, such manipulations are not always possible in applications such as food and drug delivery. Instead, it is much more convenient and elegant to choose the right polysaccharide to achieve the desired purpose for a given condition. Complexation with polysaccharides like acacia gum has been shown to alter the tertiary structure of β-lg.[142] Therefore, it is important to understand the implications of polysaccharide complexation from the perspective of the protein's natural destination, the interface. Aside from the structure of the polysaccharide, the rheological properties of interfacial films also depend on various other factors including the pH, ionic strength, temperature and nature of the hydrophobic phase.[143,56]

Although pectin by itself is not known to be surface active, a mixed solution of β-lg and pectin can exhibit enhanced or diminished surface properties as compared to a pure β-lg solution. Neutron reflectivity measurements show that the pectin resides beneath the protein interfacial film formed in such systems acting as a supporting scaffold to the adsorbed β-lg film.[45] LMP when complexed with β-lg was found to slow down the kinetics of surface pressure development by a factor of 100 as compared to the pure protein solution at air/water interfaces.[82] However, when LMP was added sequentially post-adsorption of the protein, the final interfacial strength was 5-6 times stronger than when it was added simultaneously. In contrast, equivalent systems with HMPs exhibited much shorter lag times for surface pressure buildup.[82] Interfacial shear rheology corroborated the importance of the order of addition of biomolecules in the case of LMP at oil/water interfaces.[45] These results were suggested to originate from the lack of surface activity of β-lg/LMP complexes. It was proposed that the association/dissociation step in the interfacial adsorption of protein from complexes is the critical step in determining the assembly of interfacial network.[82] Such

dependence on the charge densities of the polysaccharide has also been observed for β-lg/pullulan complexes.[144]

Although the dependence on the total charge density of the polysaccharide is evident, the above mentioned results leave behind a few outstanding questions.

- To begin with it is not clear how pectin is strengthening the interfacial films as it is not perceived to be present at the interface but rather just beneath it.
- Further, while the importance of order of addition for LMP is established it is yet to be seen if such dependencies are present for HMP.
- If the dissociation/association of β-lg complexes before interfacial adsorption plays the crucial role as suggested,[82] then what are the repercussions of the local charge density i.e. pattern of charges of the polysaccharide on adsorption kinetics?
- Amidst these factors, what role does the molecular weight of the polysaccharide play in the final structure of the interfacial assembly?

The answers to these questions will provide us with a better picture as to not only the role of polysaccharide's fine structures but also an insight into the mechanism of complexation itself. This understanding can unlock pathways into manipulating the polyelectrolyte complexes for desired applications by simply tuning the fine structures of the complexing partner.

3.3 Materials and Methods

3.3.1 Materials

High-methoxyl citrus pectins (DM$\sim$ 68%) with different local charge patterns,[145] blocky HMP_B and random HMP_R, of a molecular weight of 90-120 KDa were obtained form CP Kelco (Denmark). The different charge patterns were derived by de-esterifying highly methyl-esterified pectins using either plant pectin methylesterase (blocky) or fungal methylesterase (random).[146] Homogalacturanon (HG) having a molecular weight of around 20 KDa of DM ($\sim$ 60%) was produced by extracting short polygalacturonic acid sections from pectin followed by methylesterification using methyl iodide

(MeI).[147] Subsequently the highly methylesterified HG was demethylesterfied using alkali or pectin methylesterase as previously reported to the desired DM.[146] The oligosaccharide (Dp7) composed of 7-8 galacturonic acid (GalA) units was purchased from Elicityl (Crolles, France). Fresh stock solutions of 0.2 g.L^{-1} of β-lg and polysaccharides were prepared at pH 4.01 $\pm$ 0.02 using HCl and NaCl to a total ionic strength of 5 mM. The pH was verified after making the protein solutions. β-lg and polysaccharides were pre-mixed at various weight ratios with a fixed protein concentration of 1 mg.L^{-1} (1 nM) and rested for 1 hour for complexation before measurements unless specified otherwise. The corresponding molar quantities for the weight ratios used in the study are listed in Table 3.1.

The methodologies used for zeta potential, interfacial rheology and interfacial tension measurements are as described in section 2.3.2, 2.3.3 and 2.3.4 respectively.

TABLE 3.1: List of Protein:Polysaccharide weight ratios (W) of solutions used in this study along with their equivalent molar ratios (M) and the corresponding number of β-lg molecules per polysaccharide molecule (N) as calculated for dimeric β-lg

$W_{\beta-lg}$:W_{po}	$M_{\beta-lg}$:M_{pectin} (N)	$M_{\beta-lg}$:M_{HG} (N)	$M_{\beta-lg}$:M_{Dp7} (N)
1:0.125	1:0.04 (26)	1:0.23 (4)	1:3.4 (0.3)
1:0.25	1:0.08 (13)	1:0.46 (2)	1:6.8 (0.15)
1:0.5	1:0.16 (6.5)	1:0.92 (1)	-
1:1	1:0.32 (3.2)	1:1.8 (0.5)	-

3.3.2 Emulsion Preparation and Drop Size Measurement

Emulsions were prepared using a Fischer Scientific Powergen 125 mixer (MA, USA) operated at 16000 rpm for 5 minutes. The emulsions were prepared with 30% dodecane by volume with a total volume of 20 mL and a protein concentration of 0.1 g.L^{-1}. Measurements of particle sizes were made using a Malvern Mastersizer 3000 (Malvern Instruments, UK) with a flow rate of 100- 120 rpm. For measurements, the emulsion was inverted to mix uniformly and a small sample was taken from the middle. The samples were added to the measurement chamber filled with Milli-Q water, until the obscuration was in the reliable range. Each sample was measured three times and the uncertainty of the sizes reported were typically around $\pm$ 0.5 μm.

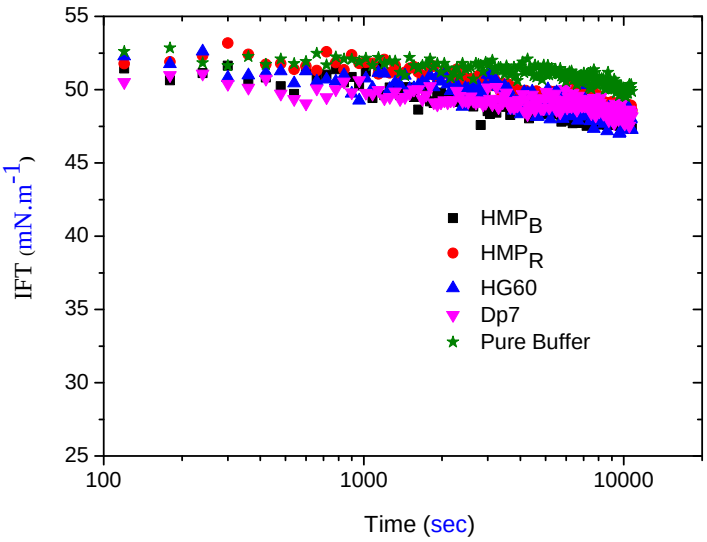

FIGURE 3.2: Dodecane/water interfacial tension (IFT) measurements of 1 mg.L^{-1} polysaccharide solutions at pH 4.

3.4 Results and discussion

3.4.1 Preliminary results

The protein is the interfacially active biomolecule in β-lg/pectin complexes. Pectins samples are not known to be surface active by themselves unless there are other impurities such as proteins present in the extracted sample. Nevertheless, the lack of surface activity of all the polysaccharides used in this study was verified using interfacial tension measurements of pure polysaccharide solutions as shown in the figure 3.2. No appreciable G_i' and G_i'' were observed even after 20 hours (data shown in appendix figure A.7). Since the polysaccharide molecules do not play any role in interfacial film formation by themselves, the interfacial results presented henceforth can be interpreted from the view point of protein adsorption.

The zeta potential values of 0.2 g.L^{-1} β-lg solutions and 0.1 g.L^{-1} HMP solutions at different pHs are presented in figure 3.3. The values show that, at pH 4, β-lg and HMPs are oppositely charged. When the biomolecules are mixed at pH 4, complexation happens almost instantly through electrostatic attraction between the positively charged residues of β-lg and the negatively charged carboxyl groups of pectin..[136,141]

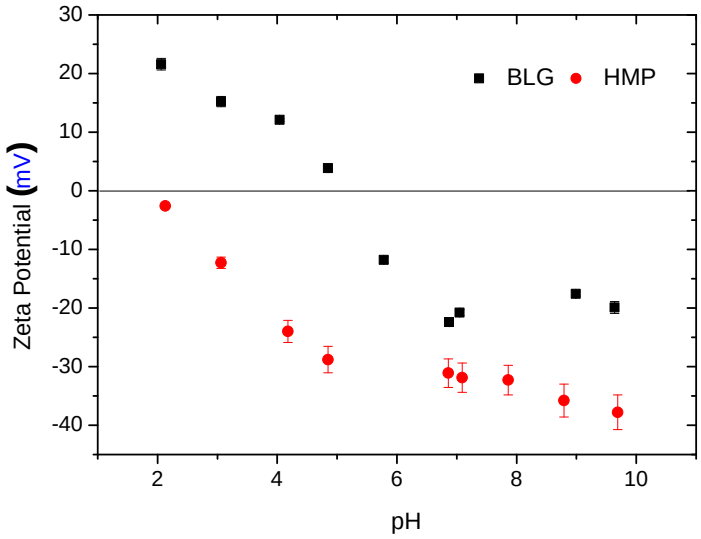

FIGURE 3.3: Zeta potentials of 0.2 g.L^{-1} β-lg and 0.1 HMP$_B$ g.L^{-1} solutions at various pHs and 5 mM NaCl

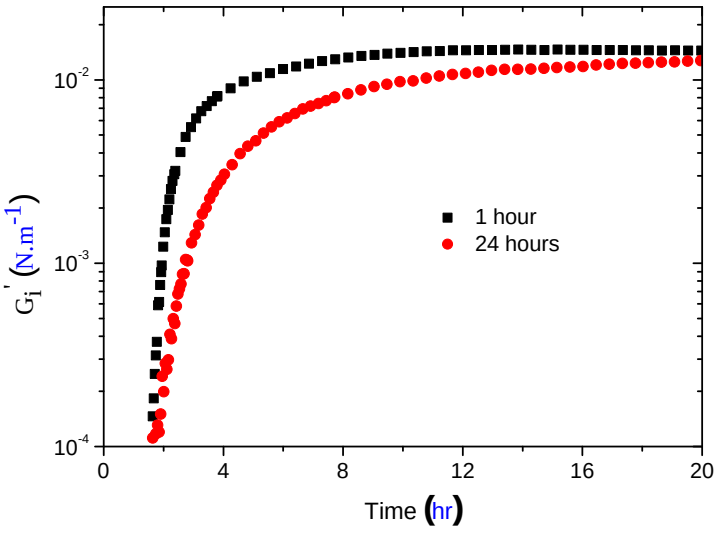

FIGURE 3.4: Time evolution of G_i' at dodecane/water interfaces of β-lg/HMP$_R$ mixtures at 1:0.125 weight ratios in pH 4 and 5mM ionic strength at different complexation durations.

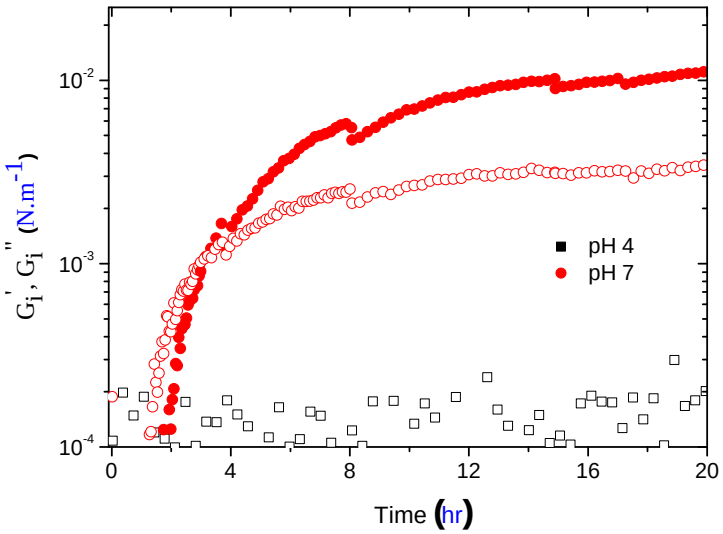

FIGURE 3.5: G_i' (solid) and G_i'' (open) from oscillatory amplitude sweeps of mixed solutions of β-lg/LMP mixtures at 1:0.5 weight ratio in pH 4 (squares) and pH 7 (circles) with 5mM ionic strength.

Similar to the measurements in chapter 2, the β-lg concentration used for the complexation studies was fixed at 1 mg.L^{-1} unless specified otherwise. Experiments were performed at different resting times and 1 hour was found to be sufficient for complete complexation. Calorimetric studies have shown that 800 seconds are suffice for complete complexation during titration.[141] Indeed, a resting time of 20 hours led to very similar finals values as seen in figure 3.4. The rest of this study was performed with a complexation duration of 1 hour.

3.4.2 Contrasting behaviors of LMP and HMP

To ascertain the electrostatic nature of the complexation, rheology measurements were performed at pH 4 and pH 7 where the protein exhibits a net positive and negative zeta potentials respectively. Transient interfacial rheology measurements of pre-mixed β-lg and LMP solutions at these pHs are presented in figure 3.5. The value at pH 7 is similar to that of pure β-lg solutions without pectin, indicating a lack of reinforcement. Although positively charged residues are present in β-lg at pH 7, the overwhelming negative charges seemingly prevents complexation. The lack of appreciable G_i'

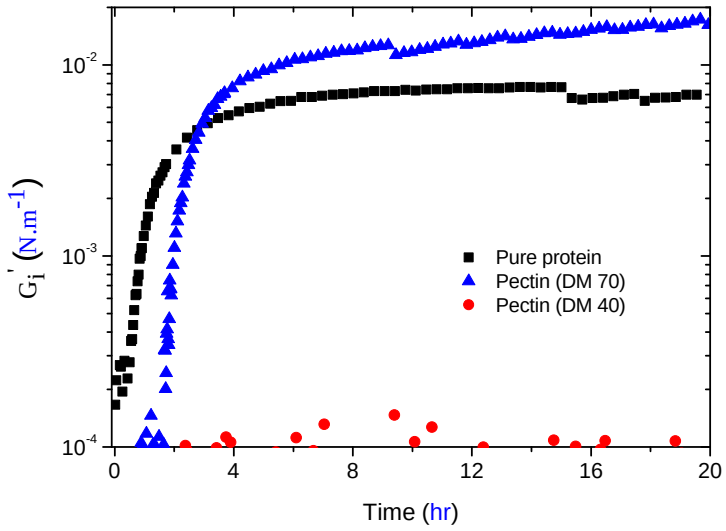

FIGURE 3.6: Time evolution of G_i' at dodecane/water interfaces of mixed solutions of β-lg/pectin with varying DMs of pectin in pH 4 and 5mM ionic strength. Corresponding G_i'' data can be found in figure A.8.

and G_i'' at pH 4 demonstrates complexation and the subsequent lack of surface activity of β-lg/LMP complexes in agreement with preceding results.[45] The origins of this lack of surface activity is not yet explicit. When LMP and HMP were complexed with β-lg the distinction between the behavior of both complexes manifests clearly at dodecane/water interfaces as shown in figure 3.6. β-lg/HMP complexes formed stronger interfaces as compared to that of pure protein solutions indicating the presence of soluble surface active complexes in complete contrast to that of β-lg/LMP complexes. This additional strength of the interface could only be attributed to the presence of HMP. It is possible that the complexed β-lg molecules could pack tighter due to the neutralization of effective net charge on complexing with pectin. In that case, however, similar behavior is expected for the β-lg/LMP. As alludied to earlier, the protein association/dissociation step during adsorption was proposed as the critical step in these contrasting behaviors.[82] During adsorption, β-lg molecules undergo structural rearrangements to reorient and expose their hydrophobic residues into the oil phase.[148] For a complexed β-lg molecule, this restructuring is presumably dictated by the nature and strength of binding between β-lg and the polysaccharide which in turn can be varied by changing the fine structures of the polysaccharide.

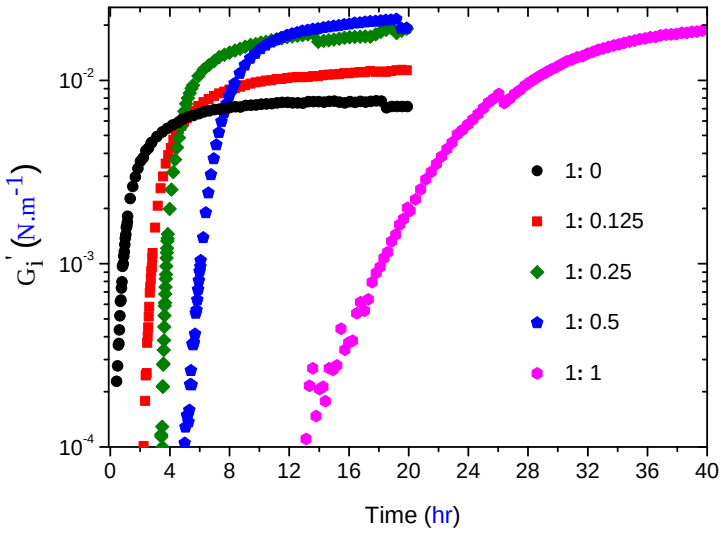

FIGURE 3.7: Time evolution of G_i' at dodecane/water interfaces of mixed solutions of β-lg/HMP$_B$ mixtures at various weight ratios in pH 4 and 5mM ionic strength. Corresponding G_i'' data can be found in figure A.9.

3.4.3 Lag time Conundrum

HMPs with two different charge patterns, namely, HMP$_B$ and HMP$_R$ were complexed with β-lg to investigate the effect of the pattern and proximity of negative charges on the pectin molecule. Transient interfacial rheology measurements of β-lg/HMP$_B$ and β-lg/HMP$_R$ pre-mixed solutions at different weight ratios are shown in figure 3.7 and figure 3.8 respectively. First and foremost, both HMPs managed to establish viscoelastic interfacial layers at all measured weight ratios. The evolution of the interfacial moduli follows the same trend displayed by the protein solutions discussed in chapter 2 with three distinct phases. Scattering studies of β-lg/pectin complexes have reported that the size of primary complexes reduces as the protein:polysaccharide molar ratio is decreased.[82,139] In other words, as the same amount of β-lg complexes with more pectin, the primary complexes become smaller as each pectin chain binds to fewer protein molecules. In other words, the size of the complexes should decrease in the order 1:0.125 > 1:0.25 > 1:0.5 > 1:1 for the weight ratios used in this study (Table 3.1). That being the case, for a fixed protein concentration, if diffusion plays the major role in determining the duration of lag phase then t_{lag} values should decrease as the concentration of polysaccharide increases. On the contrary, the t_{lag} values

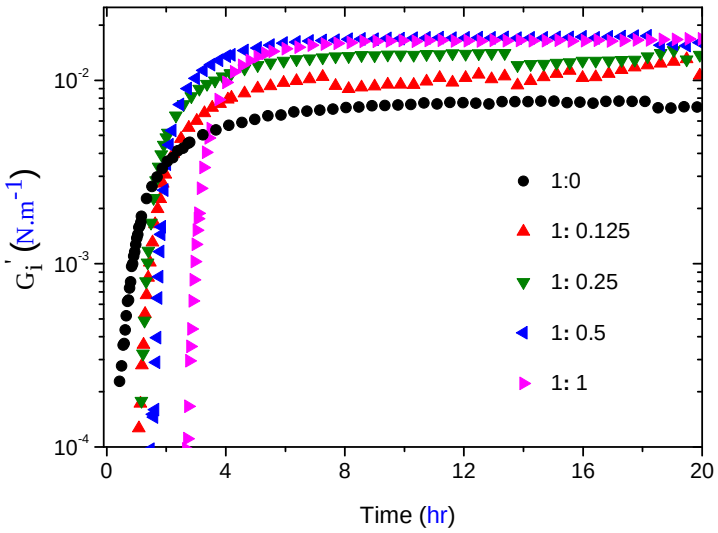

FIGURE 3.8: Time evolution of G_i' at dodecane/water interfaces of mixed solutions of β-lg/HMP_R mixtures at various weight ratios in pH 4 and 5mM ionic strength. Corresponding G_i'' data can be found in figure A.10.

monotonously increase with the polysaccharide concentration.

3.4.4 Binding Affinity Hypothesis

The t_{lag} values of β-lg/HMP_B complexes were consistently longer than that of β-lg/HMP_R. It was measured at pH 4.25 that HMP_B and HMP_R of similar charge density can complex 84 μmol and 82 μmol of β-lg per gram of pectin respectively.[149] These numbers roughly amounts to 1.5 g of β-lg per gram of pectin. This implies that in the 1:1 solutions nearly every β-lg molecule is complexed to a pectin molecule due to surplus binding sites. Accordingly there is a considerable increase in the t_{lag} value from 1:0.5 to 1:1 solutions as seen from figure 3.7 and figure 3.8. This substantial delay is the prima facie evidence that complexing with pectin delays the adsorption kinetics for β-lg. However, this also means in both HMP solutions the number of complexed and therefore uncomplexed β-lg molecules are almost similar. Although complexed β-lg molecules might exhibit a longer adsorption time, the lag time difference due to the charge pattern between HMP_B and HMP_R cannot be understood by a stoichiometric argument. The binding isotherms point out a noticeable difference in the affinity of the binding sites of HMPs. HMP_B has a few high affinity binding sites while none are

seen in case of HMP_R, consistent with the absence of blocks of negative charges. The ellipsoidal β-lg dimers have diameters of 6.9 nm and 3.6 nm on the major and minor side respectively. The length of a GalA unit containing one carboxylic group is around 0.435 nm. Therefore, for a β-lg molecule to completely bind along the minor axis requires at least 7-8 non-esterified GalA units.[138] Such patches are present in HMP_B but not in HMP_R. This high affinity of HMP_B binding sites for the protein means that the complex decoupling that is required for the protein to adsorb to the interface is delayed, which is reflected in the lag time.

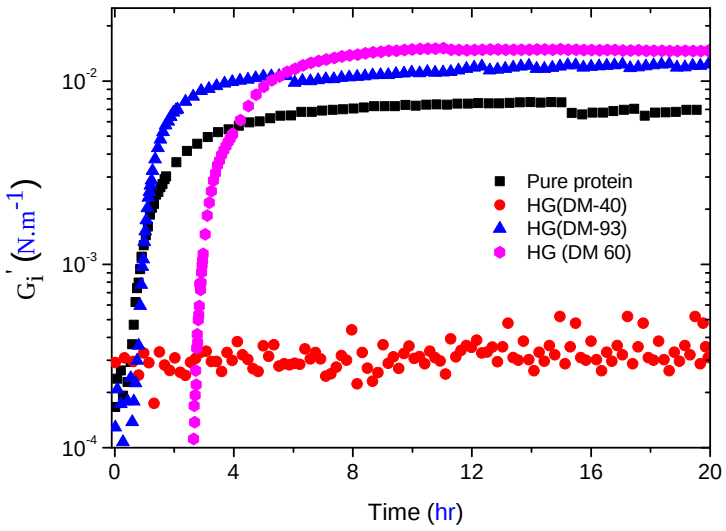

FIGURE 3.9: Time evolution of G_i' at dodecane/water interfaces of mixed solutions of β-lg/pectin with varying DMs of HG in pH 4 and 5mM ionic strength. Corresponding G_i'' data can be found in figure A.11.

3.4.5 Shorter Chain Polysaccharides

To further scrutinize this binding site argument, β-lg was complexed with smaller length pectic polysaccharides of HG and Dp7. When HGs of different DMs were complexed with β-lg, the highly charged HG-40 did not lead to surface active complexes and did not establish a viscoelastic layer as shown in figure 3.9 and consistent with previous works on LMP.[45] Interestingly, when β-lg was complexed with a HG of very low charge density (HG-93), an increase in final G_i' was still observed. This is in contrast to what was observed for a pectin with a similar charge density.[141] This could be

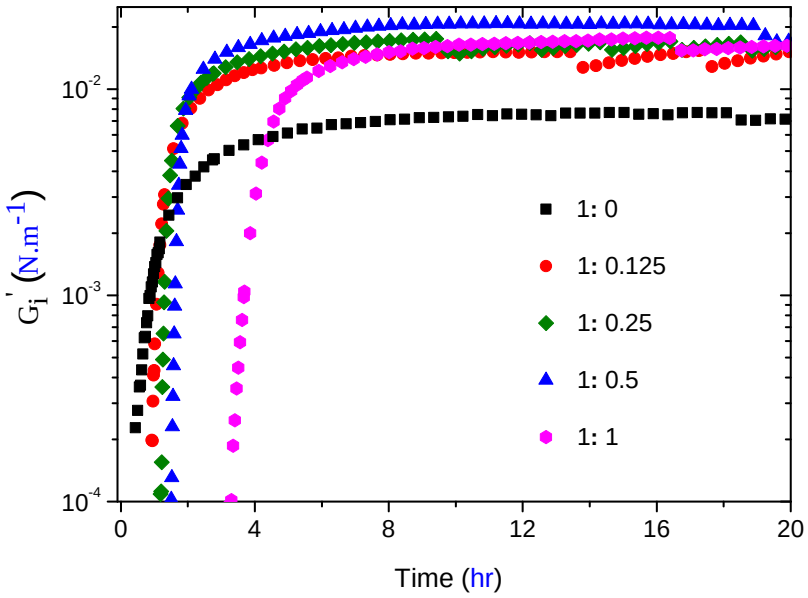

FIGURE 3.10: Time evolution of G_i' at dodecane/water interfaces of mixed solutions of β-lg/HG-60 mixtures at various weight ratios in pH 4 and 5mM ionic strength. Corresponding G_i'' data can be found in figure A.12.

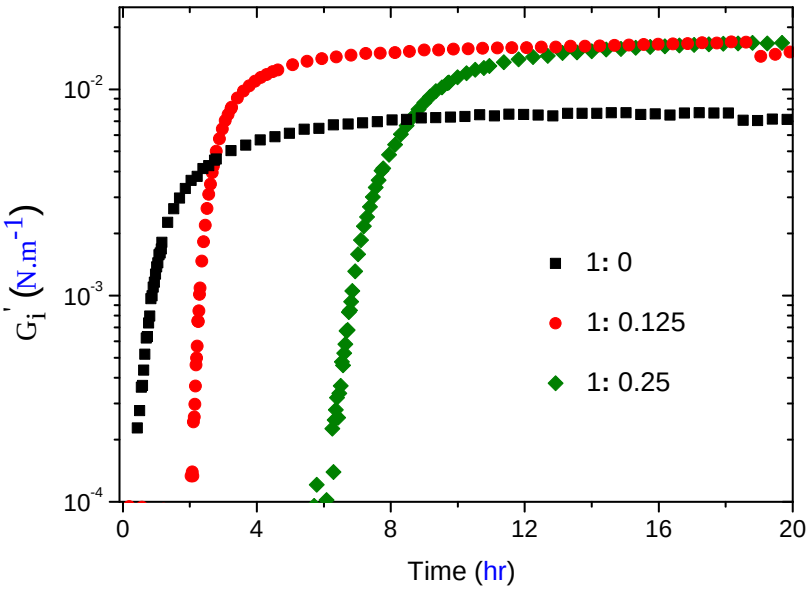

FIGURE 3.11: Time evolution of G_i' at dodecane/water interfaces of mixed solutions of β-lg/Dp7 mixtures at various weight ratios in pH 4 and 5mM ionic strength. Corresponding G_i'' data can be found in figure A.13.

due to the bulkier side chains of pectin that are not present in HG preventing access to its binding sites. Nevertheless, HG-60 is essentially HMP_R with a marginally smaller DM and chopped into roughly 5 shorter segments. If diffusion plays a crucial role in determining the lag times before which an interfacial layer forms, the smaller HG segments will have shorter t_{lag} values as compared to HMP_R. However, if the binding strength of the complexes dictate the timescale of protein escape to the interface then rates of interfacial layer formation for the HG-60 and HMP_R should be comparable. On the other hand, Dp7 is a segment of 7 or 8 charged GalA units, the smallest polymer of GalA that has been shown to complex with β-lg at pH 4. The transient rheological measurements of β-lg/HG-60 complexes and β-lg/Dp7 complexes are shown in figure 3.10 and figure 3.11 respectively. The final G_i' and t_{lag} values are compared in figure 3.12A and figure 3.12B respectively. Consistent with the binding affinity argument, t_{lag} values of the HG-60 system are comparable to those of HMP_R conclusively showing the minor role of diffusion in controlling the rate of viscoelastic interfacial layer formation. This implies that the structural rearrangement of β-lg plays the critical role in deciding the kinetics. This is further supported by the results from experiments with β-lg/Dp7 complexes which shows t_{lag} values even higher than that of HMP_B at the weight ratio of 1:0.25. This is once again consistent with the binding affinity hypothesis as Dp7 is completely charged and therefore binds with the protein strongly.

3.4.6 Adsorption Phase

Following the lag phase during which enough protein is still shackled in complexes with polysaccharide that the minimum elasticity for detection is not reached, the second phase of interfacial film formation is marked by sharp increase in G_i' values depicting more adsorption of proteins accompanied by their unfolding which leads to the strengthening of interfacial layer. As β-lg molecules accumulate at the interface, the ionic environment near the interface changes. In combination with the charge regulation mechanism around these polyelectrolytes, the interface could eventually reach different ionic conditions as compared to the bulk.[150] Therefore, the net charge of β-lg along with the interfacial charge regulation plays a critical role in the adsorption phase.[151] Complexation by electrostatic attraction not only induces a structural change in β-lg but also alters the effective charge carried by the protein.[152] This is

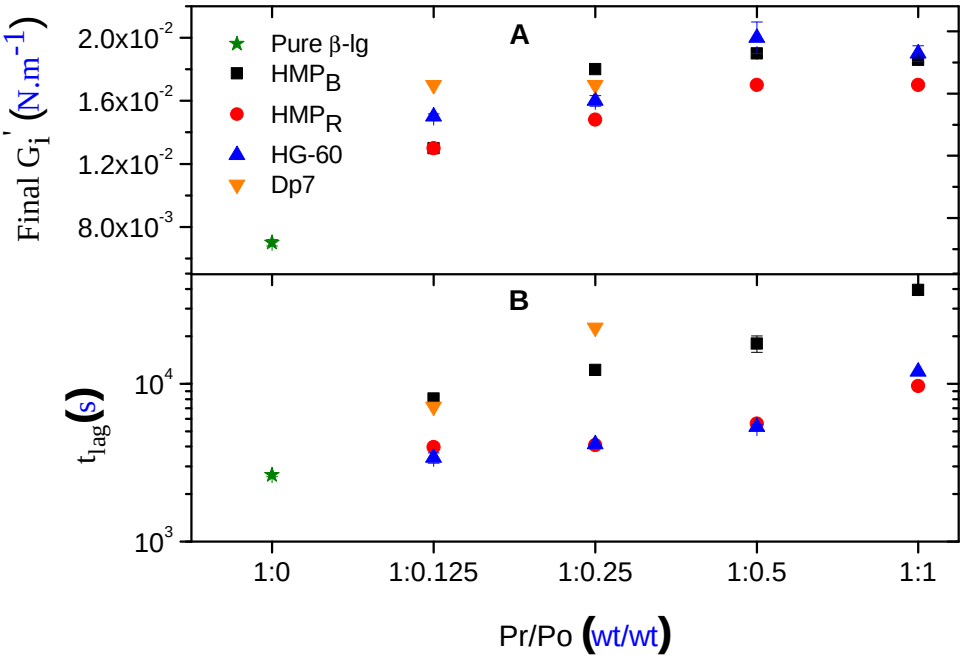

FIGURE 3.12: Final G_i' values (A) and lag time values (B) at different polysaccharide weight ratios for a fixed β-lg concentration of 1 mgL^{-1} at pH 4 and 5mM ionic strength.

supported by the dependence of β-lg adsorption on the charge density of the polysaccharide observed at other fluid/fluid interfaces.[144] The steeper rise in G_i' for mixed β-lg/polysaccharide solutions as compared to the pure β-lg is noticeable in figure 3.7 except for the 1:1 ratio. In addition, the steepness of the rise in G_i' increases at higher polysaccharide concentrations as observed in Fig.3.8. This could be a consequence of the decrease in net charge of biomolecules post-complexation leading to faster adsorption rates.[153,154,155] For 1:1 rations, the gradual rise in G_i' for HMP$_B$ as compared to the steeper rise in HMP$_R$ and HG-60 indicates a role of binding affinity. As mentioned earlier, the amount of complexed protein molecules should be similar for both pectins in this ratio and a drastic difference in rate of adsorption suggests a possible role of binding affinity. However, β-lg/Dp7 complexes do not exhibit these steep rises despite high binding affinity. This leaves behind the speculation that the slow adsorption rate for 1:1 HMP$_B$ could be due to a combination of binding affinity as well as side chain intervention in protein unfolding post-adsorption at the interface.

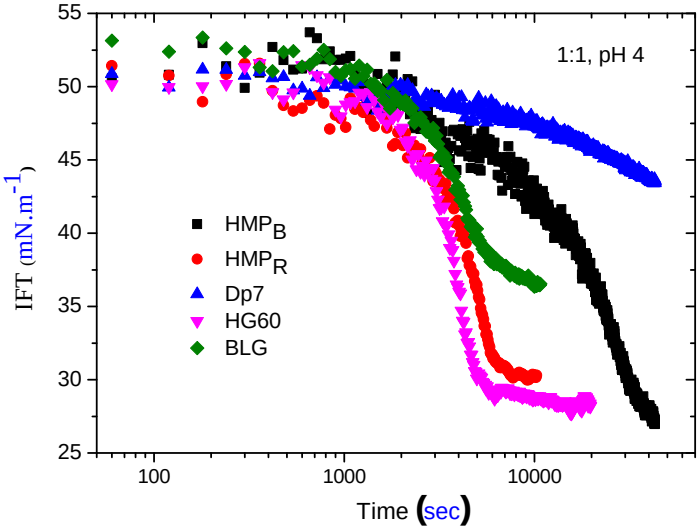

FIGURE 3.13: Dodecane/water interfacial tension (IFT) measurements of 1:1 pre-mixed β-lg/polysaccharide solutions at pH 4.

Monitoring the interfacial tension values provides us a complementary perspective as to the rate of adsorption of protein molecules. The time evolution of $\gamma_{o/w}$ values for various β-lg/polysaccharide solutions at 1:1 ratios are shown in figure 3.13. The 1:1 ratio was chosen since all the β-lg molecules have been shown to have complexed at this stoichiometry.[149] Hence, the adsorption kinetics will be a better reflection of the nature of β-lg/polysaccharide complexes containing information about the structure of complexed β-lg molecules. The rate of reduction in interfacial tension is in the order, pure β-lg $\sim$ β-lg/HG-60 $\sim$ β-lg/HMP$_R$ > β-lg/HMP$_B$ > β-lg/Dp7. This decrease in rate is in the increasing order of size of the contiguous patches of negative charges on the backbone of the complexing polysaccharide. This result once again points out that diffusion appears to be irrelevant in the rate of film formation. The slower reduction of surface tension in HMP$_B$ and Dp7 suggest a slower transfer of proteins to the interface in the most tightly bound complexes. The experiments using randomly charged HMP$_R$ and HG-60 exhibited similar rates of interfacial film formation to that of pure β-lg solutions albeit their final $\gamma_{o/w}$ was considerably lower. HMP$_B$ nearly took three times as long to reach the same $\gamma_{o/w}$ as that of HMP$_R$. These results point out that the local charge density of the binding site arising out of different charge patterns also plays a crucial role during the adsorption phase.

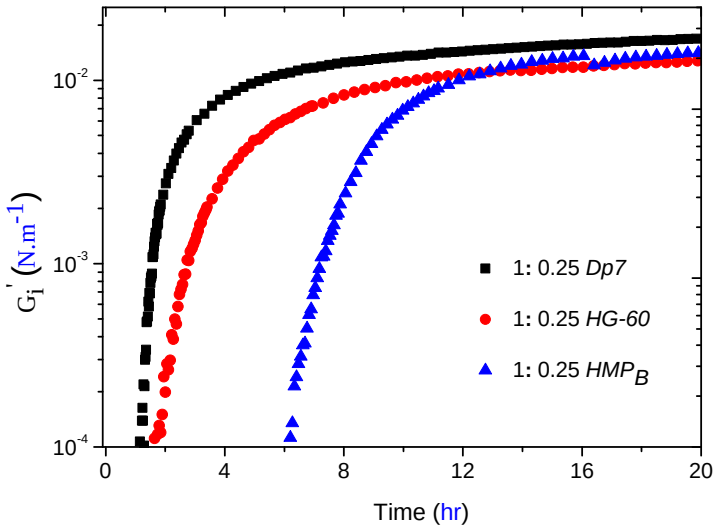

FIGURE 3.14: Time evolution of G_i' at dodecane/water interfaces of mixed solutions of β-lg and various polysaccharides at 1:0.25 weight ratio in pH 3 and 5mM ionic strength. Corresponding G_i'' data can be found in figure A.14.

3.4.7 Role of the Polysaccharide

As the G_i' value crescendos and ultimately enters the final phase of film formation, most of the protein molecules have adsorbed at the interface. The G_i' values almost reaches a plateau, although there is still a very slight increase in the strength of the network with time. All the mixed solutions of β-lg and polysaccharides show an improvement in the final G_i' after 20 hours as compared to the pure protein solution (Fig. 3.12A). Aside from the mixed solutions at 1:0.125, all other weight ratios roughly lead to similar G_i' values (15-20 mN.m^{-1}) irrespective of the length and the charge distribution of the polysaccharide. The Neutron scattering studies on the interfacial films formed by β-lg/LMP complexes have shown that the polysaccharides do not reside at the interface but rather just beneath it acting as a scaffold for the protein layer.[45] Therefore, it is entirely possible that a polysaccharide molecule strengthens the interface by simply cross-linking multiple adsorbed β-lg molecules through electrostatic binding.[156]

In our previous study on pure β-lg films at dodecane/water interfaces, we found that β-lg dimers at pH 4 form viscoelastic films while monomers at pH 3 were unable to form a film with any perceivable elasticity.[157] We attributed this to the inability

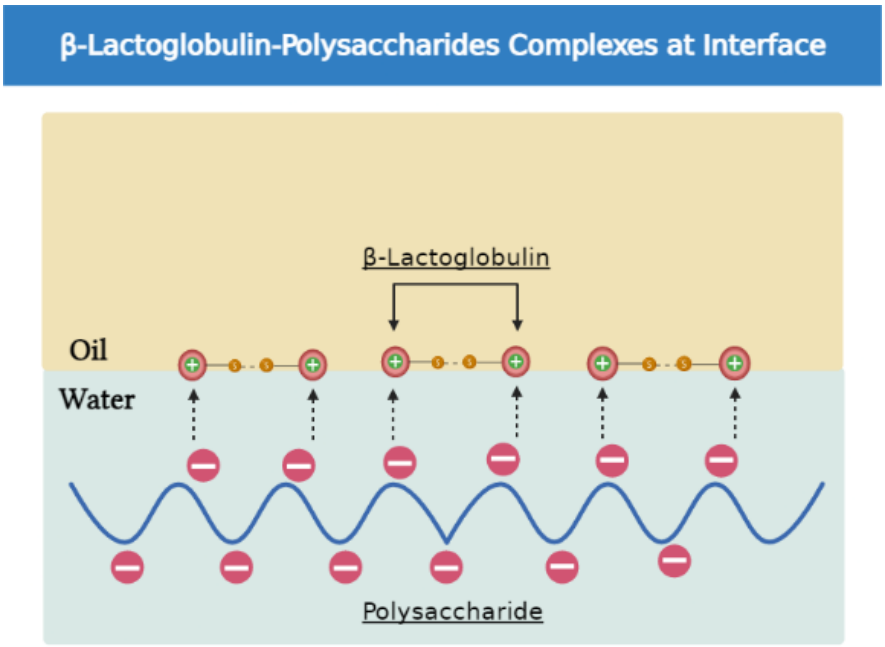

FIGURE 3.15: A schematic depiction of the possible mechanism by which a polysaccharide molecule could strengthen β-lg monomers at the interface by cross-linking.

of β-lg monomers to interconnect and form an extended, percolating interfacial network. Therefore, interfacial measurements were carried out using mixed solutions of β-lg monomers and polysaccharides at pH 3 (Fig. 3.14). Under these conditions, β-lg by itself cannot form a viscoelastic film at the concentration studied for the aforementioned reason.[157] Despite that, the solutions containing the polysaccharides gave rise to stable viscoelastic interfacial films. This result supports the notion that polysaccharide molecules reinforce the interface by concatenating adsorbed β-lg molecules and establishing interlinks beneath the interface as shown in Fig. 3.15. The successful formation of a viscoelastic film at pH 3 suggests that β-lg monomers do adsorb at the interface assuming polysaccharide complexation does not induce dimer formations in the bulk. More conclusive evidences will be provided through micrheology in the next chapter.

3.4.8 Post-adsorption β-lg Complexation

In the experiments discussed above, the polysaccharides investigated were complexed with the protein in the solution, prior to adsorption at the interface. The final G_i' values

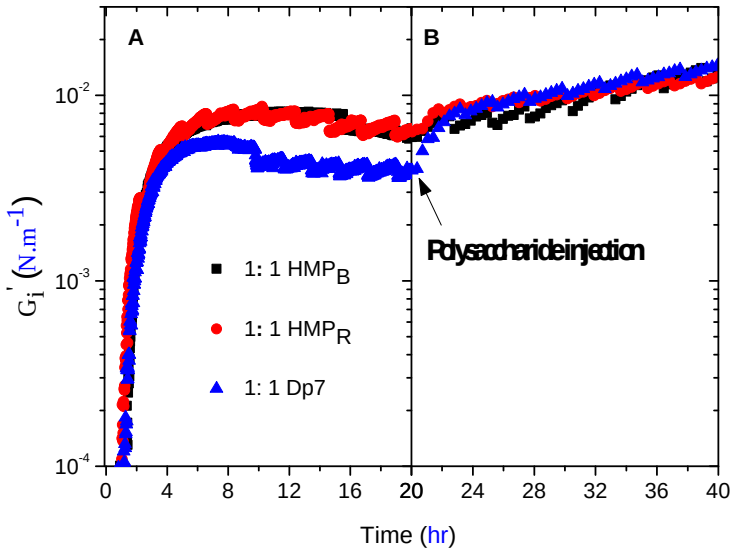

FIGURE 3.16: Time evolution of G_i' at dodecane/water interfaces of β-lg concentration of 1 mgL^{-1} at pH 4 and 5mM ionic strength (A) and after the injection of polysaccharide into the subphase (B). Corresponding G_i'' data can be found in figure A.15.

of these solutions were twice that of the pure β-lg solutions. Bertsch et al. (2019) observed a similar increase in the interfacial strength when LMP was sequentially added to a pre-formed β-lg layer.[45] However, when LMP was pre-mixed with the protein solution before protein adsorption, the interfacial strength was less than that of the pure β-lg solution.[45] To investigate such order of addition effects of the biopolymers in this study, polysaccharides were injected into the subphase of pre-formed β-lg layers using microfluidic syringe pumps. The inserted microtubes were 0.2 μm and more than 1 cm away from the 1 mm thick DWR ring. Before addition of the polysaccharide, with the microfluidic tubings still immersed in the subphase, the oil/water interfaces of protein solutions were measured for 20 hours as shown in figure 3.16A. The lag times and G_i' values of these measurements are as expected for protein adsorption at the interface.

Once nearly all the β-lg molecules have adsorbed at the interface i.e. the interfacial strength reaches a plateau (after 20 hours), the polysaccharide solutions were injected into the bottom of the subphase. About 100 μL of 0.2 g.L^{-1} polysaccharide solutions were injected at a rate of 167 nL.s^{-1}. This amounts to a complete discharge into the subphase after 600 seconds. The interface was monitored for a further 20

hours as shown in figure 3.16B to observe the effect of complexation of polysaccharide molecules with the adsorbed β-lg molecules. About 150 seconds after the onset of polysaccharide injection, a noticeable increase in G_i' is observed for both the HMPs as well as the Dp7 (figure 3.16B). The increase suggests that some polysaccharide molecules have already reached the interface and complexed with the adsorbed β-lg. This duration of time before an interfacial response is much shorter than the lag time values of the pre-mixed solutions which was > 3000 s. If the size of the polysaccharide molecules contribute considerably to the lag time values of pre-mixed solutions, then we should observe a similar duration before G_i' increase after the injection of polysaccharide into the subphase. The vast lag time difference between pre-mixed solutions and subphase injected solutions further show that the size of the polysaccharide molecules play a trivial role in the rates of interfacial film formation. Instead, the lag time is a result of the pre-adsorption commitment of the β-lg molecules and a consequence of it unshackling from the complexing polysaccharide and unraveling at the interface. If the β-lg molecules are already at the interface this lag time almost completely vanishes as seen in figure 3.16B. Furthermore, the final G_i' values were very similar to that of their pre-mixed counter parts implying the order of addition does not matter as much as it does for LMP.

3.4.9 Preliminary Emulsion Results

TABLE 3.2: Size measurements (D_{50}) in μm for dodecane droplets in β-lg/HMP_B solutions at various weight ratios

$W_{\beta-lg}$:W_{HMP_B}	D_{50} (t=0)	D_{50} (t=24 hrs)	D_{50} (t=10 days)
1:0	43.2	43.3	43.7
1:0.125	56.4	67.3	76.3
1:0.25	57.2	60	67.8
1:0.5	40.1	40.1	42.6
1:1	35.3	36.3	36.6

TABLE 3.3: Size measurements (D_{50}) in μm for dodecane droplets in β-lg/HMP_R solutions at various weight ratios

$W_{\beta-lg}$:W_{HMP_R}	D_{50} (t=0)	D_{50} (t=24 hrs)	D_{50} (t=10 days)
1:0	43.2	43.7	43.3
1:0.125	53.2	59.2	59.5
1:0.25	50.6	52.1	54.6
1:0.5	42.6	43.7	45.7
1:1	35	35.4	36.3

To understand how the interfacial rheology and interfacial tension measurements translate to emulsification behavior, emulsions were prepared using a fixed protein concentration of 0.1 g.L^{-1}. β-lg/HMP$_B$ and β-lg/HMP$_R$ complexes at various weight ratios were studied along with that of the pure protein system. In order to obtain a reasonably stable emulsion, the total protein concentration was 100 times the amount used for interfacial rheology. However, the protein surface concentration for a total oil volume of 6 ml (assuming uniform emulsion drop size of 50 μm) comes to around 2.77 mg.m^{-2} provided all the protein reaches the interface. This value is comparable to the protein surface concentration used for interfacial rheological studies (10. 6 mg.m^{-2}) with the same assumption of total protein adsorption. This is a reasonable assumption to obtain protein surface concentration as it was measured that more than 90 % of β-lg adsorbs on the emulsion droplets.[93] Moreover, the calculated surface concentration for emulsion is close to the values (1.29-1.65 mg.m^{-2}) measured in other emulsion studies for β-lg monolayer formation.[158] The drop size distributions for β-lg/HMP$_B$ and β-lg/HMP$_R$ solutions was measured on the day of emulsion preparation, after 24 hours and after 10 days in order to estimate the extent of coalescence and are listed in table 3.2 and table 3.3 respectively. At first, the addition of both pectins seem to reduce the emulsifying capability of the protein as the median size of 1:0.125 for both pectins are nearly 10 % larger than the pure protein emulsion. However, at higher polysaccharide concentration the median drop sizes decrease and at a ratio of 1:1, both pectins formed emulsions with smaller D$_{50}$ than the pure protein emulsion. This better emulsification at higher pectin concentrations is consistent with what has been observed for other similar HMPs.[159] Moreover, in the emulsions with higher pectin concentrations the increase in drop size with age was less pronounced. The emulsions with HMP$_R$ exhibited a slightly smaller D$_{50}$ and marginally better stability with age as compared to HMP$_B$. However, at a ratio of 1:1 both HMPs had very similar size and stability with age. Further comments on these results will be made in the upcoming discussion section.

3.5 Discussion

It is evident from the results of this study that the role of diffusion of β-lg/polysaccharide complexes in determining the timescale of building of an elastic interfacial layer is minimal. It appears that the binding between the β-lg molecules and the polysaccharide in the bulk delays the protein adsorption at the interface. The higher the availability of protein binding sites the longer is the delay as more protein molecules struggles to free itself and access the interface, as reflected in the lag times. Further, upon complexation with pectin at pH 4 the % of β-strands increases while the α-helix content decreases for the protein molecules.[141] It has been argued that such changes in the ratio of different secondary structure elements could promote protein oligomerization leading to β-lg rich clusters on the polysaccharide molecules.[139] SANS and SAXS measurements showed larger protein clusters and a broader size range for the strongly binding HMP_B as compared to HMP_R. Therefore, protein-protein aggregation is also a factor that could contribute to the adsorption kinetics especially in solutions with excess proteins and saturated polysaccharides.

The rises in t_{lag} observed with increases in polysaccharide concentration indicate that the protein-polysaccharide interaction plays the crucial role in hindering the adsorption of protein to the interface and delaying the formation of an interfacial layer. The interfacial tension measurements at 1:1 weight ratios showed that the higher binding affinity for the polysaccharide, slower the protein adsorption at the interface. Nevertheless, polysaccharide induced protein-protein aggregation could also contribute to the increase in t_{lag} values for mixed protein-polysaccharide solutions as compared to that of pure protein solutions. During emulsion formation, the protein molecules do not have the time they had during the interfacial rheology experiments to diffuse to the interface and then unravel. As emulsion experiments showed, pectin molecules with large β-lg clusters (1:0.125) are not superior emulsifiers to the pure protein solution. This could be due to the polysaccharide molecules hindering the efficient distribution of proteins at the interface by phase separating them into clusters. In such a case, emulsions formed with larger protein clusters would be expected to be more unstable as compared to the emulsion droplets with smaller clusters. This is consistent with the

median drop sizes of emulsions consistently reducing with increase in pectin concentration. Emulsions at 1:0.5 and 1:1 ratios had very similar drop sizes for both HMPs indicating once enough binding sites are available for the proteins, the HMPs behave similarly. More importantly, the size of 1:1 emulsions was found to be less than that of pure protein solutions. Further, the final interfacial strength of the interface also did not increase after a ratio of 1:0.5 for both the HMPs. This reaffirms that HMPs if used in the right ratios can enhance the emulsifying capability of β-lg by reinforcing the interface.

While it is understandable for a long polysaccharide to concatenate β-lg molecules, Dp7 is just long enough to bind to one β-lg monomer at pH 3 but still manages to reinforce and strengthen the interface. Moreover, for the ratios used in this study there is excess Dp7 present implying ample binding sites for the protein molecules to bind directly to Dp7 as mentioned in table 3.1. However, that doesn't rule out the possibility of complexation-induced protein oligomerization or two β-lg/Dp7 complexes combining to aggregate.[141] In that case, the amount of oligomers will be directly proportional to the number of complexed protein molecules i.e. the amount of available protein-polysaccharide binding sites. Moreover, the size of the oligomers do not play a major role as the dimer is long enough to establish a viscoelastic layer as revealed from chapter 2.

At monomeric conditions of pH 3, Dp7 results are particularly interesting as t_{lag} values at pH 3 were found to be half of that found in pH 4. In these conditions, HMP_B and HG-60 eventually lead to viscoelastic interfacial layers as well albeit considerably slower than Dp7. In fact, Dp7 which had the longest lag time at pH 4 lead to the quickest interfacial film formation at pH 3. Keeping in mind the role of β-lg's quarternary structure on interfacial elasticity, it is possible that the number of complexed protein molecules i.e. number of binding sites has a positive correlation with lag times unlike at pH 4 where a strong binding affinity retarded the film formation by shackling the molecules. Therefore, higher number of β-lg binding sites at pH 3 is implies a higher number of elasticity imparting β-lg oligomers. For a given weight of polysaccharide, Dp7 solutions have the highest number of binding sites followed by the linear HG-60 and finally the bulky HMP_B. Therefore, the amount of protein aggregation should be in the order Dp7 > HG-60 > HMP_B which does appear to be

correlated with the lag times observed at pH 3. Further, at pH 3, the polysaccharides carry less net charge which could partially contribute to a lower binding affinity during complexation. Since binding studies have not been conducted at pH 3 further comments cannot be made on the protein's structure post complexation. However, β-lg can complex with polysaccharides through different patches of positively charged residues on its structure.[160] It is therefore possible that β-lg binds to polysaccharides in a less compromising way at pH 3 as compared to that of pH 4 and therefore do not impede the adsorption of protein molecules. However, further information is needed to completely understand if β-lg monomers bind to polysaccharide in a different route than β-lg dimers.

3.6 Conclusion

The objective of this chapter was to study the effect of polysaccharide complexation on the interfacial behavior of β-lg molecules. It has been previously reported that complexation with polysaccharides retards the formation of β-lg interfacial films and has a negative impact on the final interfacial strength. However, there was little mechanistic understanding of this behavior. Here, the transient rheology of pre-mixed β-lg/polysaccharide solutions revealed an intricate role of the distribution of negative charges on the polysaccharide in controlling the stability of the complexes versus the protein's preference for the interface.

Interestingly, the size of the polysaccharide molecules did not play the deciding role in shaping the rate of interfacial film formation. This is exemplified by the fact that the system with HMP_B having comparable lag time values to those obtained with Dp7, which is nearly 600 times smaller than the pectin. However, both these polysaccharides contain concentrated patches of negative charges leading to strong binding affinity with β-lg and thereby delaying the protein's adsorption and relaxation at the interface. When β-lg molecules and a polysaccharide such as a highly negative LMP complex, it imposes too high a structural penalty to reshuffle and adsorb at the interface. This is most probably why pre-mixed β-lg/LMP solutions did not lead to an interface of any appreciable strength.

The final interfacial strengths of various protein/polysaccharide systems suggested that the number of contact points between the two biopolymers along with the binding affinity play a crucial role. Experiments at pH 3 led to the proposal that the mechanism by which these polysaccharide molecules reinforce the interface was cross-linking of adsorbed β-lg molecules and hence concatenating them to form a percolating network. These results showcase that pre-mixed solutions of β-lg/HMPs can be used as a one-shot delivery system for emulsification purposes for reinforced interfaces. Besides, this study also provides possible routes in devising β-lg/polysaccharide complexes by exploiting parameters such as the charge distribution and length of the polysaccharide for drug delivery applications.

Chapter 4

Microrheology of Beta-lactoglobulin Interfacial Films

4.1 Background

Rheology is the study of a material's response to an applied deformation or stress. Usually, this involves the application of a time-dependent stress at a particular frequency and amplitude. In shear rheology, a force that is parallel to the surface is varied with time on an interfacial area which is maintained constant. However, traditional mechanical measurements such as shear rheometers are limited in their probing frequency ranges and sensitivity. Interfacial shear rheometry assumes that the applied force does not alter the material's property as a consequence of the measurement. It perceives the lateral cohesion along the interface with the measurement value reflecting the average strength. It does not provide any information regarding how the interfacial strength might vary spatially across the interface. Hence, it is important to perceive the system with an alternative tool that will enable us to overcome these limitations. Microrheology can be used to probe different sections of the interface providing a composite perspective. Although it is statistically tedious, its superior sensitivity and large dynamic range means that the results obtained complement the measurements obtained using macro rheology.

Thermal energy manifests as random motion of constitutive atoms and molecules.

While such movements are undetectable to a naked eye, tracking the motion of colloidal particles embedded in the fluid over time and modelling their motion will provide us information about the rheological properties of the fluid in the particle's vicinity. Further, the advancements in the quality of microscopes and imaging devices gave birth to a new field called microrheology. The aim of this chapter is to gather complimentary microrheology measurements for interfaces assembled with β-lg and β-lg/polysaccharide complexes as presented in chapters 2 and 3 respectively. Interfacial microrheology has some additional challenges as compared to the reasonably well established bulk microrheology and is still evolving. Therefore, in this chapter, the current understanding regarding the motion of a particle at a fluid/fluid interface will be discussed. This will be followed by explaining the multiple particle tracking techniques along with the required mathematical models that are used to extract the rheological properties will be explained. This will be followed by an overview of the relevant works and the current understanding of how interfacial macro- and microrheological techniques correlate. Finally, the objective of this chapter will be laid out followed by the results obtained on systems of interests herein and their subsequent discussion will be presented.

4.2 Particle Motion at Fluid/Fluid Interfaces

Multiple particle tracking is facilitated at fluid-fluid interfaces due to the irreversible attachment of particles on to the interface. The attachment energy of a particle (E_p) at a fluid1/fluid2 interface can be arrived at using Young's equation and is given by,

$$\langle \Delta E_p \rangle = -\pi a^2 \gamma_{12} (1 \pm \cos\theta)^2 \tag{4.1}$$

where a is the radius of the particle, γ_{12} is the bare fluid-fluid interfacial tension and θ is the average equilibrium contact angle of the particle at the interface. The challenge of measuring the contact angle of a particle at the interface has come a long way including using nanoparticles for the measurements.[161] However, the averaging over many particles along with measurement uncertainty typically imparts an uncertainty to this variable. A review article written on the development of the techniques can be found here.[162] Furthermore, this θ is also a reflection of how much the particle's

surface is immersed in either of the bulk fluids and thereby changes in the fluid bulk viscosity will also be expected to have an effect on the particle's interfacial motion. However, studying the effect of bulk phase viscosities is difficult since it cannot be done without altering the γ_{12}. Since E_p is usually a few orders of magnitude times the thermal energy (k_BT), thermal fluctuations can not knock the particle from the interface, making its adsorption irreversible.

Therefore, staying adsorbed is energetically favourable for the particle and this new life at the interface imposes some confinements. Firstly, it cannot fluctuate in the direction perpendicular to the interface, as much as it can parallel to it. This is a consequence of the anisotropic nature of the interface and the possible energy cost required in changing its contact angle. Hence, the particle predominantly moves along the plane of the interface.[163] Secondly, there is a new interface created between the particle and the two fluids called the *triple line* where all the three materials meet. This is the contact line over which the additional force of interfacial tension will play a crucial role. The consequence of this three-phase contact line is still not crystal clear. This raises the question "what is the relationship between the bulk viscosities and the interfacial viscosity?"

For a two-dimensional fluid, the drag intrinsically becomes a non-linear function of its viscosity since no solution could satisfy the boundary conditions of the Navier-Stokes equation at the surface and infinity.[164] The coupling between the fluid bulk complicates the matter in case of real interfaces. In their seminal work, Saffman and Delbrück described the diffusion of a disk with the same thickness as that of the interface.[165] However, the thickness of micron sized particles are usually larger than that of the interfaces, which are usually of the order of few nanometers. Fischer et al. numerically calculated the drag on a spherical particle bound to an incompressible membrane separating two viscous liquids to the first order of Boussinesq number (B_o).[166] However, some experiments have shown that a particle at an air/water interface experiences an abnormally high drag, more than that would be expected from the bulk, which hinders the diffusion of the particle.[167] The authors justified this behavior by coupling the enhanced particle drag to the thermal fluctuations along the triple

line. Later, these results were used as the basis to propose that the inherent elastic nature of the interface, mediated by the surface tension generating an additional dissipative mechanism. Incidentally, such higher drag was theoretically predicted for curved fluid-fluid interfaces such as the surface of an emulsion droplet.[168] The re-circulation of the fluid due to finite volume effects inside an emulsion drop was the reasoning given for this enhanced drag. This was supported by results of charged microparticles on oil droplets obtained by confocal microscopy.[169][170]

Other major phenomena that are in play at the interface owing to its surface tension are Marangoni effects and capillary waves.[171] Marangoni effects display a mass transfer along an interface due to local surface tension gradients. A Brownian particle experiences a surface compression along the direction of motion and an expansion at the rear end leading to a compressible flow. In the presence of a surfactant film at the interface, the molecules move much faster than colloidal particles and thus, such contractions and expansions invoke Marangoni forces which counters the particle movement, slowing it down considerably.[166] This will lead to an incompressible flow around the particle. On the other hand, capillary forces do not come into play when the interface is reasonably planar and the particles are colloidal.[172] Nevertheless, they can be important in dilational rheology.[173]

4.3 One-point Microrheology

In one particle microrheology, the X and Y positions of individual particles are recorded over a series of frames, typically using conventional microscopy and a charge-coupled device (CCD). The position vectors at different times are then used to calculate the mean squared displacement (MSD) according to the equation

$$\langle \Delta r^2(\tau) \rangle = \langle (r(t+\tau) - r(t))^2 \rangle \tag{4.2}$$

where $r(t)$ is the position vector at time t and τ is the time interval or lag time between the frames. The above mentioned MSD ($\langle \Delta r^2(\tau) \rangle$) is calculated for particles at different time intervals and is typically averaged over an ensemble of particles. Hence, the final

MSD obtained is averaged over all instances of a particular lag time for each particle and over the ensemble of different individual particles. According to the Einstein-Smoluchowski equation, the MSD is given by the equation:

$$\langle \Delta r^2(\tau) \rangle = 2nD\tau \tag{4.3}$$

where n is the dimension of tracking and, D is the diffusion coefficient of the particle. Hence, for two-dimensional particle tracking n is 2 and the MSD is given by $4D\tau$. Meanwhile, the relation between the diffusion coefficient (D) of a particle suspended in a fluid of viscosity (η) is given by the Stokes-Einstein-Sutherland equation:

$$D = \frac{k_B T}{6\pi\eta a} \tag{4.4}$$

where a is the radius of the diffusing tracer particle and T is the temperature of the fluid. Hence, the viscosity of the fluid can be easily derived from these two equations provided the MSD is known. However, this can be applied only in those cases in which the fluid is completely viscous or if the elastic nature of the fluid is intangible. In the case of viscoelastic fluids, the viscosity becomes a complex viscosity ($\widetilde{\eta}$). Rheological parameters such as loss modulus (G'') and storage modulus (G') are timescale dependent parameters. Hence, to obtain a direct relationship for the complex moduli (G^*) from the MSD, we perform either a Laplace transform, or Fourier transform (FT). The generalized Stokes-Einstein-Sutherland relationship in the frequency domain can be expressed as the following:

$$G^*(\omega) = \frac{k_B T}{i\pi a \omega F_u[\langle \Delta r^2(\tau) \rangle]} \tag{4.5}$$

where $F_u[\Delta r^2(\tau)]$ is the Fourier transform of the MSD. To calculate the FT of the MSD, a method was developed by Mason et al. in which the transform is calculated algebraically by expanding $\langle \Delta r^2(\tau) \rangle$ locally around the frequency of interest using a power law and retaining the leading term.[174] This leads to the following relation,

$$|G^*(\omega)| \approx \frac{k_B T}{\pi a \langle \Delta r^2(1/\omega) \rangle \Gamma[1 + \alpha(\omega)]} \tag{4.6}$$

where $\alpha(\omega)$ is the first-order power law exponent describing the logarithmic slope of $\langle \Delta r^2(\tau) \rangle$ at t = $1/\omega$ and

$$\alpha(s) \equiv \frac{dln\langle \Delta r^2(\tau) \rangle}{dlnt} \mid_{t=1/\omega} \tag{4.7}$$

From these, the individual moduli values are given by the following equations:

$$G'(\omega) = |G^*(\omega)|cos(\pi\alpha(\omega)/2), \tag{4.8}$$

$$G''(\omega) = |G^*(\omega)|sin(\pi\alpha(\omega)/2) \tag{4.9}$$

Since the rheological properties are obtained through double numerical derivatives, calculated rheological properties can be noisy due to the inherent noise in the raw MSD data. Therefore, before transforming the MSD to the frequency domain, the relationship between the MSD and lag time is typically captured by fitting a continuous, smooth curve, which is subsequently used to calculate the rheological properties as described above. It is also worth mentioning that this approximation was modified by Dasgupta et al. for MSD data that are highly curved with a rapidly changing slope across multiple orders of magnitude of frequencies by incorporating the second-order logarithmic derivative of the MSD.[175]

4.3.1 Two-Point Microrheology

Conventional passive microrheology is based on tracking a probe particle displacement with respect to the medium. While this method works as intended for homogeneously viscous fluids, heterogeneous materials are more challenging. In fact, exploring the heterogeneous texture of cells was a major motivation in the development of two-point microrheology (TPM). Unlike 1-particle microrheology, TPM is based on the cross-correlated movement of two neighbouring tracer particles.

To give a crude analogy, 1-particle microrheology is a way of finding the stiffness of a rope by tying a ball to the end of it and pulling it in different directions. On the other hand, TPM is similar to tying a ball to both ends of the rope, pulling one and observing its effect on the other. This method is especially fruitful when tracer-medium interactions become a cause for concern. Since TPM only reflects the response

of the medium between the two tracers and not their local environment, the local confinements of individual tracer particles do not affect the measurements.

In order to calculate TPM, we need to have an idea of how the ripples generated by one tracer die down with the inter-particle distance. This information has been derived using hydrodynamic calculations of a Brownian particle at an interface. Levine and Lubinsky found that the assumption that two-point microrheology is not a function of the local environment of the tracers is only valid for interparticle distances much greater than the particle radius for incompressible fluids.[176] This is an important elucidation which enables a simple definition of the two-particle diffusion coefficient (D_{rr}),

$$D_{rr}(r,s) = \frac{k_B T}{2\pi \tilde{G}(s)} \tag{4.10}$$

where D_{rr} is the cross-correlation between the displacement vectors of the two tracer particles calculated using their projection onto the line joining the centers of the particles. It is given by the following equation

$$D_{rr}(r,\tau) = \langle \Delta r_1(\tau) \Delta r_2(\tau) \rangle \tag{4.11}$$

where Δr_1, Δr_2 are the displacements owing to the stochastic motion of tracer particles along their mutual line of centers at a lag time τ. A two-particle MSD that is equivalent to the conventional one particle MSD can be formed using a geometric factor as follows,

$$\langle \Delta r^2(\tau) \rangle_2 = \frac{2r}{a} D_{rr}(r,\tau) \tag{4.12}$$

where $\frac{2r}{a}$ rescales the correlations to the diameter of the particle. This two-particle MSD ($\langle \Delta r^2(\tau) \rangle_2$) will be equivalent to conventional 1-particle MSD ($\langle \Delta r^2(\tau) \rangle$) only if the medium is incompressible, homogeneous, isotropic on all length scales (including much less than the size of the tracer) and the no-slip boundary condition is satisfied at the surface of the tracer particles.

4.4 Interfacial Microrheology Studies

The effect of interfacial curvature on particle dynamics as proposed by Danov et al. (2000)[168] was verified experimentally by Wu et al. (2006) by capturing the probe particle displacements on emulsion droplets.[169] The curvature was defined by the ratio of droplet and particle radii. Wu et al. continued their work on curved interfaces using oil-in-water Pickering emulsions as a template. They used single particle tracking to show that the mobility of charged particles is dependent on the contact angle as well as oil phase viscosity.[177] The authors extended their work on Pickering emulsions using TPM to further explore the oil/water interface.[178]

Prasad and Weeks also explored the application of TPM to different concentrations of human serum albumin proteins at air/water interface.[179] They noticed a transition from 3D dominated particle motion to 2D dominated particle motion at higher surface viscosities. This approach was further extended to studying soap films of varying thickness (h) and tracer particle diameters (d).[180] These studies found that 3D shear gradients in the fluid layer starts to dominate tracer particle dissipation around $h/d \sim (7 \pm 3)$. They also found that in 2D, D_{rr} dies down with interparticle distance (R) according to the relation A$\ln R$ + B (A,B are constants) as compared to $1/R$ in 3D.

Peng et al. pointed out that for a planar interface, the presence of surfactants might compromise some of the original assumptions of the hydrodynamic theories developed such as those that deal with Marangoni effects.[181] They presented a relation between diffusion coefficient and area fraction occupied by the polymethylmethacrylate (PMMA) particles at decalin/water interface. An elaborate review of works and techniques can be found here.[182,183]

4.4.1 Interfacial Microrheology of Proteins

The need to understand the physiological flow behavior of blood has been an important motivation behind the development of microrheology. This lead to the branch of clinical haemorheology.[184] This was followed by studies on F-actin proteins, one of the most important building blocks of our cells.[185,186] With time it became clear

that protein-particle interactions are to be taken seriously in order to accurately measure the microrheology of protein systems with particles carrying considerable surface charge. Naturally, this led to experimenting with the chemical coating of tracer particles intending to minimize this interaction. It was shown that carboxylated particles coated with polyethylene glycol (PEG) molecules (0.75 kDa) for example were better in avoiding protein adsorption.[187] It was also demonstrated that TPM significantly reduces differences measured arising from different tracer surface chemistries. Recently, Garting et al. discussed the various problems of choosing tracer particles for protein solutions and showed that a much longer PEG (20 kDa) is ideal for such measurements.[188]

The application of microrheology in studying intricate things such as the unfolding of globular proteins in the bulk has been investigated.[189] The unfolding of bovine serum albumin (BSA) using urea was studied using tracer particles assuming the hard-sphere theory for globular proteins.[190] Active interfacial microrheology studies were carried out on BSA at air/water interfaces using magnetic nano rods and showed the increase in surface viscosity from 10^{-9} to 10^{-5} Ns/m over 2 hours while the surface pressure saturated in minutes.[190] However, the rise in surface viscosity was not accompanied by a corresponding increase in surface elasticity prompting the authors to suggest the possible annealing of the protein films. Another magnetic based technique combining active interfacial microrheology with visualization using fluorescence microscopy was developed using tailor-made magnetic 'microbuttons' as probes.[191] Microrheology also gives us the ability to study the kinetics of protein adsorption. The linear and non-linear microrheology of lysozyme layers forming at air/water interface was studied.[192] The authors observed subdiffusive behaviors of probe particles occurring in less than 200 seconds after addition signifying rapid adsorption. Moreover, no heterogeneity was observed and the distribution of the displacements of probe particles at all lag times remained Gaussian.

On the contrary, a much slower increase in surface viscosity was observed for β-lg from pHs 5.2 and 7 for similar concentrations at air/water interfaces.[193] Moreover, the three stage adsorption of β-lg involves a phase of heterogeneity in surface properties with two distinct particle subsets of considerably different diffusivities was observed. Although the evolution of protein layers were similar at both pHs 5.2 and 7, it was

noted that the former responded as an rigid elastic film while the later was much more viscous. Interestingly, a follow-up work on β-lg at decane/water interfaces at the same conditions indicated a sol-gel transition with no signs of heterogeneity.[54] The formation of the protein films were faster at oil/water interfaces as compared to that of the formation at air/water interfaces, with a larger viscoelasticity. The aforementioned two studies at similar protein concentrations indicate that the rheology evolution of protein kinetics is not universal and depends on lots of factors such as specific protein and the hydrophobic phase of interest.

4.4.2 Comparison of Macrorheology and Microrheology at Interfaces

Although macrorheology and microrheology probes the same shear interfacial properties, very large discrepancies, even around a few orders of magnitude have been reported for some systems.[194,195,196,197] This is completely different to the generally good level of agreement found in the case of the bulk measurements using these techniques.[198] In this respect, monolayers of poly(tert-butyl acrylate), PtBA, at air/water interfaces is an important system of discussion that was reported to exhibit mismatch between the measurements of both rheological techniques.[194] This discrepancy could not be explained by particle-polymer interactions and was suggested to originate from the difference in sensitivities of macrorheology and microrheology. Further investigation showed the presence of heterogeneity on the PtBA monolayers which might hinder the homogeneous distribution of the particles.[195] The authors suggested that the presence of such heterogeneity could even preclude efficient measurements by microrheology for such systems. The discrepancy was still observed when PtBA monolayers were probed using a different microrheology technique.[199] Further, incorrect flow field definitions of interfacial probes hindering accurate calculations in macrorheological measurements was not ruled out as well.[200] A direct comparison between macro- and micro- interfacial rheological techniques was partially addressed in a recent study.[201] Overall, although the frequency ranges of these two techniques overlap, interfacial macrorheology and microrheology probes the system at different length scales with different sensitivities and careful considerations of methodologies and theories are required which might also depend on the specific system being studied.

Based on the above discussion, a rigorous and direct comparison of the values obtained using macrorheology and microrheology for β-lg interfacial films is not feasible due to the extensive attention it demands. Ideally, this would require careful considerations of the definitions of the flow field around the probe geometries (DWR, microparticles), especially for viscoelastic interfaces, along with the accurate estimation of subphase drag on the measurements. From a microrheology perspective, a detailed imaging of the protein laden interface to investigate the possible presence of heterogeneity and other surface concentration gradients should be assessed. This must be followed up with rigorous testing for possible particle-protein interactions that might impact the motion of probe particles at the interfaces along with accurate measurements of the contact angle of probe particles at different protein concentrations. Such a detailed investigation is beyond the scope of this work due to the constraint of time. Therefore, the objective of this chapter is to carry out *ad hoc* microrheology measurements to obtain qualitative, complementary evidences of the macrorheological inferences obtained in chapters 2 and 3. The main objectives of this chapter are,

1. To verify the contrasting behaviors of β-lg monomers and dimers at oil/water interfaces and assess the presence of heterogeneity, if any, in the protein films.
2. To estimate the critical β-lg dimer concentration required to impart elasticity to the oil/water interface. This will be investigated by varying the surface dimer concentration as well as the salt concentration.
3. To compare the particle motions in pure β-lg laden interfaces and interfaces with β-lg/polysaccharide complexes in order to gain a better understanding of the impact of complexation.

4.5 Materials

Fluoresbrite plain polystyrene microspheres (CAT-17154) of 1 μm and 0.5 μm diameter (coefficient of variation is 3 %) obtained from Polysciences, Inc. were used as tracer particles for particle tracking. The particle's excitation maximum is 441 nm and emission maximum is 486 nm. The particle solutions were thoroughly washed to remove any residual surfactant before being used for tracking. The zeta potentials

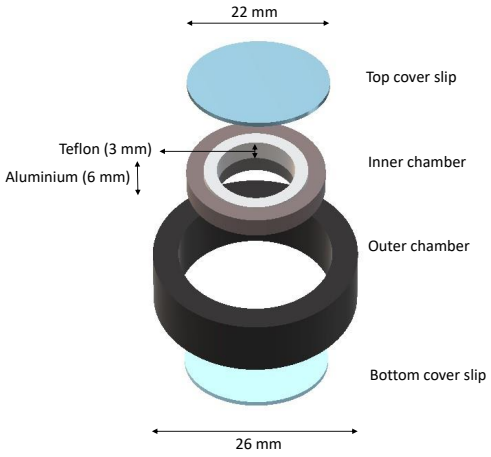

FIGURE 4.1: An exploded view of the interfacial chamber used for microrheology.

of the particles were measured to be (0.1 $\pm$ 0.5 mV) using zetasizer nano ZS. Colloidal plain polystyrene particles of similar sizes have previously been used for microrheology at β-lg laden interfaces and no issues were reported about protein-particle interactions.[193] In this study, the values of the contact angle of the particles were not measured and not used for any calculations. In the experiments of this study, the probe particles were added to air/water interfaces before the addition of dodecane on top. At the time of addition, the air/water interface is probably nearly pristine with very little protein adsorption and therefore the contact angle of the particles are assumed to be comparable for all the measurements. This implies the assumption that the contributions from the bulk phases i.e. dodecane and the protein solution are similar for all the measurements and that the particle motion is predominantly a reflection of the interfacial layer.

Standard silicone oil (PDMS) samples purchased from Sigma Aldrich were used for preliminary interfacial measurements. The sample viscosities were 100 and 1000 cSt which corresponds to 0.096 and 0.97 Pa.s respectively. All the measurements were carried out at 25°C. The protein solutions and dodecane preparation were the same as elaborated in chapter 2. The protein/polysaccharide solutions were the same as elaborated in chapter 3. The final particle concentration in the sample was around 0.0014 wt% in an attempt to limit interparticle interactions.

4.6 Methodology

4.6.1 Interfacial Chamber

Tracking particles on interfaces is precarious given the commonly found curvature of air-water and oil-water interfaces. To negate such curvature effects and to obtain a reasonably flat interface, an interfacial chamber was built with an inner surface made of half-teflon and half-aluminium to pin the interface.[202,54] The specifications of the chamber are shown in the figure 4.1. The circular cross-section area of the chamber was ~ 3.8 cm^2. The closed nature of the chamber also limits convective noise arising due to air flow from the surroundings. Preliminary experiments showed that drying and oil leaking was a problem while conducting long duration experiments. This was solved by attaching a small rubber gasket to the bottom of the chamber which presses against the bottom cover slip to form an air-tight space.

The sample was prepared by first adding around 680 µl of β-lg solution at a concentration sufficient to generate the appropriate surface concentration (10.6 mg.m^{-2} unless specified otherwise). The surface concentration was chosen to be consistent with the shear rheology measurements carried out previously. The surface concentration was calculated assuming all the protein in the solution reaches the interface. Freshly sonicated probe particles were diluted in the appropriate buffer solution as the protein and dispersed on top to the air/water interface using a 10 µL pipette. Unlike other interfacial microrheology studies,[54] no alcohol was added in the particle mixture since any residual alcohol might denature the protein adsorbed at the interface. After 10 minutes, dodecane was added on the top to complete the formation of an oil/water interface and the chamber was sealed to prevent any effect of external air flow. The area fraction of the probe particles was maintained below a density of 0.002 above which the hydrodynamic interactions become appreciable.[181] Particle tracking was commenced after the samples were equilibrated for 2 hours which was shown to be suffice to build an elastic interface from the macrorheology experiments in chapter 2. For mixed solutions of protein/polysaccharides at 1:0.125 ratio, an equilibration time of 6 hours was given for Dp7 (pH 4) and 3 hours was given for the other polysaccharides before particle tracking, based on the lag time values from macrorheology results in chapter 3.

4.6.2 Particle Tracking

Particles were tracked in an inverted microscope (Nikon Eclipse TE-2000U) with an air immersion, long working distance objective of 40× magnification (Nikon S Plan Flour ELWD, with NA = 0.6) on an air damped table illuminated using a pE-300 series white LED purchased from CoolLED. Multiple series of images were obtained at 50 frames/sec for 5 seconds using an CCD camera (Andor Neo CMOS) along with an auxiliary magnification of 1.5×. At least 60 particles were tracked for each system with a rolling shutter. It was ensured that the tracked probe particles were actually at the oil/water interface and not in the bulk by making sure that the particles did not go out of the focal plane while observing them for few hours.

After obtaining a series of images, they are analysed using polyparticle tracker algorithms in MATLAB.[203] This program uses a polynomial fitting with Gaussian weight to track the X and Y positions of the particles at each frame. The pixel co-ordinates were transformed to actual distances using the appropriate conversion factor for the magnification used (9.2558 $\pm$ 0.2 pixels/μm). This data was then used to calculate a MSD as elaborated previously in this chapter. It should be noted that, before analyzing the tracking data for MSD, de-drifting was performed to remove any global linear drift that might have contributed to the position of the particles. These static drifts could primarily arise from the mechanical vibrations of the experimental setup and tilt of the chamber causing a fluid flow across the interface. Such drifts can be typically observed as a constant rate of change in position of all particle with time. Drift removal was carried out by subtracting the averaged rate of change of position of all the particles in the frame. Prior to this, the drift was ensured to be uniform across the tracked frame by averaging particles in different sections of the frame. Subsequently, we obtained MSD plots against lag time and recorded the trajectories of the tracked particles. The minimum resolvable MSD was approximately 0.001 μm^2 measured for stationary colloids stuck to the cover slip, which corresponds to detectable displacement of around 100 nm. All fittings were performed using Origin Pro 8.5 software with adjusted R-squared values > 0.95.

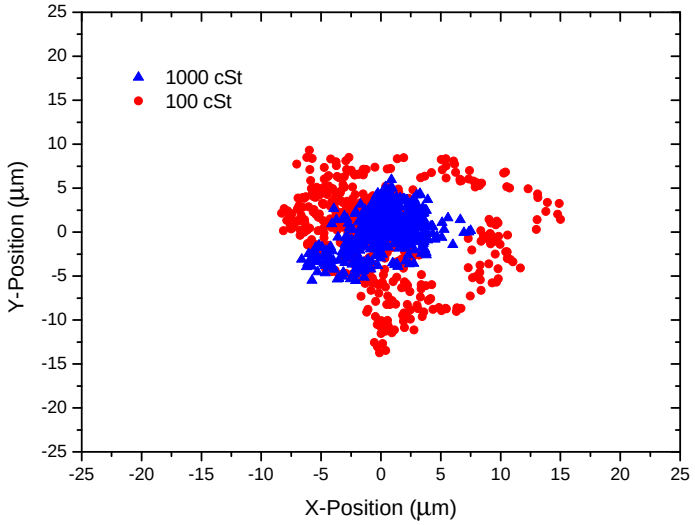

FIGURE 4.2: X-Y positions of tracer particles at PDMS/water interfaces with different oil viscosities.

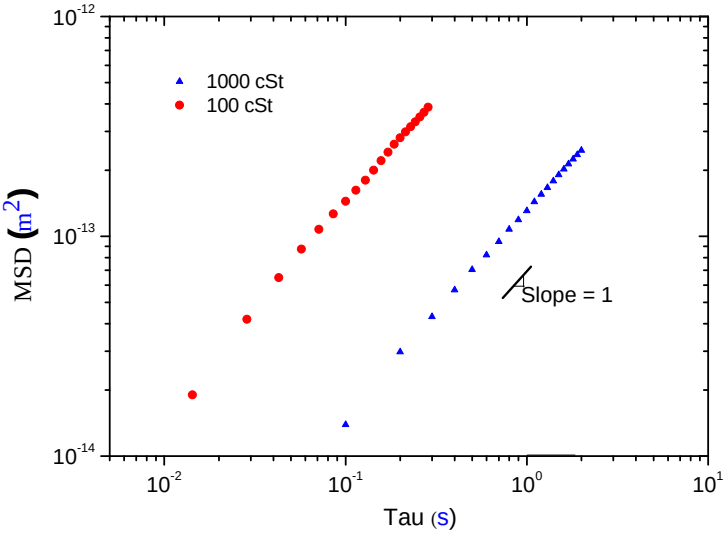

FIGURE 4.3: MSD values obtained from tracking of tracer particles at PDMS/water interfaces with different oil viscosities.

4.7 Results and Discussion

4.7.1 PDMS/Water Systems

PDMS (silicone) oils are a typical model systems to study rheology since they are available in different viscosities without changing their chemical nature. Such systems have been measured at different oil viscosities using microrheology.[204] In this study, we use PDMS/water as a control system to compare the two rheological methods. The kinematic viscosities of samples were 100 and 1000 cSt which corresponds to 0.096 and 0.97 Pa.s respectively. The tracking of probe particles at the interface was carried out using fluorescent particles of 1 μm diameter. At least 60 particles were tracked for each oil/water interface from which the particle position data was obtained as shown in figure 4.2. As expected, the average displacement of particles was found to be reduced when the more viscous 1000 cSt was studied as compared to the 100 cSt oil/water interface. The MSD data obtained from the tracking is shown in figure 4.3. The slopes of the MSD vs delay time (τ) data were almost one on a log-log plot in all cases indicating their predominantly viscous nature. Straight lines could be fitted to obtain the G_i'' using the equation 4.6. Probability density functions display the normalized histogram of the distribution of particle displacements for a given lag time. The probability density function ($P_{\Delta Y}$) of probe particle displacements at a lag time of 1 sec is shown in figure 4.4. The Gaussian distribution indicates homogeneity as expected for a pure water and oil interface.

The G″ values obtained from both rheological methods used herein are compared in figure 4.5. The lines are from the fitted MSD values of microrheology and the symbols are the values obtained from interfacial shear rheology. For a micron sized particle, the B_o number, which is the ratio of surface viscosity to the bulk viscosity, is 100 times higher than the DWR geometry used in shear rheology. Hence, less contribution from the bulk fluid is experienced by the probe particles as compared to the rheometer geometry. The slight difference in the slopes of the G″ values obtained from shear rheology and microrheology could be due to this bulk contribution. Nevertheless, for both the oils, the two methods seem to be in reasonable agreement. For such homogeneous, viscous interfaces this agreement is consistent with what has been observed in other studies.[199,195]

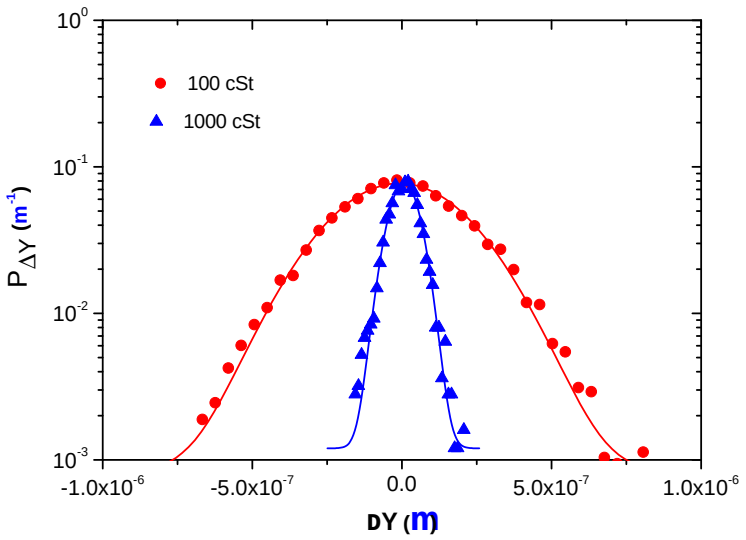

FIGURE 4.4: Probability density functions of particle displacements at 1 sec delay time of tracer particles at oil/water interface with different oil viscosities.

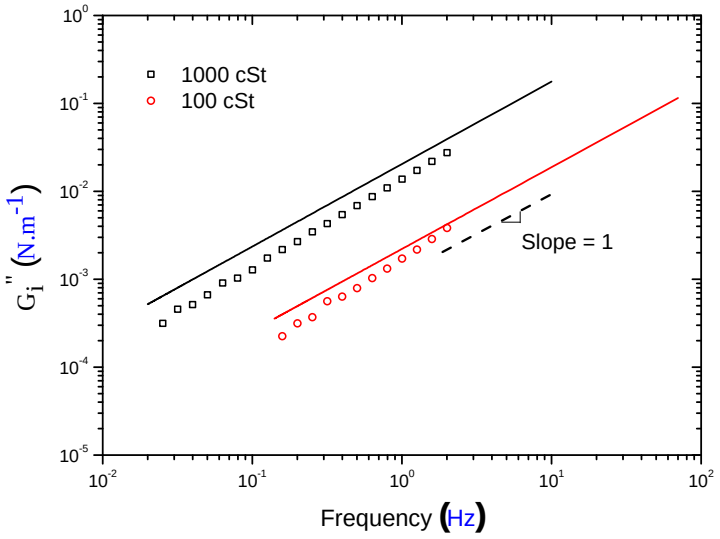

FIGURE 4.5: Comparison of G″ values obtained from microrheology (line) and shear rheology (symbols).

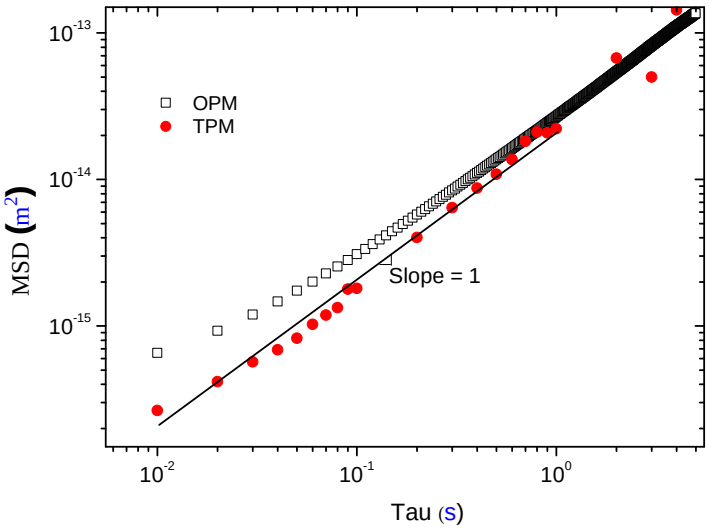

FIGURE 4.6: Comparison of MSD values at different lag times obtained from microrheology One-particle microrheology (OPM) and two-particle micrheology (TPM). The continuous line represents linearity.

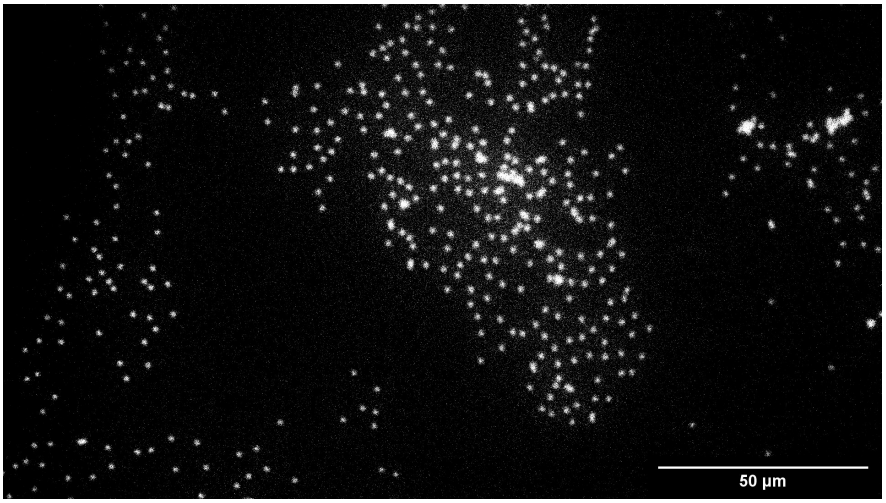

FIGURE 4.7: Fluorescent image showing aggregates of probe particles that are stuck together at dodecane/water interfaces at high particle fractions.

4.7.2 Two-point and One-Point Microrheology Comparison

The option of analysing the tracking data with two-point microrheology was explored in anticipation of possible heterogeneity of protein interfacial films. For a preliminary comparison of one-point microrheology (OPM) and two-point microrheology (TPM), a bulk (not interfacial) system was studied. A glycerol/water mixture containing equal volumes of both fluids and a highly concentrated suspension (2.6 %w/v) of 0.5 μm plain polystyrene particles was analyzed. The tracking data was used to extract the MSD of the particles using both OPM and TPM as shown in the figure 4.6. The solid line represents linearity which is the expected result for a viscous fluid such as glycerol/water. However, in such high concentrated suspensions particle-particle interactions are significant, imparting motion contributed by non-thermal forces such as particle collisions.[205] This is reflected in the difference between the MSDs especially at smaller time scales where the OPM MSD values are slightly over estimated as observed in other such systems.[206] However, to obtain the same level of accuracy of MSD values using TPM, more than 4000 particles were imaged for statistical analysis. This has been the drawback of the two-point analysis technique as it requires a large volume of tracking data.[206] When such high concentrations of particles were used at the oil/water interface rather than in the bulk, aggregation ensued and particles clustered as shown in figure 4.7. Such aggregation reduces the effective concentration of freely diffusing probe particles and modify the interface with time making their suitability questionable for this study. Therefore, lower particle concentrations were used here in order to avoid such aggregations. However, at lower particle concentrations i.e. for 20-30 particles tracked, two-point analysis leads to noisy MSD values and we conclude that, although two-point microrheology is ideal for analyzing bulk systems with potential heterogeneity arising from, for example, depletion, it is not feasible for analyzing the time evolution of protein film rheology at oil/water interfaces.

4.7.3 Monomeric and Dimeric β-lg Interfaces

Plain, non-functionalized polystyrene particles were chosen as the primary probe particles due to their neutral electrostatic nature. Image recording was typically initialized after any obvious drift effects such as sample manipulation caused due to external

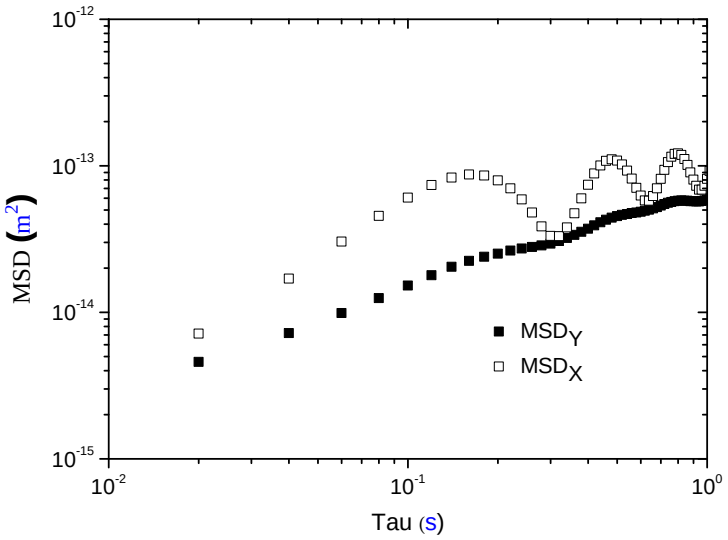

FIGURE 4.8: Typical MSD values obtained showing the static noise associated with the x-direction which is not observed in the y-direction.

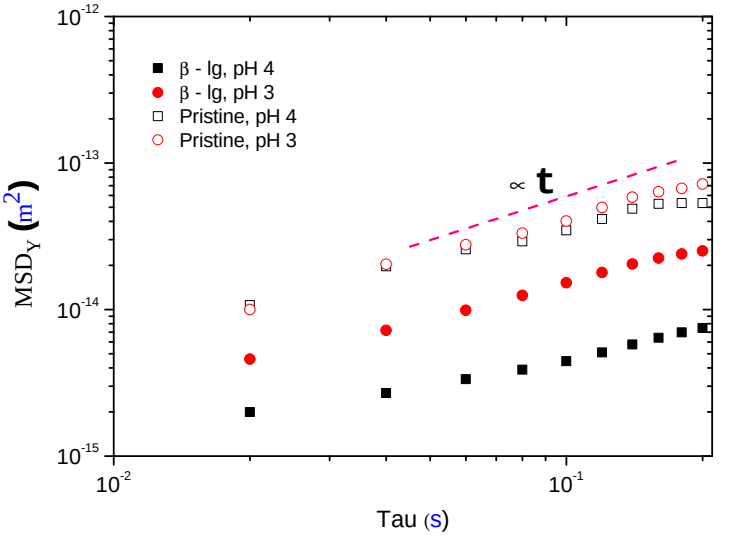

FIGURE 4.9: MSD values at different lag times compared for pristine and protein-laden dodecane/water interfaces.

stimuli dissipated which roughly amounts to around a few minutes from the formation of the oil/water interface. Despite allowing much longer equilibration times, a persistent drift as shown in figure 4.8 was often detected just in the x-direction in protein-laden and pristine interfaces. Since the measurement chamber is sealed, the source of this noise is uncertain but it is most probably related to the experimental setup such as differential heating of components from light sources, mechanical coupling from camera fans, anisotropic mechanical relaxation of the stage. As the exact origin of this noise is unknown, any data obtained using an arbitrary drift correction was assigned as questionable. Therefore, only the calculations based on y-displacements that did not display any noise issue are presented for the reminder of this study.

Our previous interfacial rheology investigation using shear rheometry revealed that the quaternary structure of β-lg directly affects the interfacial viscoelastic properties (See Chapter 2 and the paper in appendix B). The macrorheology measurements detected that interfacial films which were comprised of β-lg monomers were only viscous in contrast to the viscoelastic β-lg dimer films. To further investigate this behavior, particle tracking was carried out at dodecane/water interfaces with the same β-lg surface concentration (10.6 $mg.m^{-2}$) as that of the macrorheology measurements. The MSD values of pristine interfaces and β-lg laden interfaces are compared in figure 4.9. The displacement distributions at two different lag times for pristine dodecane/water interfaces and β-lg laden interfaces at pHs 3 and 4 are given in the figure 4.10. The probability density functions of particle displacements of the pristine interfaces are Gaussian-like and the displacements become larger at longer time scales.

Firstly, the MSD values of the protein-laden interfaces are considerably less than that of the pristine interface at pH 3. This confirms that β-lg monomers do adsorb at the interface as shown by the complexation studies at pH 3 (chapter 3) despite the fact that the monomers struggle to reduce the surface tension, or build an elastic layer (chapter 2). Secondly, when the interfacial film was made of β-lg dimers at pH 4, the MSD values are distinctly smaller than that was found for the monomeric interface which is also reflected in the probability density functions of particle displacements in figure 4.10.

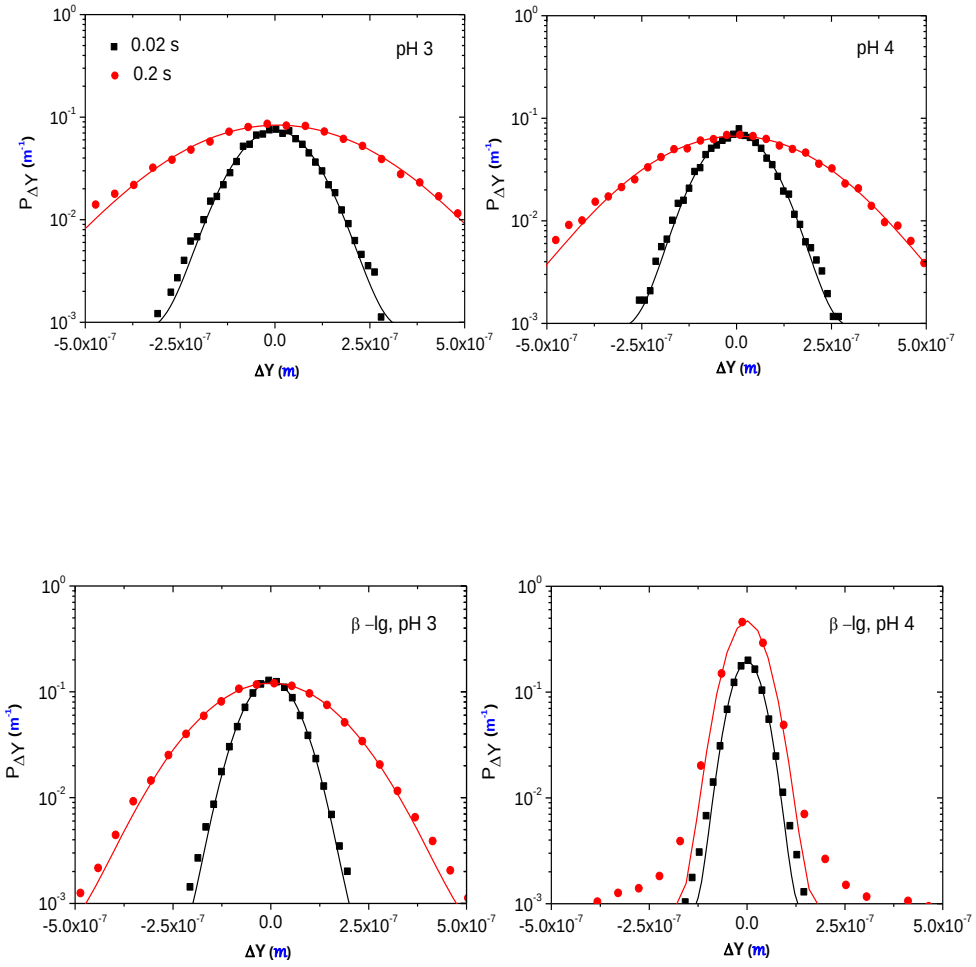

FIGURE 4.10: Probability density function of particle displacements at different lag times for plain PS 1 μm particles at pristine (top) and β-lg laden (bottom) dodecane/water interfaces at pH 3 (left) and pH 4 (right). The β-lg surface concentration is 10.6 mg.m^{-2}. The lines show the best Gaussian fit.

Further, the displacement distributions reflect a viscous interface at pH 3 as the displacements consistently increase at higher lag times. In contrast, particles at dimeric interfaces show no marked increase in displacements from a lag time of 0.02 to 0.2 seconds. Such impeded motion signifies the presence of a confinement originating from a pervasive elastic interfacial protein film structure confining the particles. This is once again in agreement with the elastic interface perceived by the shear rheology measurements. Further, the displacement distributions measured for the dimeric interface at pH 4 distinctly deviates from Gaussianity at a higher lag time of 0.2 s signalling heterogeneity at the interface.

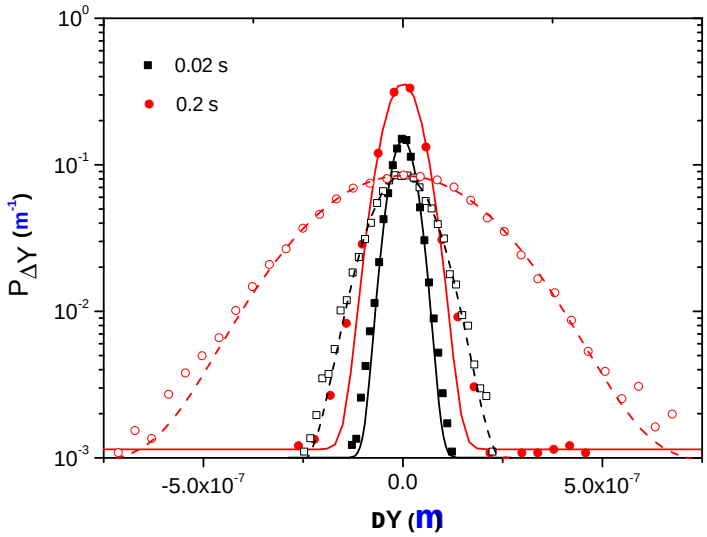

FIGURE 4.11: Probability density functions of particle displacements at various lag times of plain PS 1 µm particles (filled) and plain PS 0.5 µm particles (open) at dodecane/water interfaces at pH 4 with a β-lg surface concentration of 10.6 mg.m^{-2}. The lines show the best Gaussian fit. Lag time legends: Squares (0.02 s) and Circles (0.2 s).

The monomodal distributions of the displacements at pH 3 suggests a uniformity in protein distribution across the interface where the Gaussian variation in displacements originates from the statistics of the thermal fluctuations rather than intrinsic differences in surface rheology. However, for the β-lg dimer network at pH 4, the particle displacement distributions, reflects confined motion with a possible presence of heterogeneity due to the deviation from Gaussianity. To further investigate the nature

of this behavior, particle tracking was carried out with a smaller probe particle of diameter 0.5 μm. The probability density functions of particle displacements of the two sizes are juxtaposed in figure 4.11. The displacements of 0.5 μm particles are clearly larger than that of 1 μm at both the lag times. The dependency of particle distributions on the length scale of the probe particles, further supports pore-like confinements as shown in figure 4.13, where the smaller particle is still impeded but has a diameter length more to diffuse. Therefore, it is possible that β-lg molecules assemble at the interface eventually leading to pore-like structures of the order of ~ 1.25 μm, which is the total of diameter of the particles and the variance of the displacement distribution seen for the traced probe particles at a lag time of 0.2 sec.

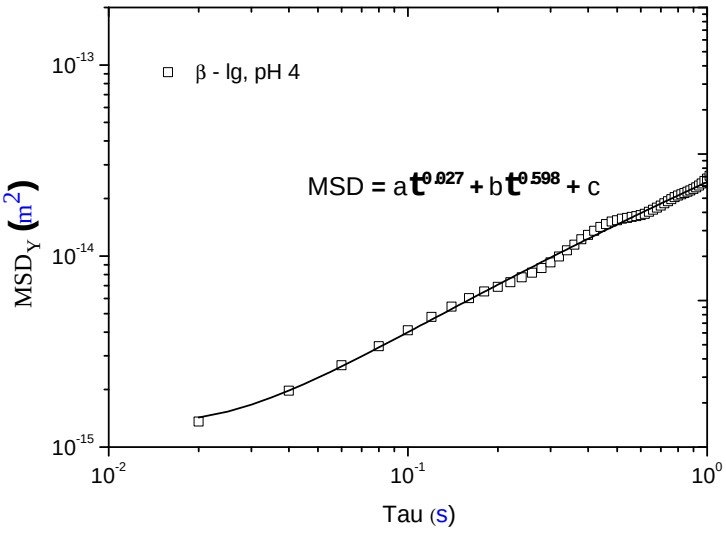

FIGURE 4.12: MSD values (symbols) of β-lg laden interfaces at pH 3 and pH 4 and their fit (lines) to the specified equations.

To compare the interfacial moduli values obtained through shear rheology and microrheology, the MSD values obtained were fitted to relevant equations to fit the time dependence of the MSD before the application of the transforms, to ensure smooth data was available for numerical differentiation as shown in figure 4.12. An equation with two time dependent power terms was used to fit the time dependence of the MSD before the application of the transforms, to ensure smooth data was available for numerical differentiation. Such functional forms have been used in the past to fit the MSDs from other viscoelastic materials, such as concentrated polyethylene oxide

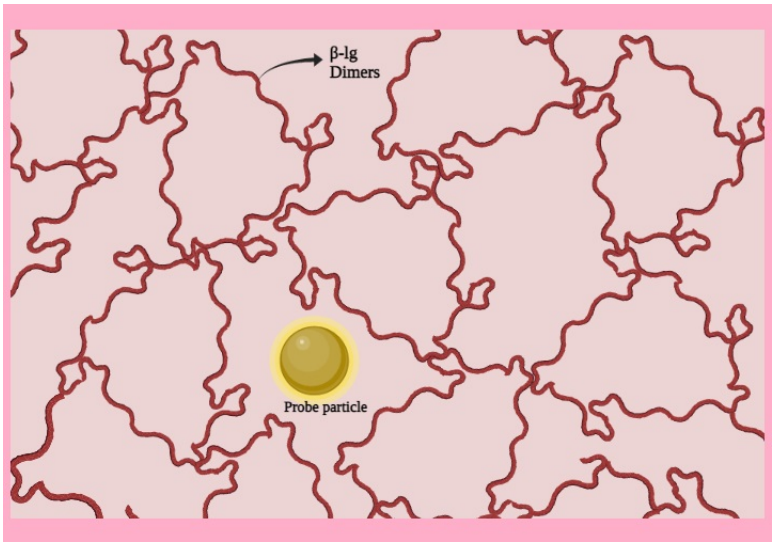

FIGURE 4.13: A depiction of a probe particle in the confinements of an entangles network established by β-lg dimers at the oil/water interface.

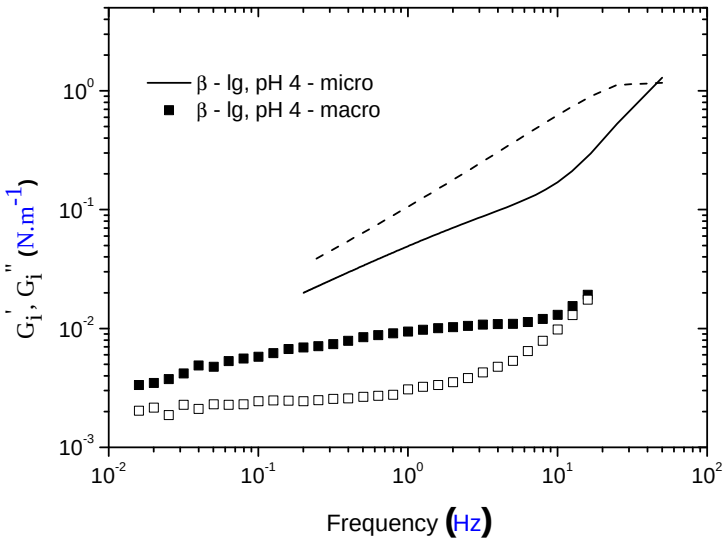

FIGURE 4.14: Comparison of G_i' (solid symbols, continuous line) and G_i'' (open symbols, dashed line) values at different frequencies obtained using shear rheology (symbols) and microrheology (lines).

solutions.[175] The fitted equations were then used to calculate the moduli values using the previously discussed method.[174] The comparison between the moduli values of the two techniques are shown in figure 4.14. Interestingly, the moduli values at pH 4 was an order of magnitude higher for microrheology as compared to shear rheology. Such order of magnitude differences have been observed in other polymer systems[194] and has been typically associated with the presence of heterogeneity.[195] Further, in contrast to shear rheology, $G_i'' > G_i'$ for microheology suggesting the particles perceive a viscous dominated region. This could be interpreted as the presence of pore-like confinements embedded in a percolating elastic dimeric network where the pores are possibly filled with viscous β-lg monomers. Moreover, both techniques indicated a region of moduli cross-over around the frequency of 20-50 Hz for the protein film at pH 4. The disparity between the moduli values obtained from both the interfacial rheology techniques will be further elaborated in the discussion section.

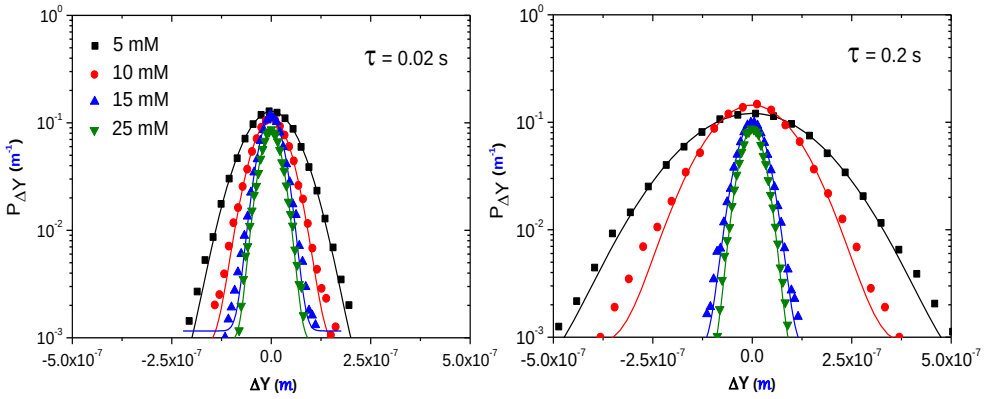

FIGURE 4.15: Probability density functions of particle displacements of plain PS 1 μm particles at dodecane/water interfaces at pH 3 and different NaCl concentrations and a β-lg surface concentration of 10.6 mg.m^{-2}. The corresponding lag times of the correlation functions shown are 0.02 s (left) and 0.2 s (right). The lines show the best Gaussian fit.

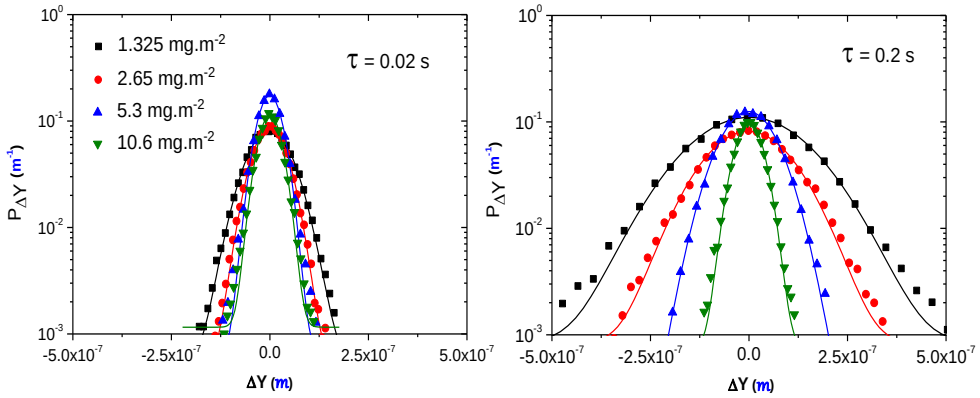

FIGURE 4.16: Probability density functions of particle displacements for plain PS 1 µm particles at dodecane/water interfaces at pH 3, 15 mM NaCl with various β-lg surface concentrations. The corresponding lag times of the correlation functions shown are 0.02 s (left) and 0.2 s (right). The lines show the best Gaussian fit.

4.7.4 Monomer-Dimer Transition

Particle motion at β-lg laden interfaces indicated a viscous-like nature at pH 3 (monomers) and a confining structure at pH 4 (dimers). Our interfacial macrorheology measurements from chapter 2 showed a clear relationship between the elastic modulus and the concentration of dimers. The rheology experiments showed that at pH 3, the oil/water interface was viscous at 5 mM NaCl and significant elasticity was observed from $\geq$ 25 mM NaCl. The C_{NaCl} at which enough dimers were present at the interface to impart elasticity and form confinements was studied further using microrheology. Particle tracking was carried out at dodecane/water interfaces prepared at 10.6 mg.m^{-2} protein concentration with 5, 10, 15 and 25 mM NaCl concentrations. The probability density function of particle displacements at various lag times are presented in figure 4.15. Although the total protein concentration was the same in all the samples, a clear reduction in particle displacement was observed with higher salt concentrations. The increase in salt concentration might in any case be expected to contribute to the denser packing of proteins. However, a considerable reduction in displacements are seen from 10 mM to 15 mM NaCl concentration which can be seen in figure 4.15. In addition, the probability density function for 10 mM at higher

lag times show a marginal deviation from Gaussianity suggesting heterogeneity. This suggests that the nature of this transition from a disordered interface to the presence of a pervasive network is drastic and not just based on salt concentration but probably on the generation of a critical percolating dimer concentration as well.

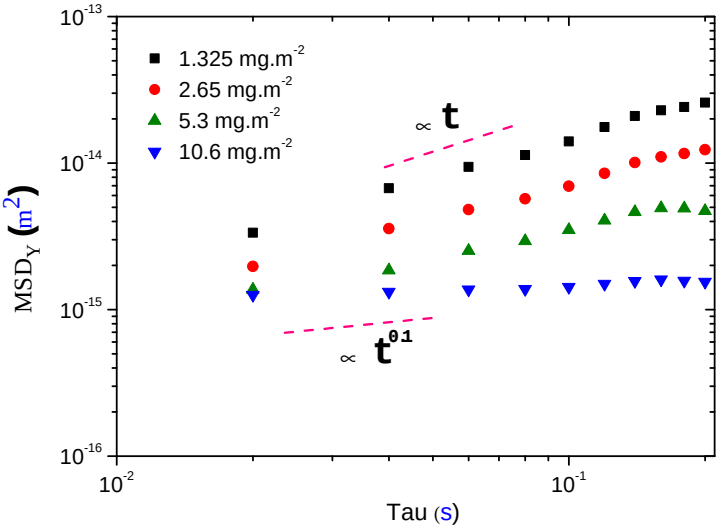

FIGURE 4.17: MSD values at different lag times compared for dodecane/water interfaces with different β-lg surface concentrations.

The surface protein concentration at the oil/water interface increases during the formation of a protein interfacial film. To further capture the nature of the transition observed at different salt concentrations as the amount of protein dimer changes concurrently, particle tracking was carried out at interfaces with 10.6, 5.3, 2.65 and 1.325 mg.m^{-2} β-lg total possible surface concentrations at pH 3. Based on the previous result the C_{NaCl} was chosen to be 15 mM NaCl to maximise the chances of observing any transition. The particle displacement distributions of these results are shown in figure 4.16. The corresponding MSD values at different lag times for these interfaces are shown in figure 4.17. The displacement distributions are very similar at a lag time of 0.02 s. However, at the lag time of 0.2 s, the distributions for concentrations $>$ 2.65 mg.m^{-2} resemble the interface at pH 4. Moreover, the displacements of probe particles of systems with $>$ 2.65 mg.m^{-2} do not change considerably at different lag times suggesting the formation of a constraining structure. It is therefore possible that β-lg

forms a percolating network with confinements at the interface at a surface concentration of > 2.65 mg.m^{-2}. These numbers are very similar to the critical interfacial β-lg concentrations (1.80 - 2.69 mg.m^{-2}) measured at oil/water interfaces using other techniques.[207] Similar transitions with time were observed for microrheology of dilute β-lg films at decane/water interfaces.[54]

4.7.5 Protein/Polysaccharide Complexes at Interfaces

We have learnt from macrorheology that the HMPs, HG-60 and Dp7 poly and oligosaccharides lead to a strengthened interface when complexed with β-lg (See Chapter 3 and the paper in appendix B). We proposed that the polysaccharide sits just beneath the interface interconnecting the adsorbed proteins and thereby providing additional elasticity by cross-linking. To gain further understanding on the aforementioned inferences, particle tracking experiments were performed at dodecane/water interfaces for β-lg/polysaccharide mixed solutions at pH 4. The protein surface concentration was 10.6 mg.m^{-2} while the weight ratio of protein/polysaccharide was maintained at 1:0.25. The probability density functions of particle displacements are shown in figure 4.18. The corresponding MSD values at different lag times for all the polysaccharide complexes are compared with that of the pure protein in figure 4.19.

All the systems with additional polysaccharides (except Dp7) clearly exhibited smaller MSD values than the pure protein solution as expected from the interfacial macrorheology. Due to the small displacements of the probe particles in these reinforced systems, the MSD values were noisy making it difficult to provide a fit for the plot to extract the moduli values, but the alignment with the results obtained in Chapter 3 is clear. The Dp7 system at pH 4 exhibits larger displacements than pure protein layer and closer to the pristine interfacial measurements. It is possible that Dp7-induced protein aggregation might lead to a few barren patches at oil/water interface leading to larger displacements. Besides, these measurements were taken after 6 hours, which might still be insufficient duration for complete layer build up (recall the slow kinetics of decoupling of this highly charged oligosaccharide and the protein). The HG-60 system showed the least MSD which was very near to the minimum

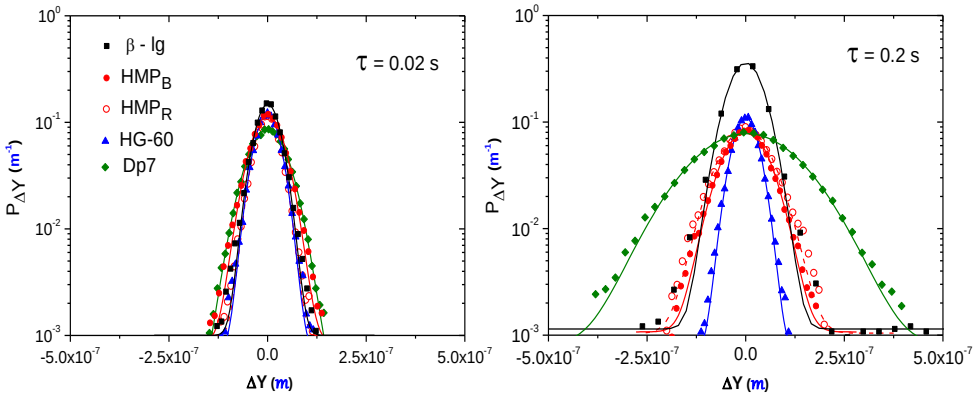

FIGURE 4.18: Probability density functions of particle displacements for plain PS 1 μm particles at dodecane/water interfaces at pH 4 with various β-lg/polysaccharide complexes at a weight ratio of 1:0.25 The corresponding lag times of the correlation functions shown are 0.02 s (left) and 0.2 s (right). The lines show the best Gaussian fit.

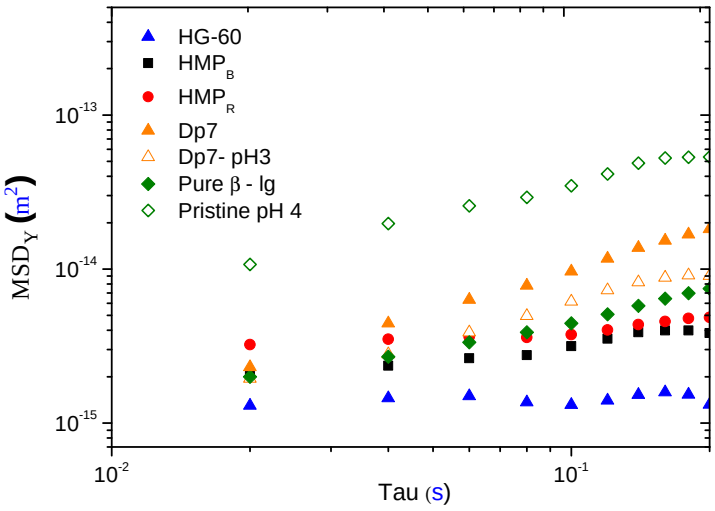

FIGURE 4.19: MSD values at different lag times compared for dodecane/water interfaces with different β-lg/polysaccharide complexes at pH 4.

resolvable MSD of 0.001 μm^2. The probability density function of particle displacements reflects the same at lag time of 0.2 s as shown in figure 4.18. Further, the deviation from Gaussianity which is observed for the pure protein at pH 4 subsides for the protein/polysaccharide complexes. The more homogeneous film structure of protein/polysaccharide complexes could be due to the presence of polysaccharides just beneath the interfacial protein films.[45] Dp7 was complexed with β-lg at pH 3 as well for further comparison as shown by the open symbols in the figure 4.19. However, β-lg/Dp7 complexes at pH 3 did form an interfacial film more quickly in further agreement with the smaller lag times observed in shear rheology for β-lg/Dp7 complexes at pH 3.

4.8 Discussion

In agreement with previous works, the interfacial network formation of β-lg at pH 4 was reflected in the shorter displacements of probe particles as compared to the pristine interface.[54] This is consistent with the macrorheology results presented in chapter 2 and is consistent with the hypothesis that β-lg dimers are the elastic network building units of the protein. Although β-lg/polysaccharide complexes at pH 3 established viscoelastic layers as shown in chapter 3, the reduced MSD values for β-lg monomers at pH 3 as compared to the pristine interface, conclusively shows that the monomers do adsorb by themselves. In addition, in contrast to β-lg dimers, the particle distribution displacements at monomeric interfaces remained Gaussian with no ordered structure perceived. Lee et al. observed localized motion for β-lg at longer adsorption times for both oil/water and air/water interfaces.[54,193] It was suggested that this could be due to the displacement of probe particles from the interface by the growing protein layer. It was also added that these displaced particles might get entrained in the secondary sub-protein layers adsorbed just beneath the interface. However, the surface β-lg concentration used in this study is 25 times less than that used in the study by Lee et al.[54] Therefore, the formation of multiple layers at the oil/water interface is highly unlikely in this study. Hence, it is proposed that the localized motion of particles observed on β-lg laden interface at pH 4 reflects the texture of the interfacial protein layer itself and not the properties of the sub-layers as previously suggested.[193]

In complete contrast to pristine PDMS/water interfaces, for β-lg laden interfaces at pH 4, the disparity between macrorheological and microrheological data was not only qualitative but also quantitative. While macrorheology perceived an elastic dominated interface, microrheology perceived viscous-dominated regions. This could be due to a variety of reasons. Firstly, it is important to be cognizant of the fact that while macrorheology measurements were performed at a higher strain amplitude as compared to the passive microrheology. Therefore, DWR geometry measures a much more strained β-lg layer as compared to the equilibrated protein layer in microrheology. Secondly, the greater immersion of the DWR geometry incorporates the values of the thinner subphase much more than a micron sized probe particle. This could be a reason for the higher moduli values for microrheology. However, this still cannot explain the qualitative contrast of $G_i'' > G_i'$ (micro) and $G_i' > G_i''$ (macro). Monolayers of hexadecanol also exhibit difference in trends in macrorheology and microrheology.[195] This discrepancy was suggested to originate from the compressibility of hexadecanol assemblies due to their fractal nature inducing complex flow fields at the interface.[208]

β-lg layers at pH 4 exhibited length-scale depended behavior when probed with particles of two different sizes. The difference in variance of the particle displacements at higher lag times were roughly the difference of their diameters, suggesting pore-like confinements at the interface of the order of 1.25 μm. In combination with the deviation from Gaussianity of the particle displacements observed at pH 4, these results strongly suggests a heterogeneity at the interface. We suspect that β-lg dimers form interlinked, elastic networks in a sea of β-lg monomers at the interface as depicted in figure 4.13. This could possibly explain as to why the microparticles, which are just of the order of the confinements perceive viscous-dominated regions as compared to the elastic-dominated network in macrorheology.

Further, pure protein layer measurements at different salt concentrations showed a sharp transition from the mildly heterogeneous interface at 10 mM NaCl to an elastic interface with pore-like confinements at 15 mM as the amount of β-lg dimers passes a critical level. The sharpness in the transition corresponds to protein surface concentration from 2.65 $mg.m^{-2}$ to 5.3 $mg.m^{-2}$. At these conditions roughly 0.002 % of β-lg exists as dimer. The surface concentrations are in very good agreement with the surface concentrations needed for β-lg monolayer formation as measured using other

techniques.[207] The sharpness of this transition resembles the substantial drop in diffusivity of the probe particles at oil/water interfaces observed by Lee et al. which happened in a span of few minutes.[54] These results point out that the elasticity of the interfacial film does not linearly increase with time, but rather it increases it a non-linear fashion, as would be expected for a percolation process. Such sharp increases in interfacial strength have also been observed for other interfacial assemblies.[201,209] These abrupt events also support the idea that breaking and reforming events may occur in β-lg film formation as the kinetically arrested system struggles towards equilibrium, as suggested from the results of chapter 2.

Particles adsorbed at oil/water interfaces laden with β-lg/polysaccharide complexes exhibited smaller displacements as compared to the pure protein film. This could either be due to denser packing of complexed protein molecules or the micron sized probe particles perceiving the polysaccharide layer just beneath the interface.[45] In either case, this is once again consistent with the higher strengths observed for complexed interfaces in shear rheology. From the particle displacement distributions it was observed that the heterogeneity which was observed for pure protein interfaces at pH 4, almost vanished for interfaces with β-lg/polysaccharide complexes. Moreover, while all the β-lg/polysaccharide complexes showed similar displacements of the probe particles at the interface, the displacements in the interface formed with β-lg/HG-60 complexes were marginally smaller. This is in agreement with the shear rheology data which also showed that β-lg/HG-60 complexes formed the strongest interfaces at higher polysaccharide concentrations. These observations indicate tighter packing of β-lg/HG-60 complexes, which could be due to the lack of side chains in HG-60 as compared to that of the HMPs. This enables a HG-60 molecule to concatenate multiple β-lg molecules at close proximity due to its more linear nature. These results point out that although the polysaccharide is not directly present at the interface, by altering the fine structures of the polysaccharide it is possible to tune the tapestry of the β-lg interfacial films.

4.9 Conclusions

The objective of this chapter was to investigate the microrheology of β-lg and β-lg/polysaccharide films and compare the results with the macrorheology inferences presented in the previous chapters. The contrasting microrheology measurements of β-lg monomers at pH 3 and β-lg dimers at pH 4 is in agreement with the macrorheology measurements of chapter 1. The impeded particle motion at dimeric interfaces indicated the presence of a pervasive structure corroborating the elastic nature of β-lg dimers and is consistent with the hypothesis that the β-lg dimers are the elastic network building units at oil/water interfaces. The probability density functions of particle displacements also uncovered evidence of pore-like confinements of the order of 1.25 μm which is presumably filled with β-lg monomers while the percolating, elastic network is made of β-lg dimers.

The transition from an inelastic to an elastic interface was found to be abrupt suggesting the protein layer formation is a critical process. These sharp transitions observed are consistent with previous microrheology of β-lg at oil/water interfaces.[54] Such abrupt interfacial evolution with increase in protein concentration supports the possible kinetic trapping and subsequent non-equilibrium evolution of the films with the potential breaking and reforming of β-lg film consistent with the events observed in shear interfacial rheology. The number of dimer units (56 ng.m^{-2}) needed to form an elastic interface corresponds to an area fraction occupancy of 5×10^{-6}, a surprisingly small occupation needed to form a percolated network at the interface but consistent with the extended linear nature of the associations previously observed and predicted by the dimer coupling model.

Microrheology of all the β-lg/polysaccharides complexes at oil/water interfaces show that they are slightly denser interfaces and more homogeneous as compared to the pure protein solution at pH 4. These observations are once again consistent with the macrorheology data and the observation that the polysaccharide lies just beneath the interface. Further, elastic-like interfaces were observed when β-lg/Dp7 complexes were made to form an interfacial film at pH 3 supporting the cross-liking mechanism of the polysaccharide molecules proposed in chapter 3. These results point out the tunability of β-lg/polysaccharide film topology and strength by controlling the fine

structures of the polysaccharide partner.

Chapter 5

Summary and Future work

5.1 Summary

The simplification of macromolecular entities such as globular proteins to rigid colloidal particles has come under considerable scrutiny recently. Sarangapani et al., pointed out that the protein's capacity to rearrange its structure and there by the nature of interprotein interactions in response to the aqueous conditions and concentration severely limits such a colloidal approach.[210,211] Such a colloidal approach can therefore hinder the fundamental understanding of the behavior of globular proteins. The underlying inferences of this thesis further questions the above mentioned colloidal approach in explaining the rheological behavior of interfacial β-lg assemblies. The effect of hydrophobic interactions on top of electrostatic interactions on the subsequent protein structure is reflected in the bi-functionality of β-lg. This thesis further gives insights into the dynamic buildup of β-lg assemblies at the oil/water interfaces. Further, the behavior of β-lg/polysaccharide complexes outlines that the importance of the role of fine structural details of the molecules rather than their overall characteristics such as the net charge and length of the polysaccharide. These findings will help in designing better molecular delivery systems by making specific recombinant proteins and polysaccharide molecules. Overall, this thesis demonstrates how interfacial rheology of proteins can be employed to infer structure-function relationship of proteins. These findings are further elaborated in the sections below.

5.1.1 Bi-Functionality of β-Lactoglobulin

The primary intention of this study was to explore the feasibility of understanding biomolecular assemblies at oil/water interfaces using rheological techniques. The results demonstrate that interfacial rheology is capable of revealing fundamental structural manifestations of protein molecules at nanomolar protein concentrations. Interfacial shear rheology proved to be sensitive enough to perceive the formation of a monolayer of β-lg molecules at very low surface concentrations ($\sim$ 2.65 mg.m^{-2}). It was deduced from the interfacial shear rheology measurements that β-lg dimers are the elastic network building blocks of the protein at oil/water interfaces. When β-lg was present predominantly in the monomeric form at the interface, no elasticity and no interfacial tension reduction was detected in tensiometry indicating lesser number of contact points at the interface. However, the complexation studies at pH 3 in chapter 3 and microrheology studies at chapter 4 conclusively showed the presence of β-lg monomers at the interface. The inability of β-lg monomers to impart elasticity to the interface was attributed to the the presence of only one free thiol group in cys 121 which can only form non-native dimers at the interface. On the other hand, native β-lg dimers with two free thiol groups can interlink through disulfide bridging to form a percolated, cross-linked network from long linear aggregates that can entangle and impart elasticity.

β-lg was conveniently classified as a lipocalin due to its structural similarity with the plasma retinol binding protein. However, the quest to find out the exact physiological functions of this whey protein is still not complete.[212] The presented results, unambiguously establish a relationship between bovine β-lg's quaternary structure i.e. monomer/dimer species and the protein's interfacial rheological properties. Such a relationship has not been revealed for any other mammalian protein to the author's knowledge. The existence of a bi-functionality shows that transport might not be β-lg's only physiological function. Another protein with a strikingly similar relationship between the quaternary structure and interfacial functionality is the bacterial hydrophobin, biofilm surface layer protein-A (BslA) from *Bacillus subtilis*.[120]

5.1.2 Heterogeneity and Non-linearity

The macro rheology inferences were corroborated by microrheology which further resembled an entangled network made of β-lg dimers confining viscous domains filled with monomers. When the buildup of this network was further investigated, a drastic change from an viscous, disordered film to an elastic, entangled network was observed above a beyond concentration of 2.65 mg.m^{-2}. Such an abrupt evolution during adsorption has been observed for β-lg, β-casein and other systems.[54,199,213] This sharp transition in protein formation indicates a non-linear way of building up the interface along with possible signs of non-equilibrium dynamics which was observed in macrorheology. The area fraction that is needed to be occupied by β-lg dimers to form a perceivable elastic film at pH 3, 15 mM NaCl is a surprisingly low number of 5×10^{-6}. This number is a further testament to the linear nature of the interfacial assemblies consistent with the proposed model.

5.1.3 Tunable β-lg/Polysaccharide Complexes

The aforementioned structural-rheology relationship of β-lg was extended to understand β-lg/polysaccharide complexes at the interface. This study demonstrated the role of polysaccharide's fine structures such as the local charge distribution and the length of the polysaccharide in determining the interfacial properties of the complexes at pH 4. Diffusion time of the complexes contributed a minimal role in the kinetics of interfacial film formation. Polysaccharides carrying blocks of negative charges delayed the protein adsorption which was evident through rheology as well as tensiometry. When the polysaccharide was added to pre-formed β-lg films at oil/water interfaces, this delay nearly vanished. This conclusively showed that the protein's reshuffling at the interface to partially dissociate from the polysaccharide and adsorb at the interface is the critical step in β-lg/polysaccharide complexes adsorption.[82] This crucial role of the local charge distribution also explains the limited surface activity of β-lg/LMP complexes.[45] Interestingly, the quaternary structure of β-lg also played a role in the kinetics of β-lg/polysaccharide adsorption. Further, microrheology perceived that the heterogeneity which was observed for the pure β-lg interfaces at pH

4 is not present for interfaces laden with β-lg/polysaccharide complexes. These results show that the fine structure of the polysaccharide partner can be used to tune the kinetics of adsorption and final interfacial strength as well as the architecture of β-lg interfacial films. The ability to dictate such parameters can be of potential use of protein/polysaccharide complexes in drug delivery applications.

5.1.4 Mechanism of Polysaccharide Reinforcement

The final interfacial strength of all the investigated polysaccharides (except LMP) reinforced the interface exhibiting greater strengths at higher polysaccharide concentrations before saturating. Interestingly, β-lg monomer which was unable to form an elastic interfacial film by itself, managed to do so when complexed with polysaccharide molecules. Based on this result, it was proposed that the mechanism by which a polysaccharide increases the strength of the interface is by establishing cross-links in the protein layer and thereby reinforcing it. These additional cross-links will decrease the mobility of the protein film at the interface and thereby imparting elasticity. Establishment of cross-links by polysaccharides can be achieved by concatenating multiple β-lg units as well as complexation-induced protein aggregation.[141] The final interfacial strength was directly related to the number of junctions as well the charge density of the protein binding sites in the polysaccharide. Preliminary emulsion studies showed that HMPs if used in the right ratios ($\sim$ 1:1) can improve the emulsifying capability of β-lg by reducing the drop size and extending the shelf life. Below this concentration the pectins retarded the emulsification by forming larger emulsion drops which was attributed to the presence of β-lg clusters that will impede effective protein distribution at the interface.

5.2 Future Work

Although this study has empirically elucidated the structure-function relationships in β-lg and β-lg/polysaccharide complexes using interfacial rheology, these findings further generate new questions. The following list includes the ideas that I feel are worth testing out, as well as experiments that were left out due to lack of time.

5.2.1 Role of β-lg Monomer

While the interfacial role of the β-lg dimers is clear to a reasonable degree, the role of the β-lg monomer still remains ambiguous. The monomer neither imparts elasticity nor reduces the interfacial tension, the two most common behavior seen in overwhelming majority of globular proteins. Dilitational rheology at monomeric interfaces with low protein concentrations might reveal if β-lg monomers contribute to the compressibility of protein films as was observed for BslA, a bacterial hydrophobin.[214] The presence of such a function for the β-lg monomer would provide further clues for other non-transport physiological functions. Further, investigating the existence of such bi-functionality in non-bovine β-lg from other suitable mammals might improve our understanding on the evolution of this whey protein.

5.2.2 Verification of Di-Sulfide Bridging

The network building ability of β-lg dimers was attributed to the availability of thiol groups to engage in percolating network formation at the interface through disulfide bridging. There is still a degree of uncertainty to this claim as it is yet to be conclusively verified despite some supporting previous measurements.[83] If such disulfide bonds are present, they should exist in the hydrophobic phase of the interface.[94] Therefore, adding a reducing agent that is soluble in organic liquids such as 2-(Dibenzylamino)-butane-1,4-dithiol[215] to break the disulfide bonds of the β-lg dimers might provide concrete evidence of the role of disulfide bonds. Alternatively, experiments at pH 4 with a modified β-lg in which the cysteine-121 is modified with mercaptopropionic acid and mercaptoethanol without affecting the secondary structure,[58] could also settle the argument.

5.2.3 Imaging of β-lg films

The microrheology results strongly suggested the presence of an heterogeneous network of β-lg films, especially at increasingly dimeric concentrations. Such a presence of heterogeneity could affect the homogeneous distribution of particles and thereby providing incorrect measurements of the films.[195] Therefore, to fully understand the topology of β-lg's film structure, imaging of Langmuir monolayers at oil/water and

air/water interfaces are required. Therefore, observing the formation of the labelled protein films through fluorescent microscopy could give us a better understanding of the structure. For this purpose, flurophores such as 6-carboxyrhodamine 6G succinimidyl ester[216] and 2-(4'-maleimidylanilino)naphthalene-6-sulfonate[217] could be employed. In addition, Brewster angle microscopy could also be used to visualize the real time formation of β-lg monolayers at different dimer concentrations. This will provide quantitative structural analysis about the lateral organization of β-lg molecules at fluid/fluid interfaces.

5.2.4 Comprehensive Microrheology

A comprehensive microrheology of β-lg/polysaccharide complexes at different protein:polysaccharide ratios was unable to be carried out due to lack of time and the COVID19 pandemic outbreak. Interfacial shear rheology in this study shows that at higher polysaccharide concentrations, the final elastic strength of the film is marginally higher till a ratio of 1:0.25 beyond which no increase in strength is seen. Passive microrheology at oil/water interfaces with a constant protein concentration but different different polysaccharide ratios such as 1:0.125, 1:0.5 and 1:1 would further enhance our understanding of the role of polysaccharide at the interface. Such a study would reveal information about the distribution of protein clusters in these complexes and how they assemble at the interface. Further, probing the interface of β-lg/polysaccharide complexes at pH 3 will provide greater understanding of the β-lg monomer/polysaccharide binding.

5.2.5 Complementary Emulsion Studies

Importantly, most emulsion results based on β-lg have to be reinterpreted to accommodate the dimer-monomer bi-functionality. This implies that theβ-lg's emulsifying behavior at extremely acidic conditions (such as pH 3) and extremely basic conditions (such as pH 9) is not just due to the net charge of the molecule but also its quaternary state in the solution. However, during emulsification, the protein is not given enough time for unraveling and therefore the lag times observed in standing interface experiments may not be relevant. Therefore, a possible way to gain the understanding of the

quaternary structure of β-lg on emulsification is to analyze the emulsions prepared at pHs 2 and 3 with salts of different chaotropicities such as NaCl and $NaClO_4$. The size of the emulsion droplets and their subsequent stability might provide some valuable insights. In addition, the rheology of such emulsion systems might reveal how the elastic nature of the droplet surfaces vary across these emulsions.

The preliminary results of β-lg/HMP complexes in chapter 3 suggested an optimum protein:pectin ratio beyond which the polysaccharide enhances the emulsification property of β-lg. This is counter intuitive to the interfacial shear rheology data which measured almost similar values of elastic strength at most protein/polysaccharide ratios. We suspect this might be due to the different size of protein clusters induced by these polysaccharides. A comparative study of the size and stability of emulsions at pHs 3 and 4 prepared with β-lg/HMP_B and β-lg/HMP_R complexes with different polysaccharide concentrations will tease out the role of such protein cluster size in the complexes. Further, probing the stability of these emulsions using shear rheology might reveal further information about the role of the polysaccharide in emulsification. For this purpose, comparing emulsions formed by β-lg/HMP_R, β-lg/HG and β-lg/Dp7 complexes could clarify the role of the viscosifying effect of the polysaccharide partner in the emulsion stability.

5.2.6 Tunable Mechanical Interfaces

The mechanical properties of extracellular matrices can dictate the functionality of cells and microorganisms. To conduct such investigations, biomimetic soft matter systems typically synthetic polymers are employed with tunable mechanical properties in analyzing the behavior of biological materials.[218] The monomer-dimer functionality makes bovine β-lg an ideal candidate for creating bio-friendly fluid/fluid interfaces with tunable elastic and loss modulus by changing the monomer/dimer ratios. Further, the fine structures of the polysaccharide can also be used to dictate the architecture of the films to analyze the cell's behaviors in different environments.

Appendix A

Supplementary Results

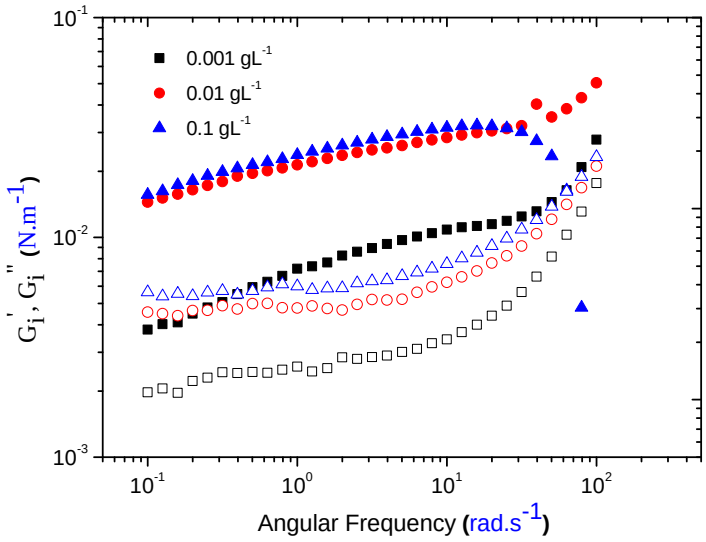

FIGURE A.1: G′ (solid) and G″ (hollow) from frequency sweeps of β-lg solutions at various concentrations at dodecane/water interface.

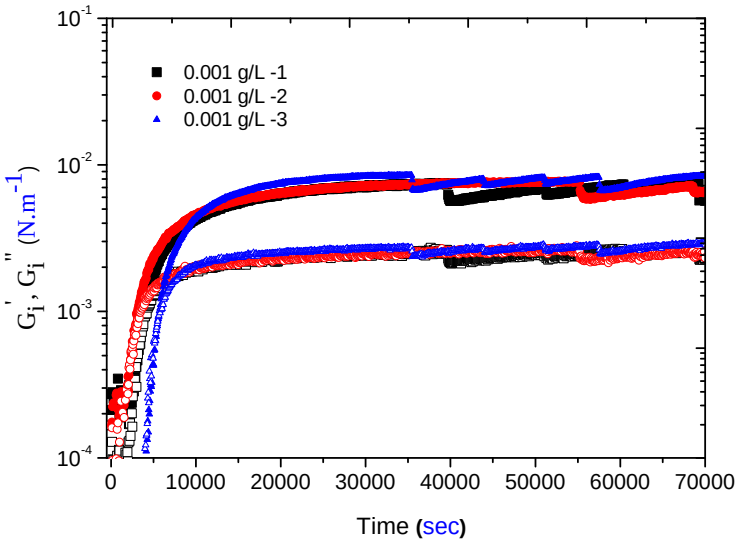

FIGURE A.2: Repetitions of time evolution of G′ (solid) and G″ (hollow) at dodecane/water interfaces with 1 mg.L^{-1} subphase β-lg concentration (pH 4, 5 mM NaCl).

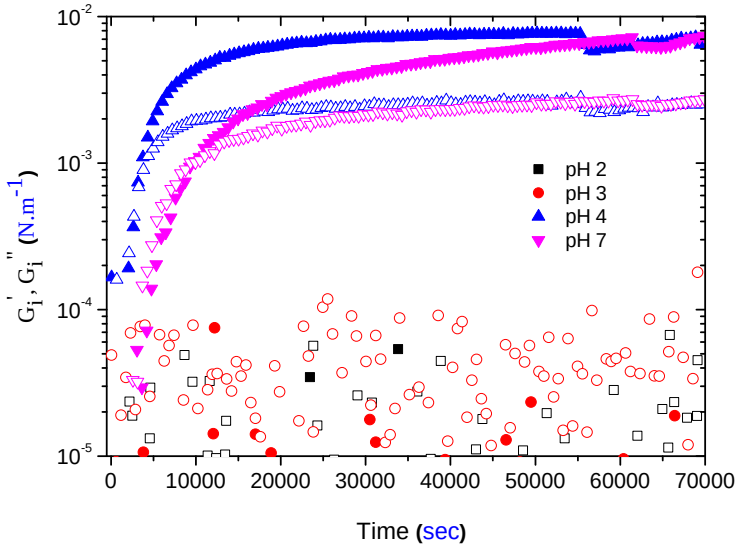

FIGURE A.3: Time evolution of G′ (solid) and G″ (hollow) at dodecane/water interfaces with 1 mg.L^{-1} β-lg subphase concentration and various pHs.

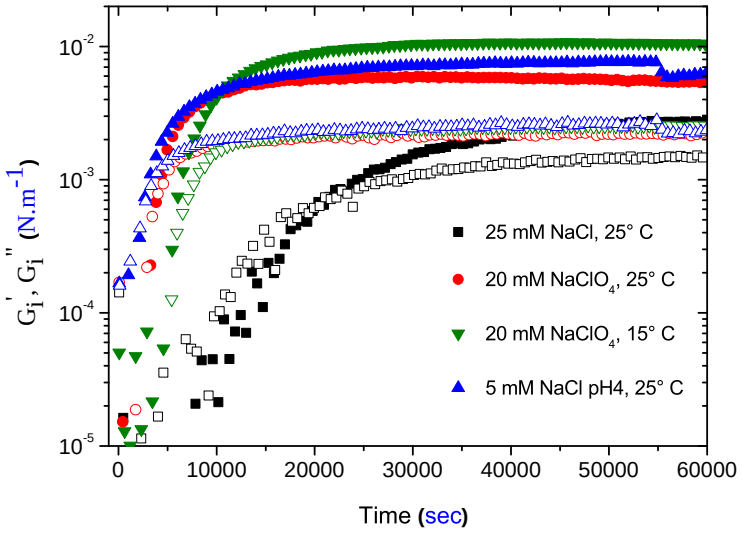

FIGURE A.4: Time evolution of G′ (solid) and G″ (hollow) at dodecane/water interfaces with 1 mg.L^{-1} β-lg subphase concentration and various ionic conditions and temperatures.

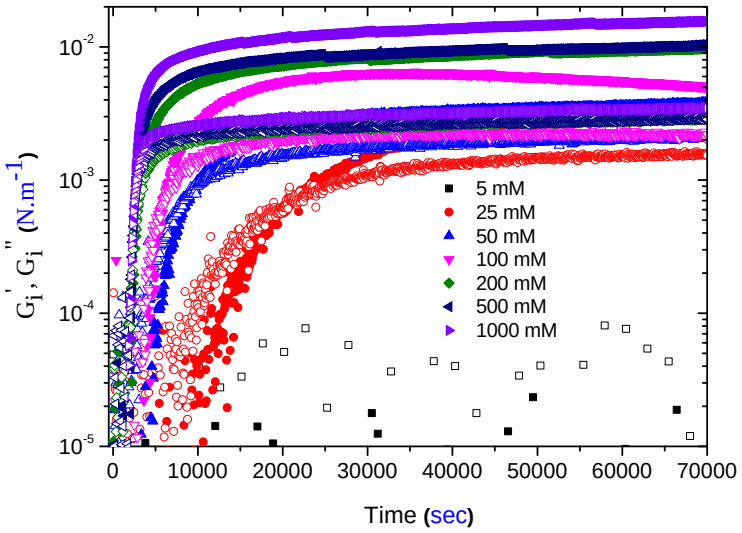

FIGURE A.5: Time evolution of G_i' (solid) and G″ (hollow) at dodecane/water interfaces with 1 mgL^{-1} β-lg subphase concentration and various NaCl concentrations at pH 3.

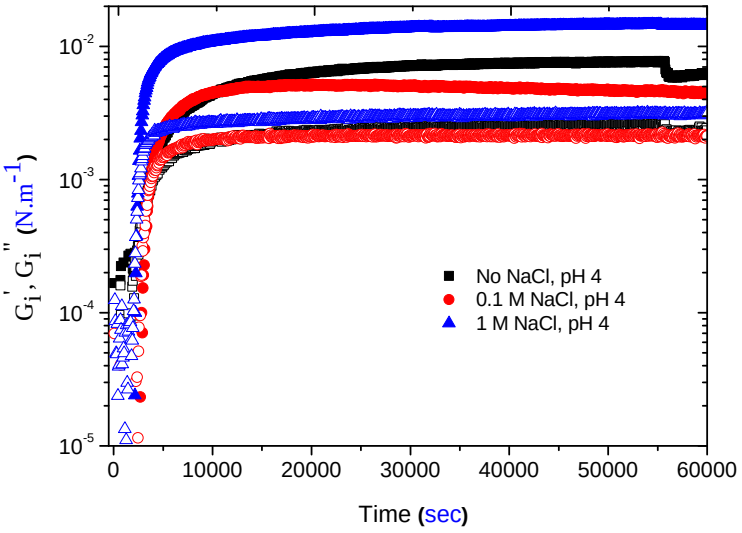

FIGURE A.6: Repetitions of time evolution of G′ (solid) and G″ (hollow) at dodecane/water interfaces with 1 mg.L^{-1} subphase β-lg concentration in pH 4 and various ionic strengths

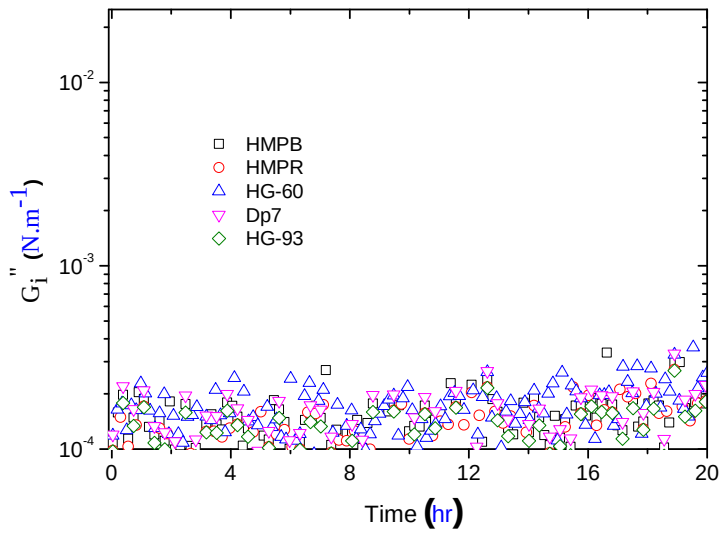

FIGURE A.7: Time evolution of G″ at dodecane/water interface with of 1 mg.L^{-1} subphase solutions of various polysaccharides at pH 4.

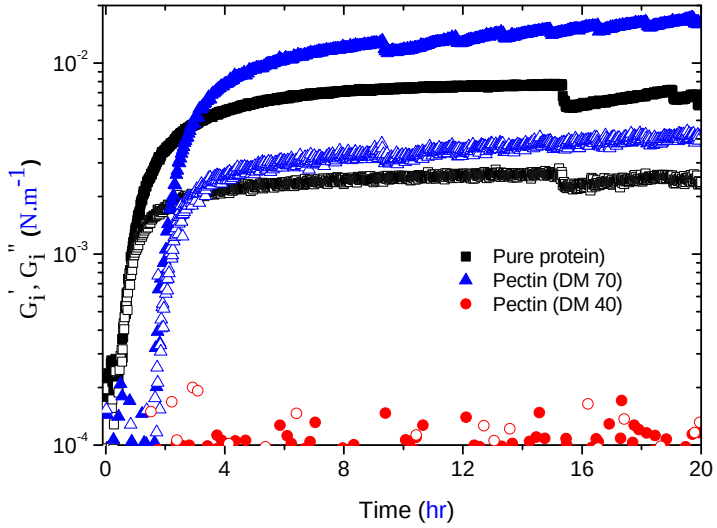

FIGURE A.8: Time evolution of G_i' (solid) and G″ (hollow) at dodecane/water interfaces with 1 mg.L^{-1} subphase mixed solutions of β-lg/pectin complexes with pectins of various DMs in pH 4.

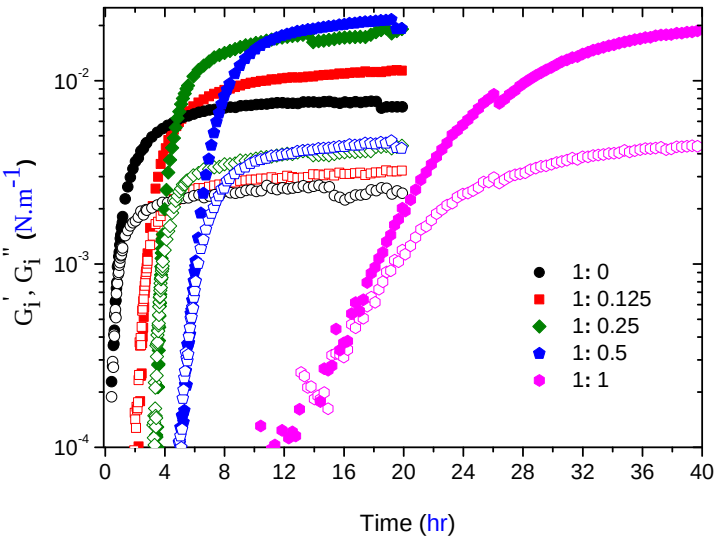

FIGURE A.9: Time evolution of G_i' (solid) and G″ (hollow) at dodecane/water interfaces with 1 mg.L^{-1} subphase mixed solutions of β-lg/HMP$_B$ complexes with various weight ratios of pectins in pH 4.

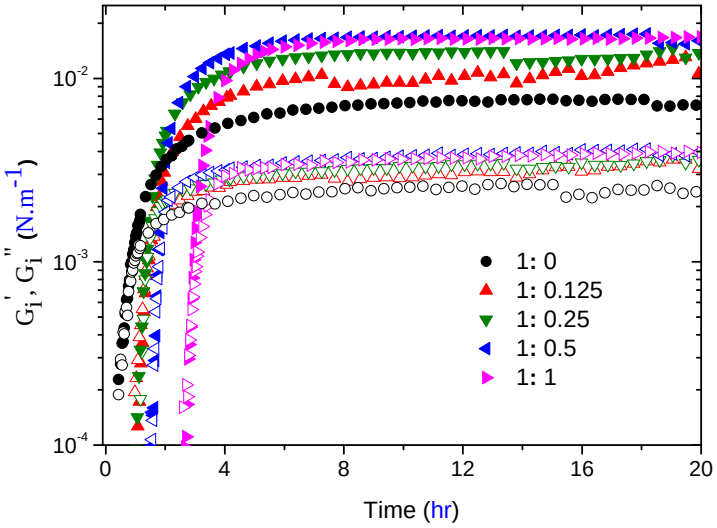

FIGURE A.10: Time evolution of G_i' (solid) and G″ (hollow) at dodecane/water interfaces with 1 mg.L^{-1} subphase mixed solutions of β-lg/HMP$_R$ complexes with various weight ratios of pectins in pH 4.

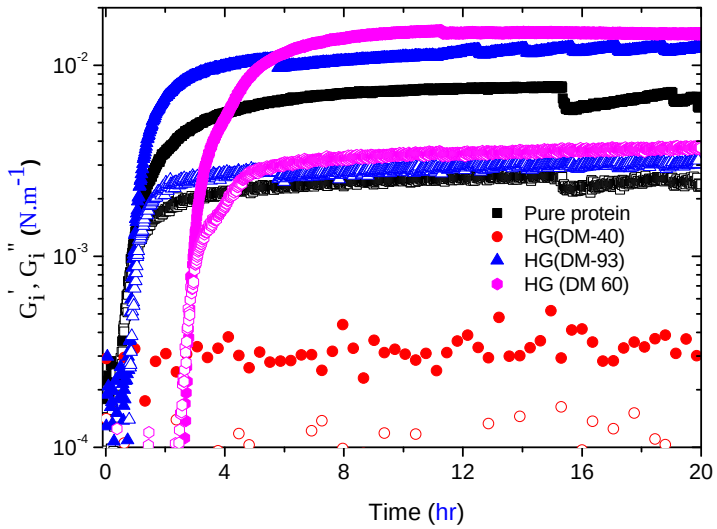

FIGURE A.11: Time evolution of G_i' (solid) and G″ (hollow) at dodecane/water interfaces with 1 mg.L^{-1} subphase mixed solutions of β-lg/pectin complexes with pectins of various HGs in pH 4.

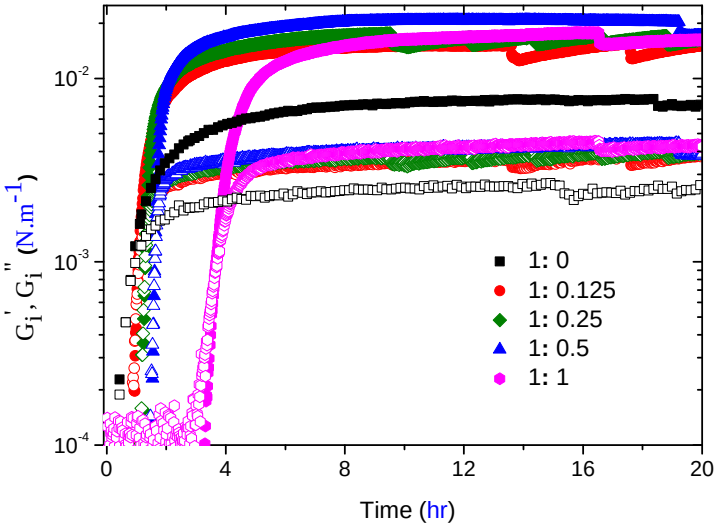

FIGURE A.12: Time evolution of G_i' (solid) and G″ (hollow) at dodecane/water interfaces with 1 mg.L^{-1} subphase mixed solutions of β-lg/HG-60 complexes with various weight ratios of pectins in pH 4.

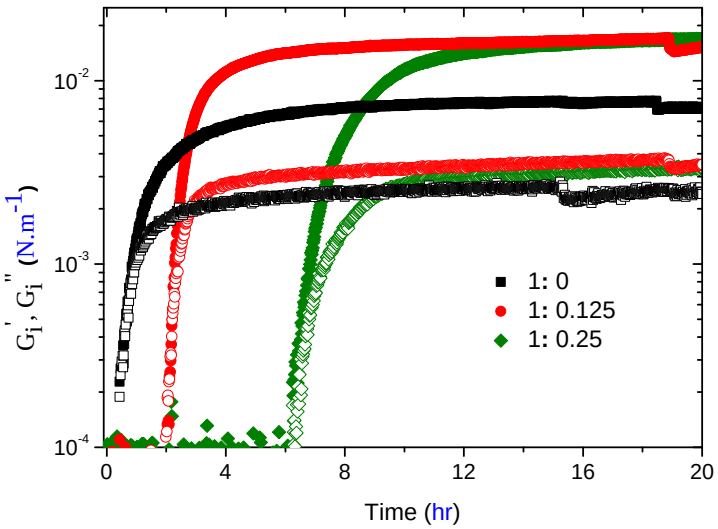

FIGURE A.13: Time evolution of G_i' (solid) and G″ (hollow) at dodecane/water interfaces with 1 mg.L^{-1} subphase mixed solutions of β-lg/Dp7 complexes with various weight ratios of pectins in pH 4.

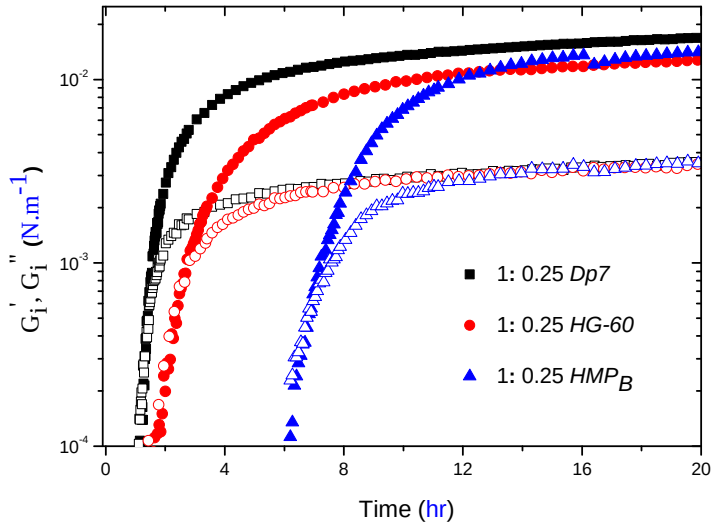

FIGURE A.14: Time evolution of G_i' (solid) and G$''$ (hollow) at dodecane/water interfaces with 1 mg.L^{-1} subphase mixed solutions of β-lg and various polysaccharides at weight ratio of 1:1 in pH 3.

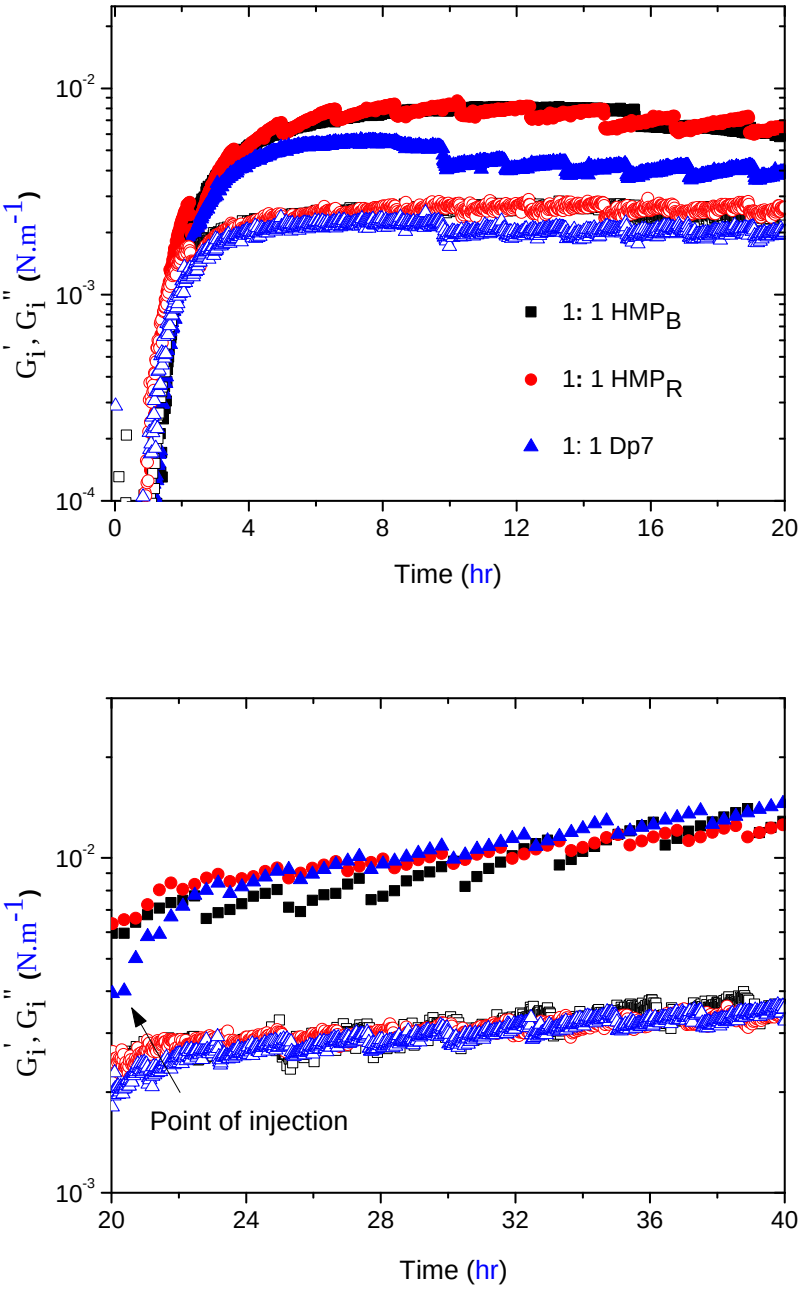

FIGURE A.15: Transient G_i' (solid) and G'' (hollow) values for a fixed β-lg concentration of 1 mgL^{-1} at pH 4 and 5mM ionic strength (A) and after the injection of polysaccharide into the subphase (B).

Appendix B

Published Works and DRC16 Forms

1. The rheological properties of bovine β-Lactoglobulin stabilized oil/water interfaces depend on the protein's quaternary structure.
   Sashikumar Ramamirtham, Catherine P. Whitby, Davoud Zare, Mike Weeks, and Martin AK Williams.
   In: *Food Hydrocolloids*. 2021
   DOI: 10.1016/j.foodhyd.2021.106834

2. Complexes of β-lactoglobulin and high methyl-esterified pectin as a one-shot delivery system for reinforcing oil/water interfaces
   Sashikumar Ramamirtham, Martin AK Williams, Davoud Zare, Mike Weeks, and Catherine P. Whitby.
   In: *Soft Matter*, 2021.
   DOI: 10.1039/D1SM00989C

MASSEY UNIVERSITY
GRADUATE RESEARCH SCHOOL

STATEMENT OF CONTRIBUTION
DOCTORATE WITH PUBLICATIONS/MANUSCRIPTS

We, the candidate and the candidate's Primary Supervisor, certify that all co-authors have consented to their work being included in the thesis and they have accepted the candidate's contribution as indicated below in the *Statement of Originality*.

Name of candidate:	Sashikumar Ramamirtham
Name/title of Primary Supervisor:	Martin A.K. Williams
Name of Research Output and full reference:	
The rheological properties of bovine β-Lactoglobulin stabilized oil/water interfaces depend on the protein's quaternary structure." Food Hydrocolloids (2021): 106834.	
In which Chapter is the Manuscript /Published work:	Chapter 2
Please indicate:	
• The percentage of the manuscript/Published Work that was contributed by the candidate:	80%
and	
• Describe the contribution that the candidate has made to the Manuscript/Published Work:	
Experimental methodology and design, data analysis, manuscript writing	
For manuscripts intended for publication please indicate target journal:	
Candidate's Signature:	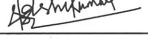
Date:	27/09/2021
Primary Supervisor's Signature:	
Date:	29/09/21

(This form should appear at the end of each thesis chapter/section/appendix submitted as a manuscript/ publication or collected as an appendix at the end of the thesis)

Food Hydrocolloids 120 (2021) 106834

Contents lists available at ScienceDirect

Food Hydrocolloids

journal homepage: www.elsevier.com/locate/foodhyd

The rheological properties of bovine β-Lactoglobulin stabilized oil/water interfaces depend on the protein's quaternary structure☆

Sashikumar Ramamirtham [a,b], Catherine P. Whitby [a,b,c], Davoud Zare [d], Mike Weeks [e], Martin A. K. Williams [a,b,c,*]

[a] School of Fundamental Science, Massey University, Palmerston North, 4442, New Zealand
[b] The Macdiarmid Institute for Advanced Materials and Nanotechnology, Wellington, 6140, New Zealand
[c] Riddet Institute, Palmerston North, New Zealand
[d] Fonterra Research and Development Center, Palmerston North, 4472, New Zealand
[e] Smart Foods Innovation Centre, AgResearch, Palmerston North, 4442, New Zealand

ARTICLE INFO

Keywords:
Whey proteins
Interfacial rheology
Acidified milk drinks
Disulfide bond
Protein adsorption

ABSTRACT

Structural manipulation of β-lactoglobulin through processes such as heat treatment and complexation with other molecules has proven fruitful in industrial formulations. To fully appreciate the ramifications of such methods on protein interfacial adsorption we have investigated assemblies of β-lactoglobulin at oil/water interfaces predominantly at pH 3 and at different conditions of ionic strength, salt type and temperature. These parameters were tuned to vary the relative amounts of two native species, namely, monomer and its smallest aggregate, the dimer, while the interface was monitored using rheology and tensiometry. Unfolding of β-lactoglobulin at the interface triggers the formation of disulfide linkages between the free thiol groups of two monomers which are located at cys121. In this way, monomers pair up to form discrete assemblies of two β-lactoglobulin molecules (non-native dimers) that are not interconnected further and this is reflected in the absence of a viscoelastic layer in solutions with high monomer concentrations. Native dimers however form primary particles capable of forming two thiol bonds allowing the formation of extended networks. A higher concentration of dimers increases the final interfacial elastic strength of the network. This fundamental relation between the quaternary structure of β-lg and its subsequent interfacial network suggests a possible interfacial role in its biological function.

1. Introduction

Proteins are biopolymers comprising various amino acids in a specific sequence. Each protein has evolved to perform a unique role which is dictated by its structure thereby establishing a structure-function relationship (Shoichet et al., 1995). The dynamic functionality of proteins arises from the fact that changes in environment can trigger a structural response that alters their functional properties. Milk proteins not only offer nutritional benefits but also other functional applications in many food formulations. β-lactoglobulin (β-lg) is the major protein of the whey family in ruminant mammalian milk. From an industrial perspective, modulating this protein's structure for better emulsification via thermal treatments has been explored (Kim et al., 2005). In order to place such phenomenology on a sound theoretical footing, it is essential to understand the adsorption behavior of native β-lactoglobulin molecules and their subsequent aggregation at the interface.

The two commonly occurring variants of bovine β-lg, β-lgA and β-lgB, differ by just two residues and display very similar properties. The native structure of a bovine β-lg monomer has 162 amino acids (~ 18300 Da) interwoven into a globular structure made of a α-helix and nine anti-parallel β-strands (Crowther et al., 2016). It contains two intramolecular disulfide linkages, cys66-cys160 and cys106-cys119, reinforcing the folded arrangement. A free thiol group in cys121 is hidden behind the α-helix. β-lg undergoes various structural transitions with changes in pH (Taulier & Chalikian, 2001). Moreover, the amphiphathic protein prefers to bury its hydrophobic residues away from the water molecules but also has to manage the intramolecular electrostatic repulsions between its charged residues. The balance between the

☆ This project was funded by New Zealand Ministry of Business, Innovation & Employment (MBIE Contract C10X1502) and AgResearch Ltd, NZ.
* Corresponding author. School of Fundamental Science, Massey University, Palmerston North, 4442, New Zealand.
E-mail address: M.Williams@massey.ac.nz (M.A.K. Williams).

https://doi.org/10.1016/j.foodhyd.2021.106834
Received 4 March 2021; Received in revised form 7 April 2021; Accepted 14 April 2021
Available online 31 May 2021

MASSEY UNIVERSITY
GRADUATE RESEARCH SCHOOL

STATEMENT OF CONTRIBUTION
DOCTORATE WITH PUBLICATIONS/MANUSCRIPTS

We, the candidate and the candidate's Primary Supervisor, certify that all co-authors have consented to their work being included in the thesis and they have accepted the candidate's contribution as indicated below in the *Statement of Originality*.

Name of candidate:	Sashikumar Ramamirtham
Name/title of Primary Supervisor:	Martin A.K. Williams
Name of Research Output and full reference:	
Complexes of β-lactoglobulin and high methyl-esterified pectin as a one-shot delivery system for reinforcing oil/water interfaces. Soft Matter (2021).	
In which Chapter is the Manuscript /Published work:	Chapter 3
Please indicate:	
• The percentage of the manuscript/Published Work that was contributed by the candidate:	80%
and	
• Describe the contribution that the candidate has made to the Manuscript/Published Work:	
Experimental methodology and design, data analysis, manuscript writing	
For manuscripts intended for publication please indicate target journal:	
Candidate's Signature:	
Date:	27/09/2021
Primary Supervisor's Signature:	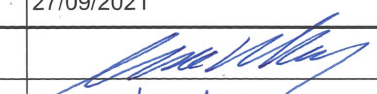
Date:	29/09/21

(This form should appear at the end of each thesis chapter/section/appendix submitted as a manuscript/ publication or collected as an appendix at the end of the thesis)

Soft Matter

PAPER

View Article Online
View Journal

Cite this: DOI: 10.1039/d1sm00989c

Complexes of β-lactoglobulin and high methyl-esterified pectin as a one-shot delivery system for reinforcing oil/water interfaces

Sashikumar Ramamirtham,[ab] Martin A.K. Williams,[abc] Davoud Zare,[d] Mike Weeks[e] and Catherine P. Whitby *[abc]

Received 4th July 2021,
Accepted 31st August 2021

DOI: 10.1039/d1sm00989c

rsc.li/soft-matter-journal

Electrostatic complexation of negatively charged polysaccharides with β-lactoglobulin (β-lg) has been shown to bolster the protein films at oil/water interfaces thereby improving emulsion stability. However, recent sub-phase exchange experiments demonstrated that highly charged polysaccharides such as low methyl-esterified pectin are complementary only if sequentially introduced to a pre-formed interfacial β-lg film. In this study, results of transient interfacial shear rheology show that, by using high-methylesterified pectins instead, complexes can be formed in pre-mixed solutions with β-lg at pH 4 that can lead to reinforced protein films at dodecane/water interfaces. Using this one-shot adsorption of such complexes, pectins as well as short chain polysaccharides like homogalacturonan nearly doubled the steady state shear elastic moduli as compared to that of a pure β-lg film. The lag times of film formation were established to be primarily decided by the charge density and pattern on the polysaccharide. Based on the results from mixed solutions of β-lg monomers, it is proposed that the polysaccharide at pH 4 strengthens the resulting interfacial layer by concatenating adsorbed β-lg molecules thereby establishing cross-links in the aqueous phase.

1 Introduction

Amphipathic proteins are an important class of emulsifiers that reduce surface tension and typically form viscoelastic interfacial films. Charged polysaccharides complex with such protein molecules through electrostatic attraction and can be used to tune the interfacial properties.[1] Such protein-polysaccharide complexes have found applications in food emulsification,[2] microencapsulation,[3,4] fat substitution,[5] protein separation[6] and bioactive deliveries.[7] Therefore, understanding the interactions between these biopolyelectrolytes have attracted the attention of soft matter scientists.

β-Lactoglobulin (β-lg) is the major whey protein (∼18 400 kDa) from ruminant mammalian milk and is a relatively well studied globular protein.[8] It primarily exists as a dimer and carries a net positive charge in acidic conditions with an isoelectric point (pI) ∼ 5.1. The bulkier pectin (∼120 000 kDa), a plant polysaccharide, is negatively charged at pHs above its pK_a of 3.5 due to carboxyl (COO^-) groups. The overall charge exhibited by pectin can be controlled by methylesterifying the COO^- groups to various extents and is referred to as the degree of methylesterification (DM). β-lg and pectin spontaneously complex in a reversible exothermic process primarily caused by a favourable enthalpy change driven by the electrostatic attraction at low ionic strengths.[9,10] Multiple β-lg molecules adhere to the charged patches along the pectin backbone causing structural changes in both biopolymers.[9] For 10–1500 μM solutions, calorimetric studies have observed intercomplex aggregation at higher protein : polysaccharide molar ratios (>15 : 1).[11]

Apart from the stoichiometry and solution conditions, the nature of these complexes also depends on various structural motifs of the charges on the backbone of pectin. When low-methoxyl pectin (LMP) (<50% DM) is mixed with β-lg at pH 4, the amount of protein molecules binding to the LMP is mediated by the electrostatic attraction between β-lg and pectin as well as the repulsion between the bound β-lg neighbours.[9] In case of high-methoxyl pectin (HMP) (>50% DM), the local charge distribution owing to the pattern of COO^- groups on the back bone of the polysaccharide plays a crucial role in the complexation.[12] The contiguity of the charges on HMPs are

[a] School of Fundamental Science, Massey University, Palmerston North, 4442, New Zealand. E-mail: C.P.Whitby@massey.ac.nz
[b] The Macdiarmid Institute for Advanced Materials and Nanotechnology, Wellington, 6140, New Zealand
[c] Riddet Institute, Palmerston North, New Zealand
[d] Fonterra Research and Development Center, Palmerston North, 4472, New Zealand
[e] Smart Foods Innovation Centre, AgResearch, Palmerston North, 4442, New Zealand

Bibliography

[1] P. G. de Gennes. "Soft matter". In: *Rev. Mod. Phys.* 64 (3 1992), pp. 645–648. DOI: 10.1103/RevModPhys.64.645.

[2] Linus Pauling, Robert B. Corey, and H. R. Branson. "The structure of proteins: Two hydrogen-bonded helical configurations of the polypeptide chain". In: *Proceedings of the National Academy of Sciences* 37 (4 1951), pp. 205–211. ISSN: 0027-8424. DOI: 10.1073/pnas.37.4.205.

[3] David Eisenberg. "The discovery of the -helix and -sheet, the principal structural features of proteins". In: *Proceedings of the National Academy of Sciences* 100 (20 2003), pp. 11207–11210. ISSN: 0027-8424. DOI: 10.1073/pnas.2034522100.

[4] Franz Hofmeister. "Zur lehre von der wirkung der salze". In: *Archiv für experimentelle Pathologie und Pharmakologie* 25 (1 1888), pp. 1–30. DOI: 10.1007/BF01918180.

[5] Jennifer M Crowther et al. "Structure, oligomerisation and interactions of β-lactoglobulin". In: *Milk Proteins-From Structure to Biological Properties and Health Aspects* (2016). DOI: 10.5772/62992.

[6] S Rowland. "The precipitation of the proteins in milk. I. Casein. II. Total proteins. III. Globulin. IV. Albumin and Proteose-peptone". In: *Journal of Dairy Research* 9 (1 1938), pp. 30–41. DOI: 10.1017/S0022029900002284.

[7] G Kontopidis, C Holt, and L Sawyer. "Invited review: β-lactoglobulin: binding properties, structure, and function". In: *Journal of dairy science* 87 (4 2004), pp. 785–796. DOI: 10.3168/jds.S0022-0302(04)73222-1.

[8] Brian K Shoichet et al. "A relationship between protein stability and protein function." In: *Proceedings of the National Academy of Sciences* 92 (2 1995), pp. 452–456. DOI: 10.1073/pnas.92.2.452.

[9] MZ Papiz et al. “The structure of β-lactoglobulin and its similarity to plasma retinol-binding protein”. In: *Nature* 324 (6095 1986), pp. 383–385. DOI: 10.1038/324383a0.

[10] Isabel Gigli. *Milk Proteins: From Structure to Biological Properties and Health Aspects*. BoD–Books on Demand, 2016. DOI: 10.5772/60465.

[11] Maulik V Trivedi, Jennifer S Laurence, and Teruna J Siahaan. “The role of thiols and disulfides on protein stability”. In: *Current Protein and Peptide Science* 10 (6 2009), pp. 614–625. DOI: 10.2174/138920309789630534.

[12] Gudipati Mualikrishna and Rudrapatnam N Tharanathan. “Characterization of pectic polysaccharides from pulse husks”. In: *Food chemistry* 50 (1 1994), pp. 87–89. DOI: 10.1016/0308-8146(94)90098-1.

[13] RD Preston. “Polysaccharide conformation and cell wall function”. In: *Annual Review of Plant Physiology* 30 (1 1979), pp. 55–78. DOI: 10.1146/annurev.pp.30.060179.000415.

[14] Beli R. Thakur, Rakesh K. Singh, and Avtar K. Handa. “Chemistry and Uses of Pectin - A Review”. In: *Critical Reviews in Food Science and Nutrition* 37 (1 1997), pp. 47–73. DOI: 10.1080/10408399709527767.

[15] Frank M Rombouts and Jean-François Thibault. “Feruloylated pectic substances from sugar-beet pulp”. In: *Carbohydrate Research* 154 (1 1986), pp. 177–187. DOI: 10.1016/S0008-6215(00)90031-4.

[16] A Miyamoto and KC Chang. “Extraction and physicochemical characterization of pectin from sunflower head residues”. In: *Journal of Food Science* 57 (6 1992), pp. 1439–1443. DOI: 10.1111/j.1365-2621.1992.tb06878.x.

[17] Rosaria Ciriminna et al. “Pectin: A new perspective from the biorefinery standpoint”. In: *Biofuels, Bioproducts and Biorefining* 9 (4 2015), pp. 368–377. DOI: 10.1002/bbb.1551.

[18] Akihiro Nakamura et al. “The stabilizing behaviour of soybean soluble polysaccharide and pectin in acidified milk beverages”. In: *International Dairy Journal* 16 (4 2006), pp. 361–369. DOI: 10.1016/j.idairyj.2005.01.014.

[19] Ana Zulueta et al. “Vitamin C, vitamin A, phenolic compounds and total antioxidant capacity of new fruit juice and skim milk mixture beverages marketed in Spain”. In: *Food Chemistry* 103 (4 2007), pp. 1365–1374. DOI: 10.1016/j.foodchem.2006.10.052.

[20] Santanu Basu and US Shivhare. “Rheological, textural, micro-structural and sensory properties of mango jam”. In: *Journal of Food Engineering* 100 (2 2010), pp. 357–365. DOI: 10.1016/j.jfoodeng.2010.04.022.

[21] Hassan Joudaki et al. “Scrutinizing the different pectin types on stability of an Iranian traditional drink “Doogh””. In: *International journal of biological macromolecules* 60 (2013), pp. 375–382. DOI: 10.1016/j.ijbiomac.2013.06.034.

[22] CM Pereira et al. “Effect of the partial substitution of soy proteins by highly methyl-esterified pectin on chemical and sensory characteristics of sausages”. In: *Food Science and Technology International* 16 (5 2010), pp. 401–407. DOI: 10.1177/1082013210366888.

[23] Henri Braconnot. “Recherches sur un nouvel acide universellement répandu dans tous les végétaux”. In: *Ann Chim Phys* 28 (2 1825), pp. 173–178.

[24] M. A. K. Williams. “Pectin Gelation and Its Assembly into Functional Materials”. In: *Pectin: Technological and Physiological Properties*. Ed. by Vassilis Kontogiorgos. Cham: Springer International Publishing, 2020, pp. 125–148. ISBN: 978-3-030-53421-9. DOI: 10.1007/978-3-030-53421-9_7.

[25] Debra Mohnen. “Pectin structure and biosynthesis”. In: *Current opinion in plant biology* 11 (3 2008), pp. 266–277. DOI: 10.1016/j.pbi.2008.03.006.

[26] Alphons GJ Voragen et al. “Pectin, a versatile polysaccharide present in plant cell walls”. In: *Structural Chemistry* 20 (2 2009), p. 263. DOI: 10.1007/s11224-009-9442-z.

[27] Yu S Ovodov. “Current views on pectin substances”. In: *Russian Journal of Bioorganic Chemistry* 35 (3 2009), p. 269. DOI: 10.1134/S1068162009030017.

[28] Kerry Hosmer Caffall and Debra Mohnen. “The structure, function, and biosynthesis of plant cell wall pectic polysaccharides”. In: *Carbohydrate research* 344 (14 2009), pp. 1879–1900. DOI: 10.1016/j.carres.2009.05.021.

[29] Beda M Yapo. “Pectin rhamnogalacturonan II: On the “Small Stem with Four Branches” in the primary cell walls of plants”. In: *International Journal of Carbohydrate Chemistry* 2011 (2011). DOI: 10.1155/2011/964521.

[30] Michael C Jarvis. “The proportion of calcium-bound pectin in plant cell walls”. In: *Planta* 154 (4 1982), pp. 344–346. DOI: 10.1007/BF00393913.

[31] Gregor T Grant et al. “Biological interactions between polysaccharides and divalent cations: the egg-box model”. In: *FEBS letters* 32 (1 1973), pp. 195–198. DOI: 10.1016/0014-5793(73)80770-7.

[32] MAV Axelos and J-F Thibault. “Influence of the substituents of the carboxyl groups and of the rhamnose content on the solution properties and flexibility of pectins”. In: *International Journal of Biological Macromolecules* 13 (2 1991), pp. 77–82. DOI: 10.1016/0141-8130(91)90052-V.

[33] David Oakenfull and Alan Scott. “Hydrophobic interaction in the gelation of high methoxyl pectins”. In: *Journal of Food Science* 49 (4 1984), pp. 1093–1098. DOI: 10.1111/j.1365-2621.1984.tb10401.x.

[34] Caroline Löfgren et al. “Effects of calcium, pH, and blockiness on kinetic rheological behavior and microstructure of HM pectin gels”. In: *Biomacromolecules* 6 (2 2005), pp. 646–652. DOI: 10.1021/bm049619+.

[35] Anton Slavov et al. “Gelation of high methoxy pectin in the presence of pectin methylesterases and calcium”. In: *Carbohydrate Polymers* 77 (4 2009), pp. 876–884. DOI: 10.1016/j.carbpol.2009.03.014.

[36] JA Lopes Da Silva, MP Goncalves, and MA Rao. “Kinetics and thermal behaviour of the structure formation process in HMP/sucrose gelation”. In: *International journal of biological macromolecules* 17 (1 1995), pp. 25–32. DOI: 10.1016/0141-8130(95)93514-X.

[37] Michael J Gidley et al. “Spectroscopic and stoicheiometric characterisation of the calcium-mediated association of pectate chains in gels and in the solid state”. In: *Journal of the Chemical Society, Chemical Communications* (22 1979), pp. 990–992. DOI: 10.1039/C39790000990.

[38] DA Powell et al. “Conformations and interactions of pectins: II. Influence of residue sequence on chain association in calcium pectate gels”. In: *Journal of molecular biology* 155 (4 1982), pp. 517–531. DOI: 10.1016/0022-2836(82)90485-5.

[39] M.A. V. Axelos and J.-F. Thibault. “CHAPTER 6 - The Chemistry of Low-Methoxyl Pectin Gelation”. In: *The Chemistry and Technology of Pectin*. Ed. by Reginald H. Walter. Food Science and Technology. San Diego: Academic Press, 1991, pp. 109–118. ISBN: 978-0-08-092644-5. DOI: https://doi.org/10.1016/B978-0-08-092644-5.50011-X.

[40] JA Lopes Da Silva and MA Rao. “CHAPTER 11 - Pectins: Structure, Functionality, and Uses”. In: ed. by Alistair M Stephen and Glyn O Phillips.

[41] Isabelle Braccini and Serge Pérez. “Molecular basis of Ca2+-induced gelation in alginates and pectins: the egg-box model revisited”. In: *Biomacromolecules* 2 (4 2001), pp. 1089–1096. DOI: 10.1021/bm010008g.

[42] Ilse Fraeye et al. “Influence of intrinsic and extrinsic factors on rheology of pectin–calcium gels”. In: *Food Hydrocolloids* 23 (8 2009), pp. 2069–2077. DOI: 10.1016/j.foodhyd.2009.03.022.

[43] Caroline Löfgren, Stéphanie Guillotin, and Anne-Marie Hermansson. “Microstructure and kinetic rheological behavior of amidated and nonamidated LM pectin gels”. In: *Biomacromolecules* 7 (1 2006), pp. 114–121. DOI: 10.1021/bm050459r.

[44] Cornelus G De Kruif, Fanny Weinbreck, and Renko de Vries. “Complex coacervation of proteins and anionic polysaccharides”. In: *Current opinion in colloid & interface science* 9 (5 2004), pp. 340–349. DOI: 10.1016/j.cocis.2004.09.006.

[45] Pascal Bertsch et al. “Transient measurement and structure analysis of protein–polysaccharide multilayers at fluid interfaces”. In: *Soft Matter* 15 (31 2019), pp. 6362–6368. DOI: 10.1039/C9SM01112A.

[46] Bjørn Jamtveit and Paul Meakin. “Growth, dissolution and pattern formation in geosystems”. In: *Growth, Dissolution and Pattern Formation in Geosystems*. Springer, 1999, pp. 1–19. DOI: 10.1007/978-94-015-9179-9_1.

[47] Ernst A. Hauser. “The history of colloid science: In memory of Wolfgang Ostwald”. In: *Journal of Chemical Education* 32 (1 1955), p. 2. DOI: 10.1021/ed032p2.

[48] Bernard F. Gibbs et al. “Encapsulation in the food industry: a review”. In: *International Journal of Food Sciences and Nutrition* 50 (3 1999), pp. 213–224. DOI: 10.1080/096374899101256.

[49] Demet Guzey and D. Julian McClements. “Formation, stability and properties of multilayer emulsions for application in the food industry”. In: *Advances in Colloid and Interface Science* 128-130 (2006), pp. 227 –248. DOI: 10.1016/j.cis.2006.11.021.

[50] Mahmood Akhtar and Eric Dickinson. “Emulsifying properties of whey protein-dextran conjugates at low pH and different salt concentrations”. In: *Colloids and Surfaces B: Biointerfaces* 31 (1-4 2003), pp. 125–132. DOI: 10.1016/S0927-7765(03)00049-3.

[51] Eric Dickinson. “Biopolymer-based particles as stabilizing agents for emulsions and foams”. In: *Food Hydrocolloids* 68 (2017), pp. 219–231. DOI: 10.1016/j.foodhyd.2016.06.024.

[52] Bach T. Nguyen, Taco Nicolai, and Lazhar Benyahia. “Stabilization of water-in-water emulsions by addition of protein particles”. In: *Langmuir* 29 (2013), pp. 10658–10664. DOI: 10.1021/la402131e.

[53] Ty B. Wagoner and E. Allen Foegeding. “Whey protein–pectin soluble complexes for beverage applications”. In: *Food Hydrocolloids* 63 (2017), pp. 130–138. DOI: 10.1016/j.foodhyd.2016.08.027.

[54] Myung Han Lee et al. “Brownian dynamics of colloidal probes during protein-layer formation at an oil–water interface”. In: *Soft Matter* 7 (17 2011), pp. 7635–7642. DOI: 10.1039/C1SM05235G.

[55] J-L Doublier et al. “Protein–polysaccharide interactions”. In: *Current opinion in Colloid & interface Science* 5 (3-4 2000), pp. 202–214. DOI: 10.1016/S1359-0294(00)00054-6.

[56] Jotam Bergfreund et al. “Effect of Oil Hydrophobicity on the Adsorption and Rheology of β-Lactoglobulin at Oil–Water Interfaces”. In: *Langmuir* 34 (16 2018), pp. 4929–4936. DOI: 10.1021/acs.langmuir.8b00458.

[57] Davoud Zare, Jane R Allison, and Kathryn M McGrath. “Molecular dynamics simulation of β-lactoglobulin at different oil/water interfaces”. In: *Biomacromolecules* 17 (5 2016), pp. 1572–1581. DOI: 10.1021/acs.biomac.5b01709.

[58] Tatiana V Burova et al. “Role of free Cys121 in stabilization of bovine beta-lactoglobulin B.” In: *Protein engineering* 11 (11 1998), pp. 1065–1073. DOI: 10.1093/protein/11.11.1065.

[59] Raffaele Mezzenga and Peter Fischer. “The self-assembly, aggregation and phase transitions of food protein systems in one, two and three dimensions”. In: *Reports on Progress in Physics* 76 (4 2013), p. 046601. DOI: 10.1088/0034-4885/76/4/046601.

[60] Kathrin Engelhardt et al. “pH effects on the molecular structure of β-lactoglobulin modified air–water interfaces and its impact on foam rheology”. In: *Langmuir* 29 (37 2013), pp. 11646–11655. DOI: 10.1021/la402729g.

[61] Stéphane Roth, Brent S Murray, and Eric Dickinson. “Interfacial shear rheology of aged and heat-treated β-lactoglobulin films: Displacement by nonionic surfactant”. In: *Journal of Agricultural and Food Chemistry* 48 (5 2000), pp. 1491–1497. DOI: 10.1021/jf990976z.

[62] F Sausset, G Biroli, and J Kurchan. “Do solids flow?” In: *Journal of Statistical Physics* 140 (4 2010), pp. 718–727. DOI: 10.1007/s10955-010-0006-9.

[63] Roger I Tanner and Kenneth Walters. *Rheology: an historical perspective*. Vol. 7. Elsevier, 1998. ISBN: 0-444-829466. DOI: 10.1017/S0022112001006036.

[64] J Murali Krishnan, Abhijit P Deshpande, and PB Sunil Kumar. *Rheology of complex fluids*. Springer, 2010. ISBN: 978-1-4419-6493-9. DOI: 10.1007/978-1-4419-6494-6.

[65] Miriam T. K. Kubo et al. “Chapter 1 Rheological Properties of Tomato Products”. In: *Tomato Chemistry, Industrial Processing and Product Development*. The

Royal Society of Chemistry, 2019, pp. 1–25. ISBN: 978-1-78801-396-3. DOI: 10.1039/9781788016247-00001.

[66] Vignesh S Balaraj et al. "Surface shear viscosity as a macroscopic probe of amyloid fibril formation at a fluid interface". In: *Soft Matter* 13.9 (2017), pp. 1780–1787. DOI: 10.1039/C6SM01831A.

[67] Mehdi Benmekhbi and Sébastien Simon. "Limitations and applicability of the interfacial shear rheology in the study of monolayer films at the air-water interface". In: *Journal of dispersion science and technology* 35.1 (2014), pp. 150–160. DOI: 10.1080/01932691.2012.757197.

[68] Steven Vandebril et al. "A double wall-ring geometry for interfacial shear rheometry". In: *Rheologica Acta* 49 (2 2010), pp. 131–144. DOI: 10.1007/s00397-009-0407-3.

[69] Albert Einstein. *Investigations on the Theory of the Brownian Movement*. Courier Corporation, 1956. ISBN: 9780486603049.

[70] Marian Von Smoluchowski. "Zur kinetischen theorie der brownschen molekularbewegung und der suspensionen". In: *Annalen der physik* 326 (14 1906), pp. 756–780. DOI: 10.1002/andp.19063261405.

[71] Robert Brown. "XXVII. A brief account of microscopical observations made in the months of June, July and August 1827, on the particles contained in the pollen of plants; and on the general existence of active molecules in organic and inorganic bodies". In: *The Philosophical Magazine* 4 (21 1828), pp. 161–173. DOI: 10.1080/14786442808674769.

[72] M Jean Perrin. "Brownian Movement and Molecular Reality: Translated from the Annales de Chimie Et de Physique, 8 Series, September 1909, by F. Soddy". In: 86 (1911), p. 105. DOI: 10.1038/086105a0.

[73] John C Crocker and David G Grier. "Methods of digital video microscopy for colloidal studies". In: *Journal of colloid and interface science* 179 (1 1996), pp. 298–310. DOI: 10.1006/jcis.1996.0217.

[74] Rep Kubo. "The fluctuation-dissipation theorem". In: *Reports on progress in physics* 29 (1 1966), p. 255. URL: 10.1088/0034-4885/29/1/306.

[75] TG Mason et al. “Particle tracking microrheology of complex fluids”. In: *Physical review letters* 79 (17 1997), p. 3282. DOI: 10.1103/PhysRevLett.79.3282.

[76] Eric Dickinson. “Interfacial structure and stability of food emulsions as affected by protein–polysaccharide interactions”. In: *Soft Matter* 4 (5 2008), pp. 932–942. DOI: 10.1039/B718319D.

[77] N Ron et al. “Beta-lactoglobulin–polysaccharide complexes as nanovehicles for hydrophobic nutraceuticals in non-fat foods and clear beverages”. In: *International dairy journal* 20 (10 2010), pp. 686–693. DOI: 10.1016/j.idairyj.2010.04.001.

[78] Wahyu Wijaya et al. “Whey protein isolate–low methoxyl pectin nanocomplexes improve physicochemical and stability properties of quercetin in a model fat-free beverage”. In: *Food & function* 10 (2 2019), pp. 986–996. DOI: 10.1039/C8FO02350F.

[79] SI Laneuville, P Paquin, and SL Turgeon. “Effect of preparation conditions on the characteristics of whey protein—xanthan gum complexes”. In: *Food Hydrocolloids* 14 (4 2000), pp. 305–314. DOI: 10.1016/S0268-005X(00)00003-5.

[80] PL Dubin, J Gao, and K Mattison. “Protein purification by selective phase separation with polyelectrolytes”. In: *Separation and Purification Methods* 23 (1 1994), pp. 1–16. DOI: 10.1080/03602549408001288.

[81] Omid Shamsara, Seid Mahdi Jafari, and Zayniddin Kamarovich Muhidinov. “Development of double layered emulsion droplets with pectin/β-lactoglobulin complex for bioactive delivery purposes”. In: *Journal of Molecular Liquids* 243 (2017), pp. 144–150. DOI: 10.1016/j.molliq.2017.08.036.

[82] Renate A Ganzevles et al. “Use of polysaccharides to control protein adsorption to the air–water interface”. In: *Food Hydrocolloids* 20 (6 2006), pp. 872–878. DOI: 10.1016/j.foodhyd.2005.08.009.

[83] Eric Dickinson and Yasuki Matsumura. “Proteins at liquid interfaces: role of the molten globule state”. In: *Colloids and Surfaces B: Biointerfaces* 3 (1-2 1994), pp. 1–17. DOI: 10.1016/0927-7765(93)01116-9.

[84] JP Davis, EA Foegeding, and FK Hansen. "Electrostatic effects on the yield stress of whey protein isolate foams". In: *Colloids and Surfaces B: Biointerfaces* 34 (1 2004), pp. 13–23. DOI: 10.1016/j.colsurfb.2003.10.014.

[85] Bénédicte Rullier et al. "β-Lactoglobulin aggregates in foam films: Effect of the concentration and size of the protein aggregates". In: *Journal of colloid and interface science* 343 (1 2010), pp. 330–337. DOI: 10.1016/j.jcis.2009.11.015.

[86] Jin-Mi Jung et al. "Structure of heat-induced β-lactoglobulin aggregates and their complexes with sodium-dodecyl sulfate". In: *Biomacromolecules* 9 (9 2008), pp. 2477–2486. DOI: 10.1021/bm800502j.

[87] Maria Dolores Pérez and Miguel Calvo. "Interaction of β-lactoglobulin with retinol and fatty acids and its role as a possible biological function for this protein: a review". In: *Journal of dairy science* 78.5 (1995), pp. 978–988. DOI: 10.3168/jds.S0022-0302(95)76713-3.

[88] Ivano Eberini et al. "Electrostatics of folded and unfolded bovine β-lactoglobulin". In: *Amino Acids* 42.5 (2012), pp. 2019–2030. DOI: 10.1007/s00726-011-0933-z.

[89] Alberto Barbiroli, Stefania Iametti, and Francesco Bonomi. "Beta-Lactoglobulin as a Model Food Protein: How to Promote, Prevent, and Exploit Its Unfolding Processes". In: *Molecules* 27.3 (2022). ISSN: 1420-3049. DOI: 10.3390/molecules27031131. URL: https://www.mdpi.com/1420-3049/27/3/1131.

[90] Varvara Mitropoulos, Annekathrin Mütze, and Peter Fischer. "Mechanical properties of protein adsorption layers at the air/water and oil/water interface: A comparison in light of the thermodynamical stability of proteins". In: *Advances in colloid and interface science* 206 (2014), pp. 195–206. DOI: 10.1016/j.cis.2013.11.004.

[91] RICHARD K OWUSU-APENTEN. "REVISED CONFORMATIONAL STABILITY PARAMETERS FOR BETA-LACTOGLOBULIN ISOTHERMAL DENATURATION BY UREA". In: *Journal of food biochemistry* 26.3 (2002), pp. 181–190. DOI: 10.1111/j.1745-4514.2002.tb00851.x.

[92] Phoebe Shih, Jack F Kirsch, and Debra R Holland. "Thermal stability determinants of chicken egg-white lysozyme core mutants: Hydrophobicity, packing

volume, and conserved buried water molecules". In: *Protein Science* 4.10 (1995), pp. 2050–2062. DOI: 10.1002/pro.5560041010.

[93] Jiali Zhai et al. "Changes in β-lactoglobulin conformation at the oil/water interface of emulsions studied by synchrotron radiation circular dichroism spectroscopy". In: *Biomacromolecules* 11 (8 2010), pp. 2136–2142. DOI: 10.1021/bm100510j.

[94] Jotam Bergfreund et al. "Globular protein assembly and network formation at fluid interfaces: effect of oil". In: *Soft Matter* (2021). DOI: 10.1039/D0SM01870H.

[95] Georgi G Gochev et al. "β-Lactoglobulin adsorption layers at the water/air surface: 3. Neutron reflectometry study on the effect of pH". In: *The Journal of Physical Chemistry B* 123.50 (2019), pp. 10877–10889. DOI: 10.1021/acs.jpcb.9b07733.

[96] Yuan Fang and Douglas G Dalgleish. "Conformation of β-lactoglobulin studied by FTIR: effect of pH, temperature, and adsorption to the oil–water interface". In: *Journal of Colloid and Interface Science* 196 (2 1997), pp. 292–298. DOI: https://doi.org/10.1006/jcis.1997.5191.

[97] Fiona A Husband et al. "Adsorbed protein secondary and tertiary structures by circular dichroism and infrared spectroscopy with refractive index matched emulsions". In: *Journal of Agricultural and Food Chemistry* 49.2 (2001), pp. 859–866. DOI: 10.1021/jf000688z.

[98] Jotam Bergfreund, Pascal Bertsch, and Peter Fischer. "Adsorption of proteins to fluid interfaces: Role of the hydrophobic subphase". In: *Journal of Colloid and Interface Science* 584 (2021), pp. 411–417.

[99] Sanaullah Khan et al. "Revealing the Dimeric Crystal and Solution Structure of β-Lactoglobulin at pH 4 and Its pH and Salt Dependent Monomer–Dimer Equilibrium". In: *Biomacromolecules* 19 (7 2018), pp. 2905–2912. DOI: 10.1021/acs.biomac.8b00471.

[100] Kazumasa Sakurai, Motohisa Oobatake, and Yuji Goto. "Salt-dependent monomer–dimer equilibrium of bovine β-lactoglobulin at pH 3". In: *Protein Science* 10 (11 2001), pp. 2325–2335. DOI: 10.1110/ps.17001.

[101] Giuseppe Graziano. "Role of hydrophobic effect in the salt-induced dimerization of bovine β-lactoglobulin at pH 3". In: *Biopolymers: Original Research on Biomolecules* 91 (12 2009), pp. 1182–1188. DOI: 10.1002/bip.21174.

[102] ZF Brotzakis and Peter G Bolhuis. "Unbiased Atomistic Insight into the Mechanisms and Solvent Role for Globular Protein Dimer Dissociation". In: *The Journal of Physical Chemistry B* 123 (9 2019), pp. 1883–1895. DOI: 10.1021/acs.jpcb.8b10005.

[103] Davide Mercadante et al. "Bovine β-lactoglobulin is dimeric under imitative physiological conditions: dissociation equilibrium and rate constants over the pH range of 2.5–7.5". In: *Biophysical journal* 103 (2 2012), pp. 303–312. DOI: 10.1016/j.bpj.2012.05.041.

[104] Michael Gottschalk et al. "Protein self-association in solution: The bovine β-lactoglobulin dimer and octamer". In: *Protein Science* 12 (11 2003), pp. 2404–2411. DOI: 10.1110/ps.0305903.

[105] Stanislava Uhrínová et al. "Structural changes accompanying pH-induced dissociation of the β-lactoglobulin dimer". In: *Biochemistry* 39 (13 2000), pp. 3565–3574. DOI: 10.1021/bi992629o.

[106] José Toro-Sierra, Alexander Tolkach, and Ulrich Kulozik. "Fractionation of α-lactalbumin and β-lactoglobulin from whey protein isolate using selective thermal aggregation, an optimized membrane separation procedure and resolubilization techniques at pilot plant scale". In: *Food and Bioprocess Technology* 6 (4 2013), pp. 1032–1043. DOI: 10.1007/s11947-011-0732-2.

[107] Aly Franck et al. "Double wall ring geometry to measure interfacial rheological properties". In: *5th international symposium on food rheology and structure*. 2008.

[108] CJ Beverung, Clayton J Radke, and Harvey W Blanch. "Protein adsorption at the oil/water interface: characterization of adsorption kinetics by dynamic interfacial tension measurements". In: *Biophysical chemistry* 81 (1 1999), pp. 59–80. DOI: 10.1016/S0301-4622(99)00082-4.

[109] ERA Lima et al. “Specific ion effects on the interfacial tension of water/hydrocarbon systems”. In: *Brazilian Journal of Chemical Engineering* 30 (2013), pp. 55–62. DOI: 10.1590/S0104-66322013000100007.

[110] Kyu Hyun et al. “A review of nonlinear oscillatory shear tests: Analysis and application of large amplitude oscillatory shear (LAOS)”. In: *Progress in Polymer Science* 36 (12 2011), pp. 1697–1753. DOI: 10.1016/j.progpolymsci.2011.02.002.

[111] Peter J Atkinson et al. “Neutron reflectivity of adsorbed β-casein and β-lactoglobulin at the air/water interface”. In: *Journal of the Chemical Society, Faraday Transactions* 91 (17 1995), pp. 2847–2854. DOI: 10.1039/FT9959102847.

[112] Palatasa Havea, Harjinder Singh, and Lawrence K Creamer. “Characterization of heat-induced aggregates of β-lactoglobulin, α-lactalbumin and bovine serum albumin in a whey protein concentrate environment”. In: *Journal of Dairy Research* 68 (3 2001), pp. 483–497. DOI: 10.1017/S0022029901004964.

[113] Gunda Panick, Ralf Malessa, and Roland Winter. “Differences between the pressure-and temperature-induced denaturation and aggregation of β-lactoglobulin A, B, and AB monitored by FT-IR spectroscopy and small-angle X-ray scattering”. In: *Biochemistry* 38 (20 1999), pp. 6512–6519. DOI: 10.1021/bi982825f.

[114] Raymond F Greene and C Nick Pace. “Urea and guanidine hydrochloride denaturation of ribonuclease, lysozyme, α-chymotrypsin, and β-lactoglobulin”. In: *Journal of Biological Chemistry* 249 (17 1974), pp. 5388–5393. DOI: 10.1016/S0021-9258(20)79739-5.

[115] Eric Dickinson and Yasuki Matsumura. “Time-dependent polymerization of β-lactoglobulin through disulphide bonds at the oil-water interface in emulsions”. In: *International Journal of Biological Macromolecules* 13 (1 1991), pp. 26–30. DOI: 10.1016/0141-8130(91)90006-G.

[116] Vera Petkova et al. “Structure of a Freestanding Film of β-Lactoglobulin”. In: *Langmuir* 19 (17 2003), pp. 6942–6949. DOI: 10.1021/la027025r.

[117] Paul J Flory, Norman Rabjohn, and Marcia C Shaffer. "Dependence of elastic properties of vulcanized rubber on the degree of cross linking". In: *Journal of Polymer Science* 4 (3 1949), pp. 225–245. DOI: 10.1002/pol.1949.120040301.

[118] Matthew D Biviano et al. "Viscoelastic characterization of the crosslinking of β-lactoglobulin on emulsion drops via microcapsule compression and interfacial dilational and shear rheology". In: *Journal of colloid and interface science* 583 (2021), pp. 404–413. DOI: 10.1016/j.jcis.2020.09.008.

[119] Y Serfert et al. "Characterisation and use of β-lactoglobulin fibrils for microencapsulation of lipophilic ingredients and oxidative stability thereof". In: *Journal of Food Engineering* 143 (2014), pp. 53–61. DOI: 10.1016/j.jfoodeng.2014.06.026.

[120] Sofia Arnaouteli et al. "Bifunctionality of a biofilm matrix protein controlled by redox state". In: *Proceedings of the National Academy of Sciences* 114 (30 2017), E6184–E6191. DOI: 10.1073/pnas.1707687114.

[121] Keith M Bromley et al. "Interfacial self-assembly of a bacterial hydrophobin". In: *Proceedings of the National Academy of Sciences* 112 (17 2015), pp. 5419–5424. DOI: 10.1073/pnas.1419016112.

[122] Liesbeth M Veenhoff, Esther HML Heuberger, and Bert Poolman. "Quaternary structure and function of transport proteins". In: *Trends in biochemical sciences* 27 (5 2002), pp. 242–249. DOI: 10.1016/S0968-0004(02)02077-7.

[123] Nicolas Taulier and Tigran V Chalikian. "Characterization of pH-induced transitions of β-lactoglobulin: ultrasonic, densimetric, and spectroscopic studies". In: *Journal of molecular biology* 314 (4 2001), pp. 873–889. DOI: 10.1006/jmbi.2001.5188.

[124] Dennis A Kim, Michel Cornec, and Ganesan Narsimhan. "Effect of thermal treatment on interfacial properties of β-lactoglobulin". In: *Journal of Colloid and Interface Science* 285 (1 2005), pp. 100–109. DOI: 10.1016/j.jcis.2004.10.044.

[125] Georgi G Gochev et al. "β-Lactoglobulin Adsorption Layers at the Water/Air Surface: 5. Adsorption Isotherm and Equation of State Revisited, Impact of pH". In: *Colloids and Interfaces* 5 (1 2021), p. 14. DOI: 10.3390/colloids5010014.

[126] Amy J Hector et al. “Whey Protein Supplementation Preserves Postprandial Myofibrillar Protein Synthesis during Short-Term Energy Restriction in Overweight and Obese Adults–3”. In: *The Journal of nutrition* 145 (2 2014), pp. 246–252. DOI: 10.3945/jn.114.200832.

[127] Mikael Nilsson, Jens J Holst, and Inger ME Björck. “Metabolic effects of amino acid mixtures and whey protein in healthy subjects: studies using glucose-equivalent drinks”. In: *The American journal of clinical nutrition* 85 (4 2007), pp. 996–1004. DOI: 10.1093/ajcn/85.4.996.

[128] Tasleem A Zafar et al. “Whey protein sweetened beverages reduce glycemic and appetite responses and food intake in young females”. In: *Nutrition research* 33 (4 2013), pp. 303–310. DOI: 10.1016/j.nutres.2013.01.008.

[129] SL Turgeon, Christophe Schmitt, and Christian Sanchez. “Protein-polysaccharide complexes and coacervates”. In: *Current Opinion in Colloid & Interface Science* 12 (4-5 2007), pp. 166–178. DOI: 10.1016/j.cocis.2007.07.007.

[130] J Leroux et al. “Emulsion stabilizing properties of pectin”. In: *Food hydrocolloids* 17 (4 2003), pp. 455–462. DOI: 10.1016/S0268-005X(03)00027-4.

[131] R Hans Tromp et al. “On the mechanism of stabilisation of acidified milk drinks by pectin”. In: *Food hydrocolloids* 18 (4 2004), pp. 565–572. DOI: 10.1016/j.foodhyd.2003.09.005.

[132] CL Cooper et al. “Polyelectrolyte–protein complexes”. In: *Current opinion in colloid & interface science* 10 (1-2 2005), pp. 52–78. DOI: 10.1016/j.cocis.2005.05.007.

[133] Vladimir Tolstoguzov. “Some thermodynamic considerations in food formulation”. In: *Food Hydrocolloids* 17 (1 2003), pp. 1–23. DOI: 10.1016/S0268-005X(01)00111-4.

[134] Eric Dickinson. “Interfacial structure and stability of food emulsions as affected by protein–polysaccharide interactions”. In: *Soft Matter* 4 (5 2008), pp. 932–942. DOI: 10.1039/B718319D.

[135] Thepkunya Harnsilawat, Rungnaphar Pongsawatmanit, and DJ McClements. "Characterization of β -lactoglobulin-sodium alginate interactions in aqueous solutions: a calorimetry, light scattering, electrophoretic mobility and solubility study". In: *Food Hydrocolloids* 20 (5 2006), pp. 577–585. DOI: 10.1016/j.foodhyd.2005.05.005.

[136] Maude Girard, Sylvie L Turgeon, and Sylvie F Gauthier. "Thermodynamic parameters of β-lactoglobulin- pectin complexes assessed by isothermal titration calorimetry". In: *Journal of Agricultural and Food Chemistry* 51 (15 2003), pp. 4450–4455. DOI: 10.1021/jf0259359.

[137] Evan Spruijt, Martien A Cohen Stuart, and Jasper van der Gucht. "Linear viscoelasticity of polyelectrolyte complex coacervates". In: *Macromolecules* 46 (4 2013), pp. 1633–1641. DOI: 10.1021/ma301730n.

[138] Amy Y Xu et al. "Sugar-coated proteins: the importance of degree of polymerisation of oligo-galacturonic acid on protein binding and aggregation". In: *Soft Matter* 13 (14 2017), pp. 2698–2707. DOI: 10.1039/C6SM02660E.

[139] Amy Y Xu et al. "Effects of polysaccharide charge pattern on the microstructures of β-lactoglobulin-pectin complex coacervates, studied by SAXS and SANS". In: *Food Hydrocolloids* 77 (2018), pp. 952–963. DOI: 10.1016/j.foodhyd.2017.11.045.

[140] Bram LHM Sperber et al. "Overall charge and local charge density of pectin determines the enthalpic and entropic contributions to complexation with β-lactoglobulin". In: *Biomacromolecules* 11 (12 2010), pp. 3578–3583. DOI: 10.1021/bm1010432.

[141] Amy Y Xu et al. "Structural mechanism of complex assemblies: characterisation of beta-lactoglobulin and pectin interactions". In: *Soft Matter* 11 (34 2015), pp. 6790–6799. DOI: 10.1039/C5SM01378J.

[142] Christophe Schmitt et al. "Study of β-lactoglobulin/acacia gum complex coacervation by diffusing-wave spectroscopy and confocal scanning laser microscopy". In: *Colloids and Surfaces B: Biointerfaces* 20 (3 2001), pp. 267–280. DOI: 10.1016/S0927-7765(00)00200-9.

[143] V Ulaganathan et al. "β-Lactoglobulin adsorption layers at the water/air surface: 1. Adsorption kinetics and surface pressure isotherm: Effect of pH and ionic strength". In: *Colloids and Surfaces A: Physicochemical and Engineering Aspects* 519 (2017), pp. 153–160. DOI: 10.1016/j.colsurfa.2016.03.008.

[144] Renate A Ganzevles et al. "Polysaccharide charge density regulating protein adsorption to air/water interfaces by protein/polysaccharide complex formation". In: *The Journal of Physical Chemistry B* 111 (45 2007), pp. 12969–12976. DOI: 10.1021/jp075441k.

[145] Piet JH Daas et al. "Investigation of the non-esterified galacturonic acid distribution in pectin with endopolygalacturonase". In: *Carbohydrate Research* 318 (1-4 1999), pp. 135–145. DOI: 10.1016/S0008-6215(99)00093-2.

[146] Beda M. Yapo and Dago Gnakri. "Pectic Polysaccharides and Their Functional Properties". In: *Polysaccharides: Bioactivity and Biotechnology*. Ed. by Kishan Gopal Ramawat and Jean-Michel Mérillon. Cham: Springer International Publishing, 2015, pp. 1729–1749. ISBN: 978-3-319-16298-0. DOI: 10.1007/978-3-319-16298-0_62.

[147] Jean-François Thibault et al. "Studies of the length of homogalacturonic regions in pectins by acid hydrolysis". In: *Carbohydrate Research* 238 (1993), pp. 271–286. DOI: 10.1016/0008-6215(93)87019-0.

[148] Davoud Zare, Kathryn M McGrath, and Jane R Allison. "Deciphering β-Lactoglobulin Interactions at an Oil–Water Interface: A Molecular Dynamics Study". In: *Biomacromolecules* 16 (6 2015), pp. 1855–1861. DOI: 10.1021/acs.biomac.5b00467.

[149] Bram LHM Sperber et al. "Binding of β-lactolobulin to pectins Varying in their Overall and Local Charge Density". In: *Biomacromolecules* 10 (12 2009), pp. 3246–3252. DOI: 10.1021/bm900812x.

[150] P Maarten Biesheuvel, Marijn van der Veen, and Willem Norde. "A modified Poisson- Boltzmann model including charge regulation for the adsorption of ionizable polyelectrolytes to charged interfaces, applied to lysozyme adsorption on silica". In: *The Journal of Physical Chemistry B* 109 (9 2005), pp. 4172–4180. DOI: 10.1021/jp0463823.

[151] Thepkunya Harnsilawat, Rungnaphar Pongsawatmanit, and David J McClements. "Stabilization of model beverage cloud emulsions using protein- polysaccharide electrostatic complexes formed at the oil- water interface". In: *Journal of agricultural and food chemistry* 54 (15 2006), pp. 5540–5547. DOI: 10.1021/jf052860a.

[152] Lydie Moreau et al. "Production and characterization of oil-in-water emulsions containing droplets stabilized by β-lactoglobulin- pectin membranes". In: *Journal of Agricultural and Food Chemistry* 51 (22 2003), pp. 6612–6617. DOI: 10.1021/jf034332+.

[153] Peter A Wierenga et al. "Quantitative description of the relation between protein net charge and protein adsorption to air- water interfaces". In: *The Journal of Physical Chemistry B* 109 (35 2005), pp. 16946–16952. DOI: 10.1021/jp050990g.

[154] Renate A Ganzevles et al. "Structure of mixed β-lactoglobulin/pectin adsorbed layers at air/water interfaces; a spectroscopy study". In: *Journal of colloid and interface science* 317 (1 2008), pp. 137–147. DOI: 10.1016/j.jcis.2007.09.030.

[155] Helena Kieserling et al. "Conformational state and charge determine the interfacial film formation and film stability of β-lactoglobulin". In: *Food Hydrocolloids* 114 (2021), p. 106561. DOI: 10.1016/j.foodhyd.2020.106561.

[156] Sashikumar Ramamirtham et al. "Complexes of -lactoglobulin and high methylesterified pectin as a one-shot delivery system for reinforcing oil/water interfaces". In: *Soft Matter* (2021), pp. –. DOI: 10.1039/D1SM00989C.

[157] Sashikumar Ramamirtham et al. "The rheological properties of bovine β-Lactoglobulin stabilized oil/water interfaces depend on the protein's quaternary structure". In: *Food Hydrocolloids* (2021), p. 106834. DOI: 10.1016/j.foodhyd.2021.106834.

[158] Slavka Tcholakova et al. "Coalescence in β-lactoglobulin-stabilized emulsions: effects of protein adsorption and drop size". In: *Langmuir* 18.23 (2002), pp. 8960–8971. DOI: 10.1021/la0258188.

[159] Demet Guzey and David Julian McClements. "Impact of electrostatic interactions on formation and stability of emulsions containing oil droplets coated by β-lactoglobulin- pectin complexes". In: *Journal of agricultural and food chemistry* 55 (2 2007), pp. 475–485. DOI: 10.1021/jf062342f.

[160] Maude Girard, Sylvie L Turgeon, and Sylvie F Gauthier. "Quantification of the interactions between β-lactoglobulin and pectin through capillary electrophoresis analysis". In: *Journal of Agricultural and Food Chemistry* 51 (20 2003), pp. 6043–6049. DOI: 10.1021/jf034266b.

[161] Manigandan Sabapathy et al. "Visualization of the equilibrium position of colloidal particles at fluid–water interfaces by deposition of nanoparticles". In: *Nanoscale* 7 (33 2015), pp. 13868–13876. DOI: 10.1039/C5NR03369A.

[162] Armando Maestro et al. "Contact angle of micro-and nanoparticles at fluid interfaces". In: *Current opinion in colloid & interface science* 19 (4 2014), pp. 355–367. DOI: 10.1016/j.cocis.2014.04.008.

[163] Antonio Stocco et al. "Evanescent-wave dynamic light scattering at an oil-water interface: Diffusion of interface-adsorbed colloids". In: *Physical Review E* 83 (1 2011), p. 011601. DOI: 10.1103/PhysRevE.83.011601.

[164] Howard A Stone. "Interfaces: in fluid mechanics and across disciplines". In: *Journal of Fluid Mechanics* 645 (2010), pp. 1–25. DOI: 10.1017/S0022112009994186.

[165] PG Saffman and M Delbrück. "Brownian motion in biological membranes". In: *Proceedings of the National Academy of Sciences* 72 (8 1975), pp. 3111–3113. DOI: 10.1073/pnas.72.8.3111.

[166] Th M Fischer, P Dhar, and P Heinig. "The viscous drag of spheres and filaments moving in membranes or monolayers". In: *Journal of Fluid Mechanics* 558 (2006), pp. 451–475. DOI: 10.1017/S002211200600022X.

[167] Giuseppe Boniello et al. "Brownian diffusion of a partially wetted colloid". In: *Nature materials* 14 (9 2015), pp. 908–911. DOI: 10.1038/nmat4348.

[168] Krassimir D Danov, Rumiana Dimova, and Bernard Pouligny. "Viscous drag of a solid sphere straddling a spherical or flat surface". In: *Physics of Fluids* 12 (11 2000), pp. 2711–2722. DOI: 10.1063/1.1289692.

[169] Chih-yuan Wu, Sowmitri Tarimala, and Lenore L Dai. "Dynamics of Charged Microparticles at Oil- Water Interfaces". In: *Langmuir* 22 (5 2006), pp. 2112–2116. DOI: 10.1021/la0525978.

[170] Jhoan Toro-Mendoza, Gieberth Rodriguez-Lopez, and Oscar Paredes-Altuve. "Brownian diffusion of a particle at an air/liquid interface: the elastic (not viscous) response of the surface". In: *Physical Chemistry Chemical Physics* 19 (13 2017), pp. 9092–9095. DOI: 10.1039/C6CP07442A.

[171] Meisam Pourali et al. "Drag on a spherical particle at the air–liquid interface: Interplay between compressibility, Marangoni flow, and surface viscosities". In: *Physics of Fluids* 33 (6 2021), p. 062103. DOI: 10.1063/5.0050936.

[172] Dirk GAL Aarts, Matthias Schmidt, and Henk NW Lekkerkerker. "Direct visual observation of thermal capillary waves". In: *Science* 304 (5672 2004), pp. 847–850. DOI: 10.1126/science.1097116.

[173] Christophe Dicharry et al. "Stability of water/crude oil emulsions based on interfacial dilatational rheology". In: *Journal of colloid and interface science* 297 (2 2006), pp. 785–791. DOI: 10.1016/j.jcis.2005.10.069.

[174] Thomas G. Mason. "Estimating the viscoelastic moduli of complex fluids using the generalized Stokes–Einstein equation". In: *Rheologica Acta* 39 (4 2000), pp. 371–378. DOI: 10.1007/s003970000094.

[175] Bivash R Dasgupta et al. "Microrheology of polyethylene oxide using diffusing wave spectroscopy and single scattering". In: *Physical review E* 65 (5 2002), p. 051505. DOI: 10.1103/PhysRevE.65.051505.

[176] Alex J Levine and TC Lubensky. "One-and two-particle microrheology". In: *Physical review letters* 85 (8 2000), p. 1774. DOI: 10.1103/PhysRevLett.85.1774.

[177] Jian Wu and Lenore L Dai. "Apparent Microrheology of Oil- Water Interfaces by Single-Particle Tracking". In: *Langmuir* 23 (8 2007), pp. 4324–4331. DOI: 10.1021/la0625190.

[178] Chih-yuan Wu, Yanmei Song, and Lenore L Dai. "Two-particle microrheology at oil-water interfaces". In: *Applied Physics Letters* 95 (14 2009), p. 144104. DOI: 10.1063/1.3243334.

[179] V Prasad, SA Koehler, and Eric R Weeks. "Two-particle microrheology of quasi-2D viscous systems". In: *Physical review letters* 97 (17 2006), p. 176001. DOI: 10.1103/PhysRevLett.97.176001.

[180] V Prasad and Eric R Weeks. "Two-dimensional to three-dimensional transition in soap films demonstrated by microrheology". In: *Physical review letters* 102 (17 2009), p. 178302. DOI: 10.1103/PhysRevLett.102.178302.

[181] Yuan Peng et al. "Short-time self-diffusion of nearly hard spheres at an oil–water interface". In: *Journal of fluid mechanics* 618 (2009), pp. 243–261. DOI: 10.1017/S0022112008004114.

[182] Francisco Ortega, Hernán Ritacco, and Ramón G Rubio. "Interfacial microrheology: particle tracking and related techniques". In: *Current opinion in colloid & interface science* 15 (4 2010), pp. 237–245. DOI: 10.1016/j.cocis.2010.03.001.

[183] Alma J Mendoza et al. "Particle laden fluid interfaces: dynamics and interfacial rheology". In: *Advances in colloid and interface science* 206 (2014), pp. 303–319. DOI: 10.1016/j.cis.2013.10.010.

[184] Timo Somer and Herbert J Meiselman. "Disorders of blood viscosity". In: *Annals of medicine* 25 (1 1993), pp. 31–39. DOI: 10.3109/07853899309147854.

[185] Thomas Gisler and David A Weitz. "Scaling of the microrheology of semidilute F-actin solutions". In: *Physical review letters* 82 (7 1999), p. 1606. DOI: 10.1103/PhysRevLett.82.1606.

[186] Dmitry Ershov, Martien Cohen Stuart, and Jasper van der Gucht. "Mechanical properties of reconstituted actin networks at an oil–water interface determined by microrheology". In: *Soft Matter* 8 (21 2012), pp. 5896–5903. DOI: 10.1039/C2SM25381J.

[187] MT Valentine et al. "Colloid surface chemistry critically affects multiple particle tracking measurements of biomaterials". In: *Biophysical journal* 86 (6 2004), pp. 4004–4014. DOI: 10.1529/biophysj.103.037812.

[188] Tommy Garting and Anna Stradner. "Optical microrheology of protein solutions using tailored nanoparticles". In: *Small* 14 (46 2018), p. 1801548. DOI: 10.1002/smll.201801548.

[189] Raymond S Tu and Victor Breedveld. "Microrheological detection of protein unfolding". In: *Physical Review E* 72 (4 2005), p. 041914. DOI: 10.1103/PhysRevE.72.041914.

[190] Prajnaparamita Dhar et al. “Active interfacial shear microrheology of aging protein films”. In: *Physical review letters* 104 (1 2010), p. 016001. DOI: 10.1103/PhysRevLett.104.016001.

[191] SQ Choi et al. “Active microrheology and simultaneous visualization of sheared phospholipid monolayers”. In: *Nature communications* 2 (1 2011), pp. 1–6. DOI: 10.1038/ncomms1321.

[192] Daniel B Allan et al. “Linear and nonlinear microrheology of lysozyme layers forming at the air–water interface”. In: *Soft Matter* 10 (36 2014), pp. 7051–7060. DOI: 10.1039/C4SM00484A.

[193] Myung Han Lee et al. “Combined passive and active microrheology study of protein-layer formation at an air- water interface”. In: *Langmuir* 26 (4 2010), pp. 2650–2658. DOI: 10.1021/la902881f.

[194] Armando Maestro et al. “Surface rheology: macro-and microrheology of poly (tert-butyl acrylate) monolayers”. In: *Soft Matter* 7 (17 2011), pp. 7761–7771. DOI: 10.1039/C1SM05225J.

[195] Joseph R Samaniuk and Jan Vermant. “Micro and macrorheology at fluid–fluid interfaces”. In: *Soft matter* 10 (36 2014), pp. 7023–7033. DOI: 10.1039/C4SM00646A.

[196] Roie Shlomovitz et al. “Measurement of monolayer viscosity using noncontact microrheology”. In: *Physical review letters* 110 (13 2013), p. 137802. DOI: 10.1103/PhysRevLett.110.137802.

[197] Zachary A Zell et al. “Linear and nonlinear microrheometry of small samples and interfaces using microfabricated probes”. In: *Journal of Rheology* 60 (1 2016), pp. 141–159. DOI: 10.1122/1.4937931.

[198] Pietro Cicuta and Athene M Donald. “Microrheology: a review of the method and applications”. In: *Soft matter* 3 (12 2007), pp. 1449–1455. DOI: 10.1039/B706004C.

[199] Eduardo Guzmán et al. “Shear rheology of fluid interfaces: Closing the gap between macro-and micro-rheology”. In: *Current opinion in Colloid & interface science* 37 (2018), pp. 33–48. DOI: 10.1016/j.cocis.2018.05.004.

[200] J Tajuelo, MA Rubio, and JM Pastor. "Flow field based data processing for the oscillating conical bob interfacial shear rheometer". In: *Journal of Rheology* 62 (1 2018), pp. 295–311. DOI: 10.1122/1.5012764.

[201] J Tajuelo et al. "Magnetic microwire probes for the magnetic rod interfacial stress rheometer". In: *Langmuir* 31 (4 2015), pp. 1410–1420. DOI: 10.1021/la5038316.

[202] Dong Woo Kang, Jin Hyun Lim, and Bum Jun Park. "Heterogeneous interface adsorption of colloidal particles". In: *Soft matter* 13 (36 2017), pp. 6234–6242. DOI: 10.1039/C7SM00618G.

[203] Salman S Rogers et al. "Precise particle tracking against a complicated background: polynomial fitting with Gaussian weight". In: *Physical Biology* 4 (3 2007), p. 220. DOI: 10.1088/1478-3975/4/3/008.

[204] Chih-yuan Wu. "Particle dynamics and microrheology at liquid-liquid interfaces". PhD thesis. Texas Tech University, 2009. URL: http://hdl.handle.net/2346/21001.

[205] Indira Sriram, Alexander Meyer, and Eric M Furst. "Active microrheology of a colloidal suspension in the direct collision limit". In: *Physics of Fluids* 22 (6 2010), p. 062003. DOI: 10.1063/1.3450319.

[206] John C Crocker et al. "Two-point microrheology of inhomogeneous soft materials". In: *Physical Review Letters* 85 (4 2000), p. 888. DOI: 10.1103/PhysRevLett.85.888.

[207] Helena Schestkowa, Stephan Drusch, and Anja Maria Wagemans. "FTIR analysis of β-lactoglobulin at the oil/water-interface". In: *Food chemistry* 302 (2020), p. 125349. DOI: 10.1016/j.foodchem.2019.125349.

[208] Dubravko Risović, Sanja Frka, and Zlatica Kozarac. "Application of Brewster angle microscopy and fractal analysis in investigations of compressibility of Langmuir monolayers". In: *The Journal of chemical physics* 134 (2 2011), p. 024701. DOI: 10.1063/1.3522646.

[209] AK Sachan et al. "Interfacial rheology of coexisting solid and fluid monolayers". In: *Soft Matter* 13 (7 2017), pp. 1481–1492. DOI: 10.1039/C6SM02797K.

[210] Prasad S Sarangapani et al. “The limitations of an exclusively colloidal view of protein solution hydrodynamics and rheology”. In: *Biophysical journal* 105.10 (2013), pp. 2418–2426. DOI: 10.1016/j.bpj.2013.10.012.

[211] Prasad S Sarangapani et al. “Critical examination of the colloidal particle model of globular proteins”. In: *Biophysical journal* 108.3 (2015), pp. 724–737. DOI: 10.1016/j.bpj.2014.11.3483.

[212] Lindsay Sawyer and George Kontopidis. “The core lipocalin, bovine β-lactoglobulin”. In: *Biochimica et Biophysica Acta (BBA)-Protein Structure and Molecular Enzymology* 1482 (1-2 2000), pp. 136–148. DOI: 10.1016/S0167-4838(00)00160-6.

[213] F Martínez-Pedrero et al. “Linear shear rheology of aging β-casein films adsorbing at the air/water interface”. In: *Journal of colloid and interface science* 511 (2018), pp. 12–20. DOI: 10.1016/j.jcis.2017.09.092.

[214] Laura Hobley et al. “BslA is a self-assembling bacterial hydrophobin that coats the Bacillus subtilis biofilm”. In: *Proceedings of the National Academy of Sciences* 110 (33 2013), pp. 13600–13605. DOI: 10.1073/pnas.1306390110.

[215] Sinenhlanhla N Mthembu et al. “2-(Dibenzylamino) butane-1, 4-dithiol (DABDT), a Friendly Disulfide-Reducing Reagent Compatible with a Broad Range of Solvents”. In: *Organic letters* 21 (24 2019), pp. 10111–10114. DOI: 10.1021/acs.orglett.9b04106.

[216] Alan R Mackie et al. “Orogenic displacement in mixed β-lactoglobulin/β-casein films at the air/water interface”. In: *Langmuir* 17 (21 2001), pp. 6593–6598. DOI: 10.1021/la010687g.

[217] Henrik Stapelfeldt, Carl E Olsen, and Leif H Skibsted. “Spectrofluorometric Characterization of β-Lactoglobulin B Covalently Labeled with 2-(4 ‘-Maleimidylanilino) naphthalene-6-sulfonate”. In: *Journal of agricultural and food chemistry* 47 (10 1999), pp. 3986–3990. DOI: 10.1021/jf9812026.

[218] Elisabeth E Charrier et al. “Control of cell morphology and differentiation by substrates with independently tunable elasticity and viscous dissipation”. In: *Nature communications* 9 (1 2018), pp. 1–13. DOI: 10.1038/s41467-018-02906-9.